AN ATTEMPT TO QUANTIFY PERMAFROST DISTRIBUTION

AN ATTEMPT TO QUANTIFY PERMAFROST DISTRIBUTION NEAR SCHEFFERVILLE, QUEBEC

Ian G. Jones

A thesis submitted to the Faculty of Graduate Studies and Research in partial fulfillment of the requirements for the degree of Master of Science

Department of Geography,
McGill University,
Montreal,
Quebec.

February, 1976

ABSTRACT

Relationships between ground temperature and environmental factors are examined at a site which is partially underlain by permafrost. A major section of the study concerns the collection of ground temperature and environmental factor data in a form which is suitable for use in production of large-scale predictions. Linear correlation analysis shows that relief, snow depth, vegetation, ground thermal properties and groundwater are all significantly correlated with ground temperature, the highest coefficients being those obtained with snow depth. The importance of snow depth is confirmed by stepwise multiple regression. This variable, together with either thermal conductivity (above 5 m) or elevation (below 5 m), explains approximately 90 percent of the variance in ground temperature, at depths down to 30m. A set of equations is derived for predicting ground temperature and incorporated into a simple heat flow model, which allows the distribution of permafrost and unfrozen ground to be projected in three dimensions. This model indicates that approximately 60 percent of the Timmins 4 Permafrost Experimental Site is underlain by permafrost, with a maximum thickness of about 150 m. The model is also tested at two other sites in the Schefferville area. It is concluded that, although the procedure is site-specific to some degree, due to the inclusion of the elevation variable, it provides a reasonable approximation for permafrost distribution at sites lying within the same elevation range as Timmins 4.

RESUME

Les relations entre la température du sol et les facteurs in situ sont étudiés à un site partiellement affecté par le pergélisol. Une section majeure de l'étude traite de la collection des données sur la température du sol et les facteurs in situ sous une forme qui puisse être utilisable pour des prédictions à grande échelle. L'analyse de la corelation linéaire montre que le relief, l'épaisseur de la neige, la végétation, les propriétés thermiques du sol et les eaux souterraines sont tous en rapport de façon significative avec la température du sol; les coefficients les plus élevés étant ceux obtenus avec l'épaisseur de la neige. L'importance de l'épaisseur de la neige est confirmée par la méthode statistique "Step-wise multiple regression". Cette variable, ajoutée à la conductivité thermique (au-dessus de 5 m) ou à l'altitude (au-dessous de 5 m) explique environ 90 pourcent de la variation de la température du sol, jusqu'à 30 m de profondeur. Un ensemble d'équations est derivé pour prédire les températures du sol et incorporé à un simple modèle de flux thermique, lequel permet d'obtenir une projection tri-dimentionnelle sur la distribution du pergélisol et du sol non gelé. Ce modèle indique qu'environ 60 pourcent du site expérimental de Timmins 4 est affecté par le pergélisol, avec une épaisseur maximum de 150 m. Le modèle a aussi été expérimenté à deux autres endroits de la région de Schefferville. Nous en concluons que, même si cette façon d'agir est spécifique au site par sa variable élévation, elle fournit

une approximation raisonnable pour connaître la distribution du pergélisol à d'autres sites sensiblement de la même altitude que Timmins 4.

ACKNOWLEDGEMENTS

A number of individuals and organisations provided assistance and encouragement during the course of this study.

Dr. Frank Nicholson supervised the study. He provided assistance and made suggestions for improvement at all stages of the study.

The Iron Ore Company of Canada has provided material assistance to the permafrost studies program since its inception. I am personally grateful also for the provision of topographic and geological maps, as well as for access to unpublished reports. Of the many IOCC employees who gladly provided assistance, I would especially like to thank Jim Orth, who arranged for me to collect samples for the thermal conductivity determinations, and Om Garg, with whom I worked on permafrost problems for two summers while employed by IOCC.

Two members of the Earth Physics Group, EMR, Ottawa gave assistance during the data collection stage of the study. Dr. A. Jessop sent copies of two computer programs for conversion of raw temperature data, while Dr. A. Judge made thermal conductivity determinations on samples which I submitted.

The study was funded by le Ministère de l'Education, Gouvernement du Québec, and the National Research Council of Canada.

Colleagues and friends of McGill who have given assistance and encouragement are too numerous to mention indi-

vidually. However, I can perhaps single out Hardy Granberg, Bryan Grey, Peter Mountford, Margaret Nicholson, Don Petzold, and Tony Price.

Not least my typists. Mrs. Valerie Lagacé produced a first draft from a practically illegible manuscript and typed the tables. Mrs. Shirley Peteran typed the final version, with an ever-shortening deadline. I thank them both.

TABLE OF CONTENTS

Continued/....

TABLE OF CONTENTS (Continued)

Continued/....

TABLE OF CONTENTS (Continued)

Continued/....

TABLE OF CONTENTS (Continued)

Continued/....

TABLE OF CONTENTS (Continued)

LIST OF FIGURES

Continued/....

LIST OF FIGURES (Continued)

LIST OF PLATES

LIST OF TABLES

LIST OF SYMBOLS

Symbol		Units
A	Ground heat flux	$Jm^{-2}s^{-1}$
A_o	Surface temperature amplitude	^oC
G	Temperature gradient	$^oCm^{-1}$
H	Sensible heat flux	$Jm^{-2}s^{-1}$
K	Thermal conductivity	$Wm^{-1}K^{-1}$
LE	Latent heat flux	$Jm^{-2}s^{-1}$
q*	Terrestrial heat flux	Wm^{-2}
Rn	Net radiation flux	$Jm^{-2}s^{-1}$
T_a	Average annual ground temperature	^oC
T_o	Surface temperature	^oC
Tz	Temperature at depth, z	^oC
Tz_a	Temperature at level of zero annual amplitude	^oC
z	Arbitrary depth beneath surface	m
Δz	Arbitrary depth increment	m
z_a	Level of zero annual amplitude	m
z_p	Depth to base of permafrost	m
α	Thermal diffusivity	$cm^{-2}s^{-1}$
ρ	Density	$gmcm^{-3}$
ω	Angular frequency of oscillation	$rad.s^{-1}$

ABBREVIATIONS

CRREL	Cold Regions Research and Engineering Laboratory
MSARL	McGill Sub-Arctic Research Laboratory
IOCC	Iron Ore Company of Canada
NRCC	National Research Council of Canada

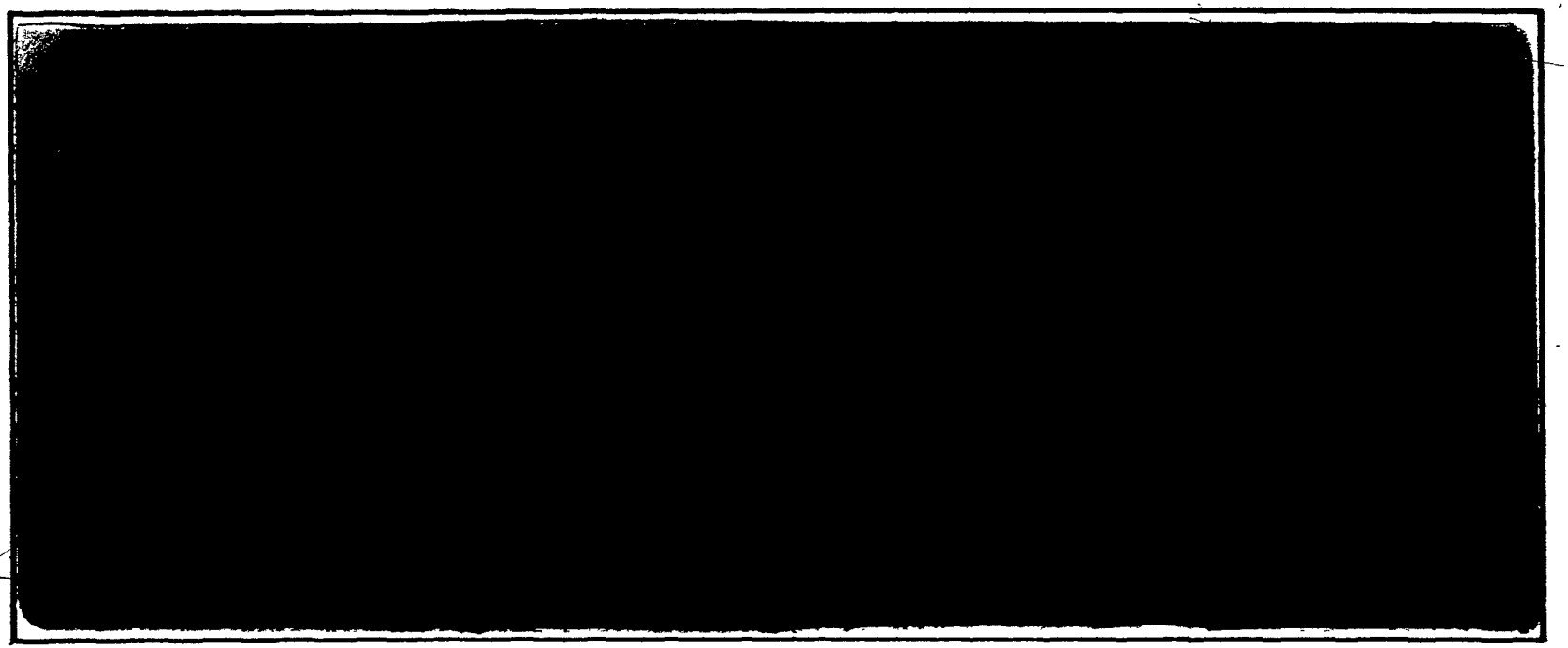

Frontispiece: View across the lower part of the Timmins 4 Permafrost Experimental Site. Irony Mountain is seen in the background. In general, permafrost underlies the sparsely-vegetated ridge areas, while the areas between ridges are essentially unfrozen. The small red shacks mark the locations of thermocables at this site, and the white stakes are snow stakes.

CHAPTER I

INTRODUCTION

1.1 GENERAL

1.11 Statement of the problem

Permafrost, or perennially frozen ground, is defined as the thermal condition which exists in earth material when its temperature remains below $0^{\circ}C$ for a period of greater than one year. Near Schefferville, Quebec (54° 48'N, 66° 49'W), in the northern part of the discontinuous permafrost zone, sufficient data are now available to justify attempts to statistically relate permafrost to the factors controling its occurrence. A major objective of the present study is therefore to define the factors which influence ground temperature distribution in the area, and to arrive at some estimate of their quantitative importance. These results form the basis for attempts to model the ground thermal regime, and hence the distribution of permafrost and unfrozen ground.

Permafrost is extensively developed, yet discontinuous, beneath upland ridge and valley terrain to the west and northwest of Schefferville. Its presence poses serious problems for open pit iron ore mining in the area. Thus, the development of techniques whereby the three-dimensional distribution of permafrost and unfrozen ground may be delineated, prior to mining, also has considerable practical application.

1.12 Objectives of the study

The objectives of the present study may be stated, formally, as follows:

i An assessment of the influence of environmental factors on the ground thermal regime in the discontinuous permafrost zone, with especial reference to conditions in the Schefferville area.

ii Derivation of improved equations relating shallow ground temperatures to such variables.

iii Development of a simple physically-based model for predicting the distribution of permafrost in three dimensions.

1.13 Outline of the thesis

A detailed outline of this thesis is contained in the Table of Contents (p.ii). Broadly, the three problems are considered in turn. A description of the study site and review of previous permafrost studies in the Schefferville area are given in Chapter 1, while Chapter 2 considers the thermal regime in permafrost. Chapter 3 is concerned with data collection, and Chapter 4 with assessing the influence of the various environmental parameters on temperature distribution. A semi-empirical model for permafrost distribution at Timmins 4 is developed and tested in Chapter 5, and applied to a new site, Timmins 2, in Chapter 6. Chapter 7 provides a summary and conclusions.

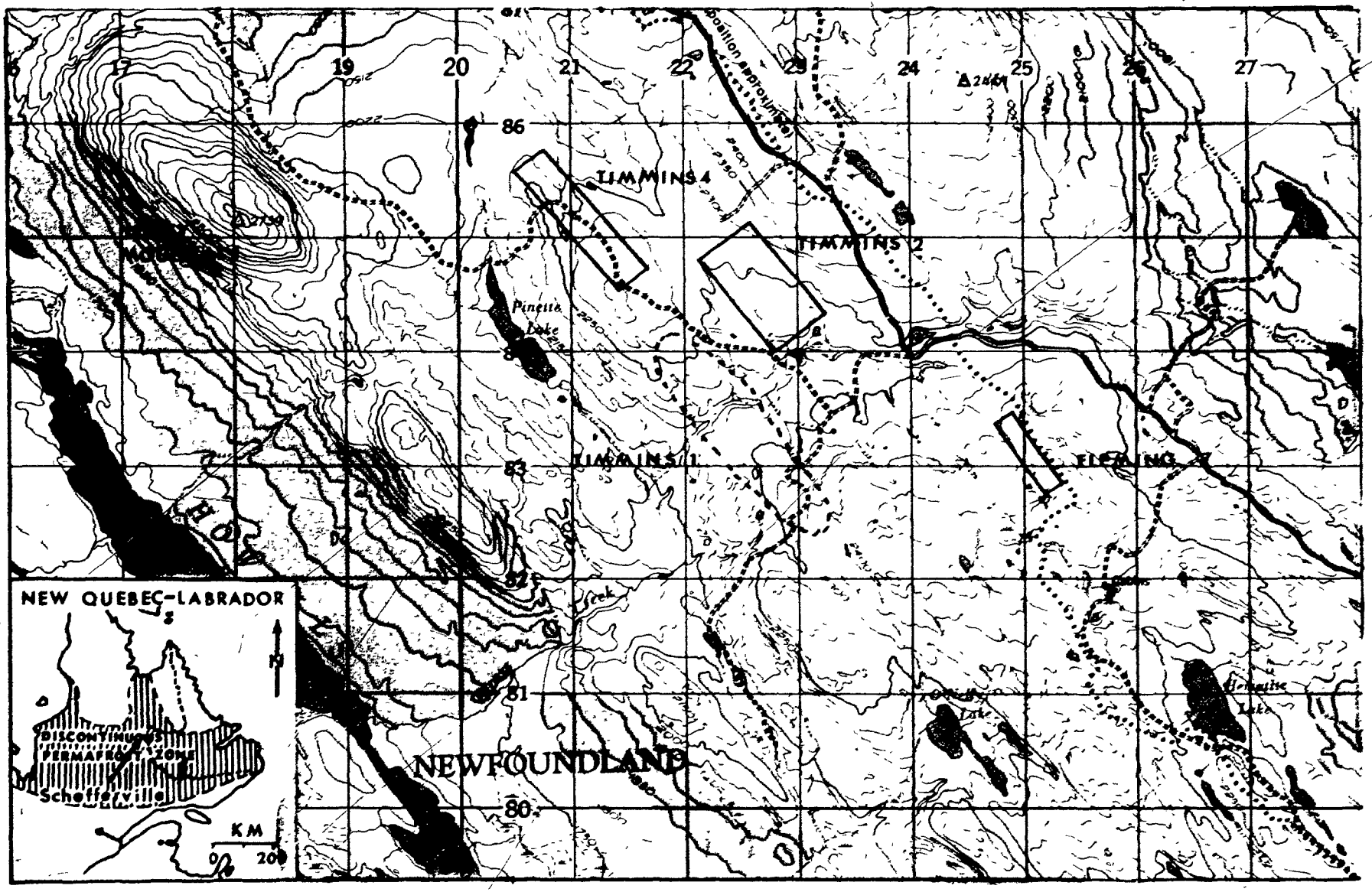

Figure 1: Location of study areas. Scale 1:50,000 (N.B. Elevations given elsewhere in the thesis refer to the IOCC datum, which is 72.5 m higher than North American datum used here).

1.2 TIMMINS 4 PERMAFROST EXPERIMENTAL SITE

The study was carried out at Timmins 4, a future mine site, situated 18 km northwest of Schefferville (Figure 1). This site lies at an elevation of between 750 m and 800 m (IOCC datum)*. Since 1968, it has been an experimental site for permafrost studies. Its physical environment is described in detail by Nicholson and Thom (1973).

1.21 Physiography

The approximately 1100 m by 350 m site is aligned with its long axis parallel to the trend of the regional topography, i.e. southeast-northwest (Figure 2). The highest ground, in the southern part of the site, comprises a valley flanked by broad flat ridges. In the central portion, the ground falls away steeply, with a predominantly northwesterly aspect and is dissected by a number of channels and small valleys. This drainage pattern becomes discontinuous, and includes a series of small ephemeral ponds, in the area of gentle, undulating relief at the northwest end of the site.

Due to differential erosion, the topography is closely related to underlying geology and structure. Ridges tend to be composed of competent material, while valleys are underlain by less competent (often altered) material and guided by strike faults.

---

* IOCC datum is 72.5 m above North American datum, see caption to Figure 1.

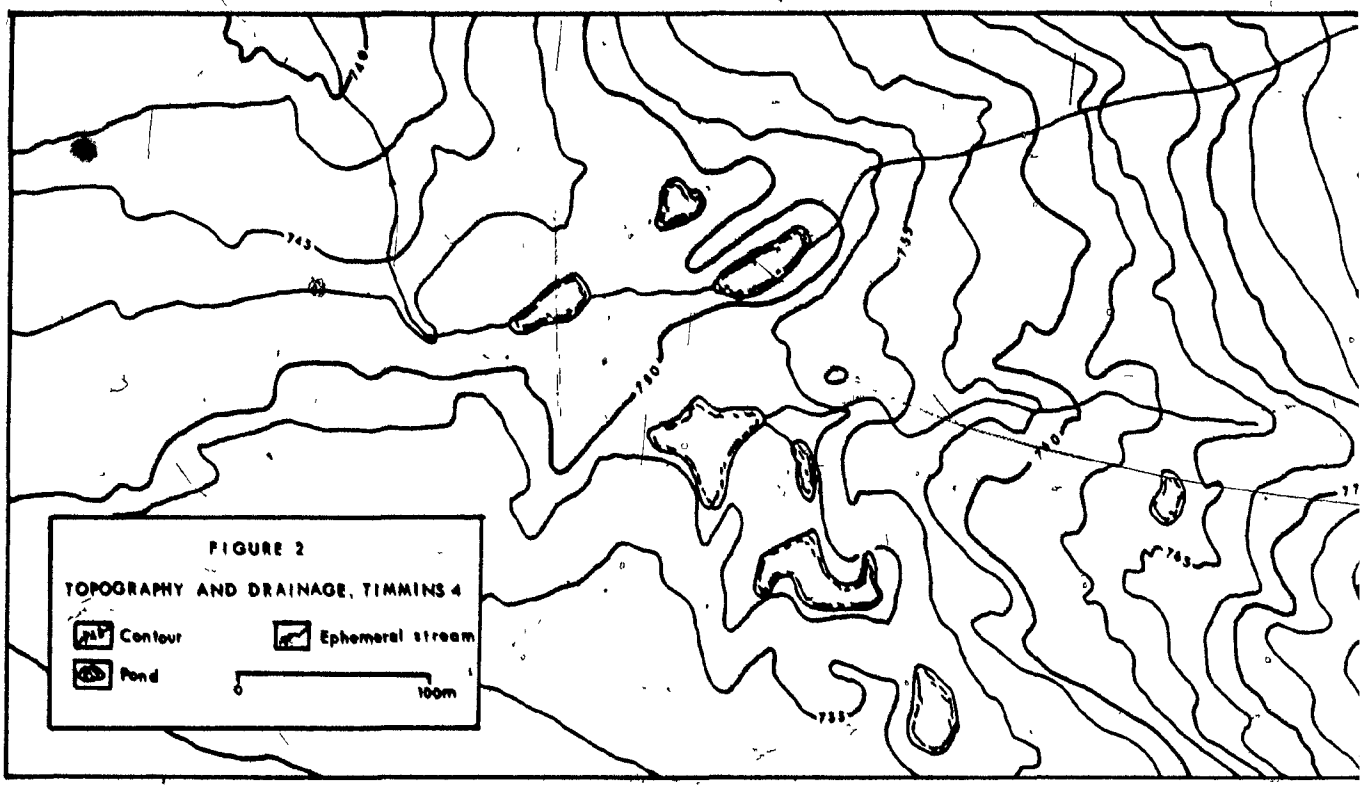

FIGURE 2

TOPOGRAPHY AND DRAINAGE, TIMMINS 4

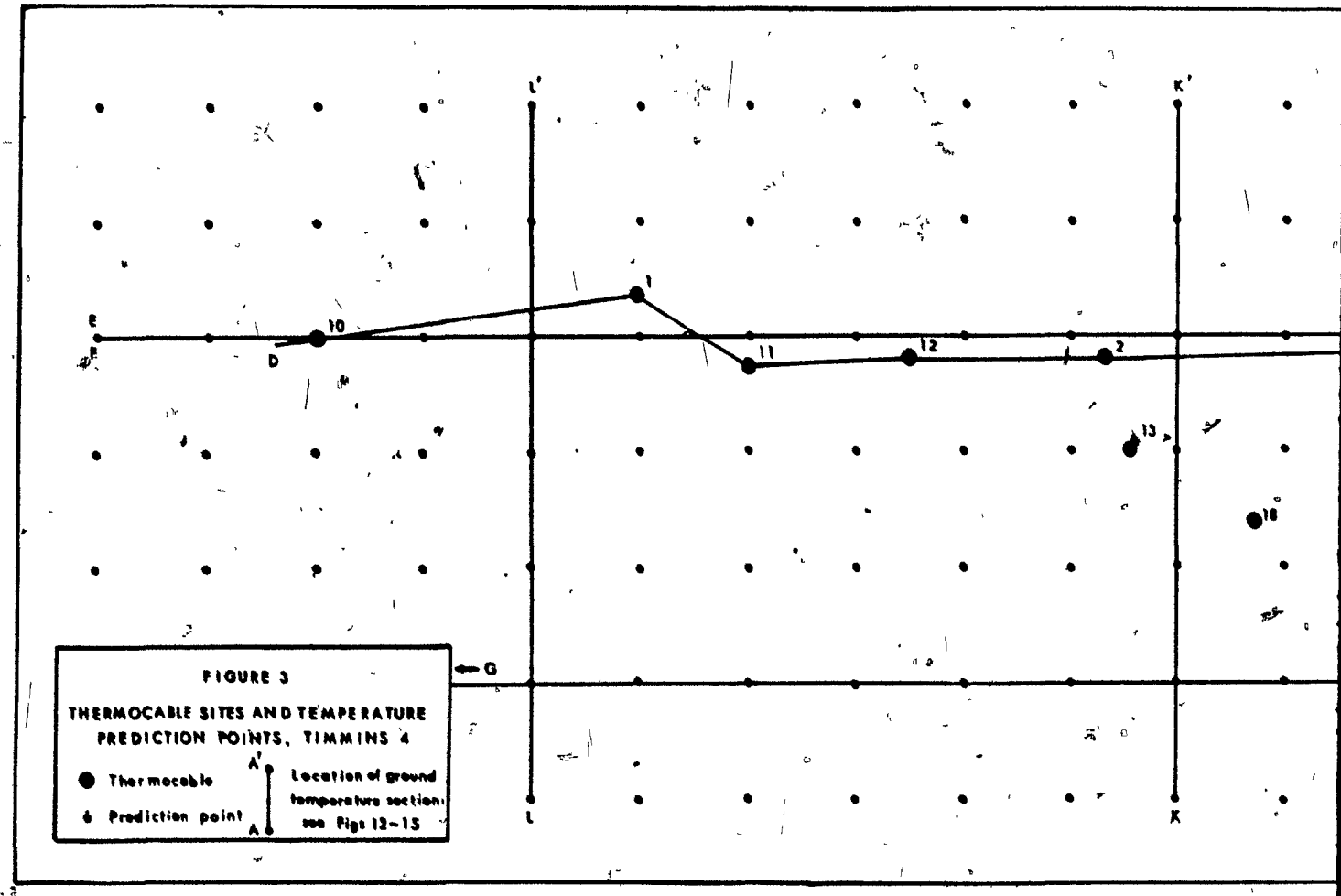

FIGURE 3

THERMOCABLE SITES AND TEMPERATURE PREDICTION POINTS, TIMMINS 4

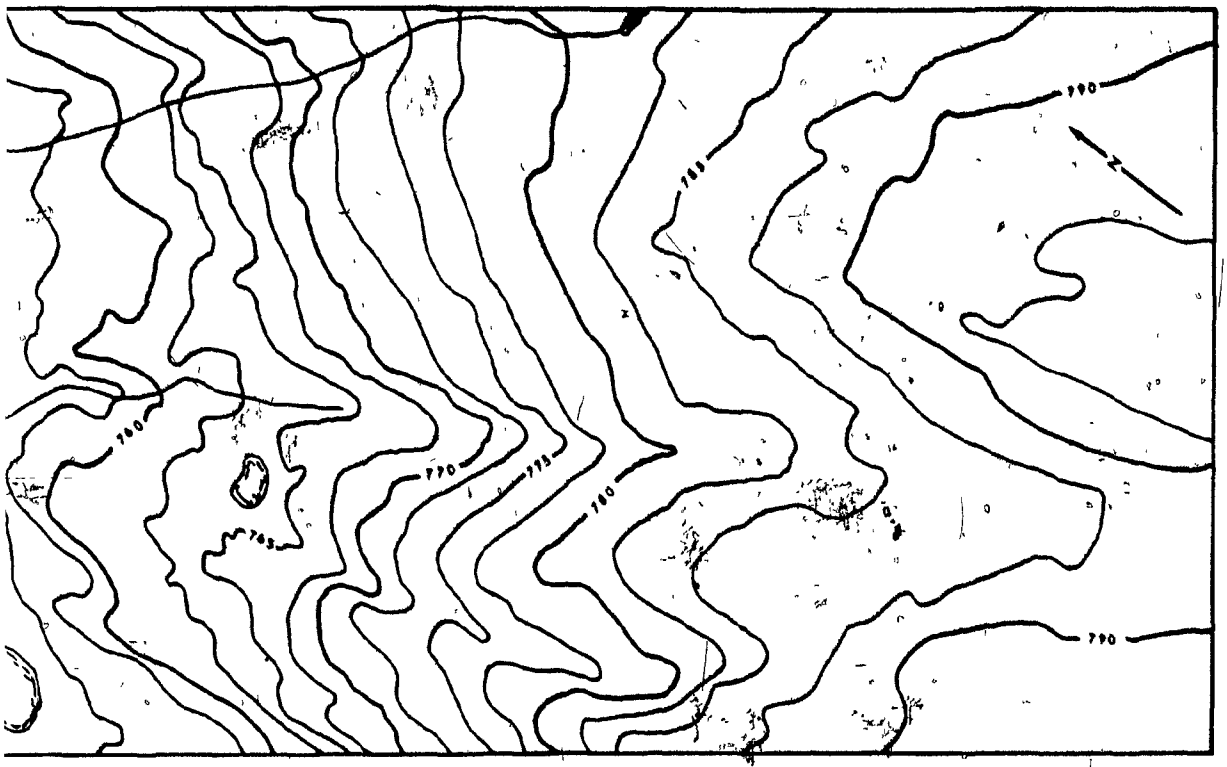
790
785
780
775
770
765
760
790
N

2 of 2

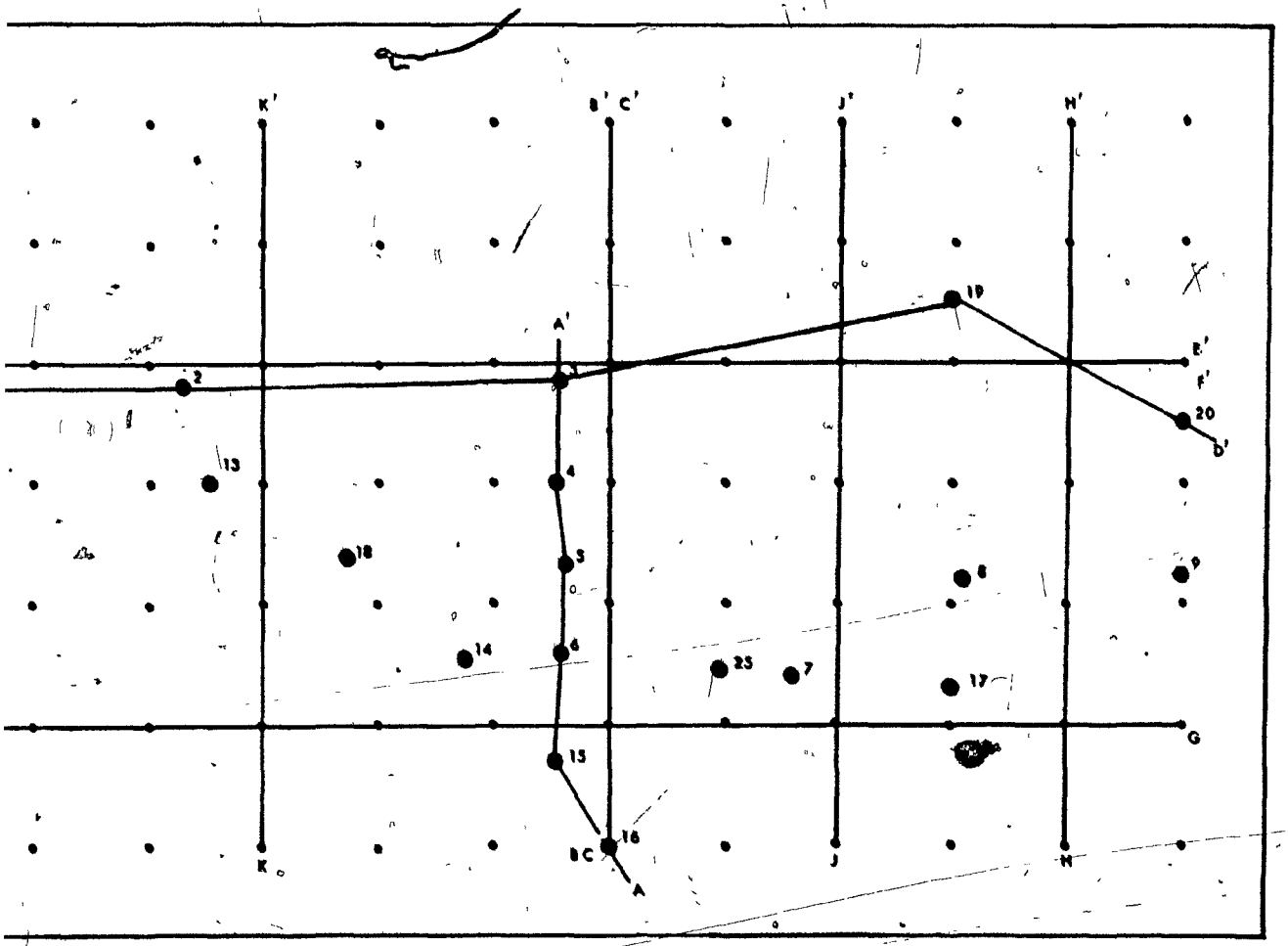
K'
B' C'
J'
H'
A'
E'
F'
b'
19
20
2
13
4
18
3
8
9
14
6
25
7
17
G
13
16
BC
A
K
J
H

1.22 Geology

The Schefferville area is underlain by low-grade metasediments of the Knob Lake Group, which comprise a miogeosynclinal sequence within the late Proterozoic Labrador Trough (Gross, 1968; Harrison, Howells and Fahrig, 1972; Zajac, 1974). The stratigraphy of the Group is summarized in Table I.

Structurally, the area is dominated by northwest-southeast trending folds and faults, the result of orogenic forces from the northeast (Stubbins, Blais and Zajac, 1960). Three periods of deformation are recognized. During the last of these, in the late Cretaceous, leaching and enrichment of the economically important Sokoman Iron Formation are believed to have occurred (Stubbins et al., op cit.; Gross, op cit.).

Due to facies changes, not all members of the Knob Lake Group are present in the Timmins area (Zajac, op cit.). The Timmins 4 site is underlain by a Sokoman Iron Formation syncline, bounded to southwest and northeast by Attikamagen Slate and unaltered iron formation respectively, in faulted contact. Leaching and enrichment of the iron formation in part of the syncline have produced the Timmins 4 orebody (Iron Ore Company, internal report).

There is a thin, discontinuous till cover, up to 1 m thick, over most of the site (Nicholson and Thom, 1973).

TABLE I

PRECAMBRIAN GEOLOGY OF THE SCHEFFERVILLE AREA

(after Gross, 1968. Table 1A)

FORMATION	LITHOLOGY
MARYJO DIABASE	Intrusive green-grey diabase
U n c o n f o r m i t y	
MENIHEK	Grey to black carbonaceous shale
SOKOMAN	Banded silicate, jasper and cherty iron formation with lean cherty and slate members.
RUTH	Black to green ferruginous slate
WISHART	Massive, often arkozic orthoquartzite
FLEMING	Massive chert breccia
DENAULT	Dolomite with minor chert, slate and quartzite interbeds
ATTIKAMAGEN	Varicoloured slate
U n c o n f o r m i t y	
ASHUANIPI	Schists and gneisses of the basement complex.

1.23 Climate

The subarctic climate experienced at the Schefferville townsite has been summarized by Tout (1964), and more recently Wilson (1971). Conditions on nearby ridges are more severe, notably with respect to wind speed and direction (Davies, 1962). Data from Timmins 4 indicate a mean annual air temperature of approximately -6°C, and mean wind speed throughout the year of 7 to 8 m^{-1} s^{-1} (Nicholson & Granberg, 1973). Precipitation totals are probably very similar to those at the townsite (an average of 745 mm, of which 312 mm water equivalent occurs as snow). The proportion of solid precipitation should be somewhat greater at the higher elevation of the Timmins 4 site.

1.24 Vegetation

Schefferville is situated within the forest-tundra sub-zone of the boreal forest (Hare, 1959). The distribution of cover types is diverse, and is closely related to drainage and microclimatic factors, most importantly snow depth and exposure (Nicholson, 1973). The vegetative cover ranges from open lichen woodland in sheltered lowland and valley locations to tundra and rock desert on the ridge tops.

The vegetation at Timmins 4 has been mapped in the field by Thom (1970), and from colour infra-red aerial photographs by Granberg (1972). Five cover types were distinguished by

Granberg (op cit. Figure 3):

1. Bare ground
2. Discontinuous cover (lichen, Vaccinium spp., Betula spp.)
3. Continuous lichen mat with scattered woody plants (Mainly Betula spp. and Ledum groenlandicum).
4. Continuous scrub (Betula spp.)
5. Sphagnum, mosses and sedge.

When the Granberg vegetation map is compared with a topographic map of Timmins 4 (Figure 2), a close relationship is apparent between topography and vegetation. Bare ground is restricted to ridge crests, while sphagnum and moss are largely confined to the valley bottoms and lower, northern part of the site. Occasional, isolated black and white spruce (Picea spp.) occur in the latter area.

Nicholson (op cit.) has demonstrated that soil formation at Timmins 4 is similarly related to drainage and microclimate.

1.3 PREVIOUS PERMAFROST STUDIES IN THE SCHEFFERVILLE AREA

The literature concerning permafrost, its distribution and the factors affecting its occurrence is so large that a detailed survey is beyond the scope of the present study. For such a review, reference should be made to the CRREL Permafrost Biblio-

graphy (CRREL, 1951 -), or to one of the existing bibliographic or summary papers (e.g. Williams, 1965; Brown and Péwé, 1973; Gold and Lachenbruch, 1973). The emphasis here will be on developments in the Schefferville area.

1.31 Ferriman Ridge

The first thermocables for direct measurement of ground temperatures in the Schefferville area were installed on the Ferriman No. 1 orebody in 1957, following the discovery of extensive permafrost at this site (Bonnlander, 1958). Subsequently, this initial investigation prompted the first regional appraisal of permafrost conditions, when vegetation and elevation were identified as factors of potential predictive value (Bonnlander and Major-Marothy, 1964). Furthermore, it suggested that permafrost in the area is in equilibrium with the present day climatic conditions; rather than a relict condition as had previously been supposed (Henderson, 1959).

In 1959, the number of thermocables was increased with the initiation of a joint project on Ferriman Ridge, involving the Iron Ore Company of Canada (IOCC), the McGill Sub-Arctic Research Laboratory (MSARL) and the National Research Council of Canada (NRCC) (Ives, 1961). A program of meteorological and snow depth observations was set up at the same time. These studies confirmed Bonnlander's conclusions, and indicated that the winter

snow cover was a major factor explaining the distribution of permafrost in the area (Ives, op cit). Meteorological data for the period (1959-61) have been analyzed and compared with conditions at the townsite by Davies (1962).

In 1961, Annersten began an evaluation of the influence of different cover types on the ground thermal regime (Annersten, 1962). He confirmed the over-riding importance of snow cover, and indicated that vegetation and elevation were of secondary importance (Annersten, 1964).

Routine ground temperature observations have been continued at Ferriman since 1962 by the staff of the McGill Laboratory. Some of the data collected have been analyzed by Gray (1966), while Barnett (1963) has compared snow depth-ground temperature relationships at the site with those on the Denault No. 2 orebody, 5 km north of the Schefferville townsite.

1.32 Timmins mining area

The decision to begin mining the Timmins group of deposits prompted relocation to this new area which was believed to be underlain by extensive permafrost. This situation was confirmed by a preliminary appraisal carried out at the site of the Timmins No. 1 mine (Thom, 1969; 1970). Using snow cover, vegetation and drainage relationships to extrapolate limited temperature data,

frozen ground was estimated to be extensive yet discontinuous with a maximum depth of approximately 90m (Thom, 1969 Table).

Studies at Timmins 1 were curtailed by the onset of stripping operations in 1968. Permafrost investigations have since continued at the Timmins 4 Permafrost Experimental Site, which was specially established, 2 km to the northwest (Nicholson and Thom, 1973). Research here has been directed primarily toward solution of two related problems (F.H. Nicholson, McGill Lab. Internal Reports):

i Development of techniques for permafrost prediction as an aid in sub-arctic mining operations (Nicholson and Granberg, 1973; Nicholson, 1974).

ii Investigation of thermal amelioration of permafrost, using snow fences and other semi-natural means.

1.33 Other studies

Ground temperature studies, in relation to permafrost distribution, have been concentrated to date on Ferriman Ridge and in the Timmins area. This is not to say that other areas or types of investigation have been neglected. For example, pre-production permafrost appraisals have been compiled for a number of sites, in connection with mining operations, by both McGill Laboratory (Internal Files) and the Geotechnical Section, Iron Ore Company of Canada (Garg

and Stacey, 1973). The latter group makes extensive use of geophysical techniques, such as seismic refraction and resistivity sounding, for permafrost delineation on a routine basis in operating mines (Garg, 1973; Séguin, 1974a, 1974b; Séguin and Garg, 1974). Yap (1972) has studied the engineering properties of frozen ores at different temperatures.

CHAPTER 2

GROUND THERMAL REGIME IN A PERMAFROST AREA

Studies of the ground thermal regime must take account of the changing distribution of ground temperatures in both space and time. On an annual basis, the thermal regime may be illustrated graphically by plotting depth-temperature profiles at monthly intervals throughout the year. Data from a thermocable at Timmins 4 have been treated in this way, as an example (Figure 4). Thermocable No. 1 (for location, see Figure 3) is unusual, in the Schefferville area, in that it penetrates the base of permafrost. It is ideal for illustrating the boundary conditions, terminology and sub-divisions of the regime, which are employed in the ensuing discussion. Plotted profiles for other thermocables at Timmins 4 are shown in Figures 11a and 11b.

2.1 UPPER BOUNDARY CONDITION -- THE GROUND SURFACE

The thermal regime is primarily a function of surface boundary temperature conditions, suggesting a possible close relationship between air and ground temperatures. Such a relationship does exist (Brown, 1966a), but the position of the permafrost boundaries and air temperature isotherms on published permafrost maps (Brown, 1967; Baranov, 1959; Ferrians, 1965), shows it is not a simple one. The discrepancy, generally in the order of 3 to 4°C (Brown, 1969. Table 3), is explained by the influence of

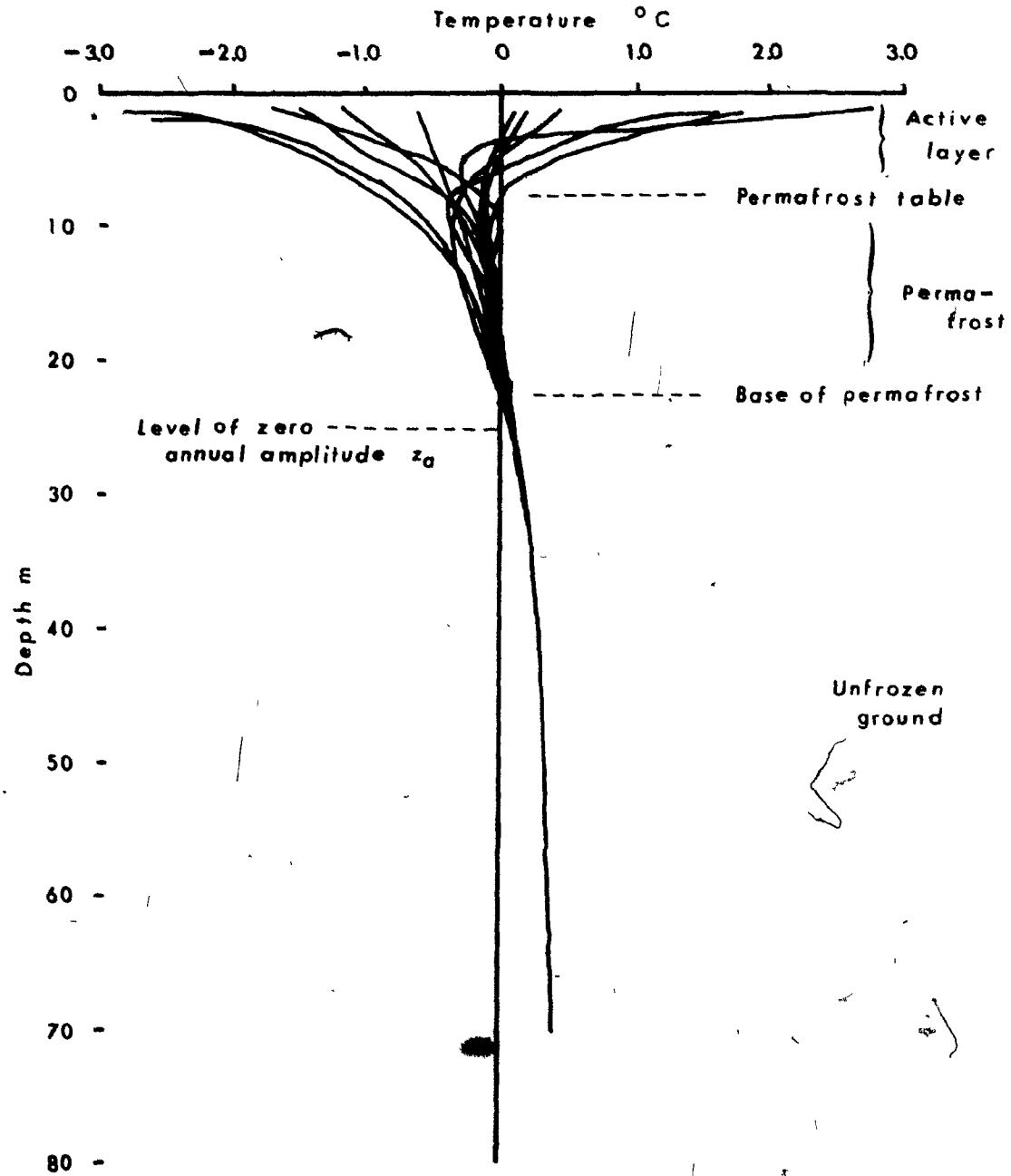

Figure 4: Components of the ground thermal regime in permafrost (Thermocable No. 1, Timmins 4).

what will be termed "environmental" factors. In the present study, these are considered to correspond to the "terrain factors", as defined by Brown (1969). The environmental factors include relief, snow cover and vegetation, which modify surface temperatures by influencing the microclimate.

The range of temperatures produced by the influence of environmental variables may be seen in Table II. Although the mean annual air temperature at Timmins 4 is approximately -6°C (Nicholson & Granberg, 1973), mean shallow temperatures, at a depth of 1.5m for example, range from -5°C to +1.3°C. This suggests an insulating effect, due to the environmental factors, of 1° to 7°C.

2.11 Components of the surface energy balance

The most important elements of the diurnal and annual exchanges of energy at the earth's surface are summarized in the following equation (after Budyko, 1958):

$$A = Rn - H - LE \qquad (1)$$

where A = Ground heat flux: the flow of heat into or out of the ground

Rn = Net radiation flux: the difference between incoming and outgoing fluxes of shortwave and longwave radiation.

H = Sensible heat flux: the loss or gain of energy, via sensible heat transfer.

LE = Latent heat flux: the energy loss or gain due to evaporation and condensation.

The magnitude and direction of the ground heat flux varies on a daily basis, as the relative importance of the turbulent fluxes changes to ensure a balance with net radiation. Thus, A is positive by day, but negative at night. On an annual basis, however, it is usual to assume that storage is constant, and therefore that A is equal to zero.

Few evaluations of the energy balance are available from the permafrost region. Daily measurements have been made over natural and burned lichen woodland (Rouse and Kershaw, 1971), and tundra (Ahrnsbrak, 1968) surfaces in the Hudson Bay lowland, and on Devon Island, N.W.T. by Addison (1972) and Courtin (1972). Other studies have been carried out over different surfaces by Brown (1965), Williams (1971) and Kelley and Weaver (1969). F.H. Nicholson (personal communication) is conducting studies of the surface energy balance at Timmins 4, in connection with permafrost amelioration studies at this site.

2.12 Environmental modification of the energy balance components

The existence of a discrepancy between average air and ground temperatures, due to the net insulating effect of environmental

factors, is well known. In the continuous permafrost zone, such effects are not generally large enough to counteract the low ambient air temperatures, although changes in existing permafrost thicknesses may result (Brown, 1966a). Further south, where mean annual air temperatures are closer to 0°C, their influence may be great enough to modify the distribution of permafrost, so that it becomes discontinuous, or may even prevent its formation entirely (Brown, op cit).

The influence of different environmental factors on the energy balance components can be considered under three sub-headings. All three sets of factors are complexly inter-related, both amongst themselves and with the permafrost (Brown, 1970. Table I).

2.121 Relief

An important micro-climatic attribute of relief is the influence of slope and aspect on incoming shortwave radiation (Garnier and Ohmura, 1970), which strongly effects soil heating. Permafrost conditions are most severe (Brown, 1969) and active layers generally least well developed (Annersten, 1964) on north-facing slopes. Studies at Thompson, Manitoba indicate the importance of even micro-relief, in determining the occurrence of frozen ground, at the southern edge of the discontinuous zone (Johnston, Brown and Pickersgill, 1963). The present writer found differences of up to 2.95°C at 50 cm depth between northeast and southwest facing slopes at Timmins 4.

Relief "shape", i.e. convexity or concavity, is important for its influence on the magnitude of the turbulent energy exchanges (Shul'gin, 1957). Both fluxes are increased over convex terrain segments, such as ridges and hills. The development of snow and vegetation covers is inhibited, in such areas, by the scouring action of the wind. To some extent the reverse is true over valleys and other depressions in the terrain (Shul'gin, op cit).

On a much large scale, when height differences of hundreds of meters are considered, ground temperatures decrease with increasing elevation (Kudryavtsev, 1965).

The occurrence of permafrost near Schefferville appears, at first sight, to be closely related to relief. Frozen ground is extensively developed under exposed ridge tops, yet absent or sporadic in lowland areas. However, the relationship is more likely essentially an indirect one, with relief controlling the distribution of other factors, such as snow and vegetation, which, in turn, control ground temperature (Annersten, 1966).

2.122 Vegetation

Vegetation forms an insulating layer, between atmosphere and ground surface, the effectiveness of which is a function of cover thickness and density (Tyrtikov, 1964; Brown, 1966b;

Balobaev, 1974). Since the accumulation of a snow cover progressively decreases the influence of vegetation in winter, this factor is most significant during the summer. At this season, the incidence of shortwave radiation, is reduced by the presence of vegetation, as a function partly of direct interception by the vegetation, and partly of reflection, due to the albedo characteristics of its surface (Brown, op cit). At night, longwave emission is similarly reduced. Ground heat loss is also increased due to evapotranspiration and sensible heat transfer. The magnitude of this effect again varies with cover density and roughness.

In winter, the vegetation cover may retard ground heat loss, but as has been suggested, the importance of this is minimized as accumulation of the snow cover proceeds.

The distribution of vegetation in the Schefferville area is related to exposure and snow accumulation (Nicholson, 1973). Annersten (1964, Figure 9) has provided data on shallow ground temperatures under different cover types. Coldest temperatures occur under tundra vegetation and bare ground and the warmest beneath lichen woodland. Annersten (1966) suggested that this distribution was related to vegetation only insofar as the cover reflects exposure and snow conditions at the site.

2.123 Snow

The winter snow cover acts as an insulator, interposing a layer of low conductivity between the atmosphere and ground surface (Gold, 1963; Krinsley, 1963). Its overall efficiency, in preventing ground heat losses, is related to snowfall pattern and effective cover period (Brown, 1969). The insulating qualities of the cover vary with depth, density and temperature (Shvetsov, 1964).

A number of equations have been proposed for quantifying the insulating influence of a snow cover (Lachenbruch, 1959; Kudryevtsev, 1965; Gold, op cit). Unfortunately, all three are difficult to apply, and it has been found profitable, in the Schefferville area, to adopt a more empirical approach.

Using a type of degree-oover day approach, Annersten (1964) suggested that a snow depth of 40 cm, during the coldest part of the winter, was critical for maintenance of a perennially frozen condition. From a consideration of extrapolated thermocable surface temperature intercepts, he also proposed an alternative value of 75 cm, placing less confidence in this figure (Annersten, op cit). More recently, Nicholson and Granberg (1973) have derived a critical value of 68 to 78 cm, using a simple linear regression model, which relates mean annual ground temperature to variations in snow depth. This latter critical

value applies, in fact, to peak snow depths but, nonetheless, agrees closely with the second value, proposed by Annersten (op cit). Both Krinsley (op cit) and Mackay and Mackay (1974) record an exponential relationship between minimum winter ground temperature and snow depth.

2.2 ACTIVE LAYER

The active layer is a seasonally freezing and thawing zone which lies between the ground surface and the upper surface of the permafrost table.

2.21 Heat transfer

The thermal regime of the active layer is complex, since this zone is a porous medium, and includes both frozen and unfrozen material, according to season. When the active layer is frozen, heat transfer occurs almost entirely by conduction, as in permafrost (Section 2.3). However, when unfrozen material is present, either as unfrozen active layer or within a talik zone, mass transfer may also be important. Changes in latent heat which accompany freezing and thawing are a further complicating factor.

The general theory of simultaneous heat and mass transfer in porous media which experience a phase change has been considered by Harlan (1971). However, to date, a lack of understanding of the exact processes involved, has made it necessary

to avoid the complexities of the theory in practical considerations of the permafrost thermal regime. Thus, it is either assumed that conductive transfer is dominant (e.g. Lachenbruch, 1959), or an approximation for the mass transfer component is included, for example, by the use of Neumann's solution (e.g. W.C. Brown, 1964).

The present study is not concerned with the active layer per se, nor in more than a general sense, with processes occurring within it. Hence the adoption of a "simple conduction" approach (Heginbottom, 1973) is perhaps appropriate. The mechanisms of conductive and mass heat transfer within the active layer will be discussed separately.

2.211 Conduction

It is usual to consider that solar insolation reaches the ground surface in a symmetrically periodic fashion, generating temperature waves which are transmitted downward with an approximately sinusoidal form (Sellers, 1968). Assuming a surface temperature amplitude, A_o, and an angular frequency of oscillation, ω (equal to $2\pi/P$, where P is period), an upper (surface) boundary condition may be defined as follows:

$$T(0,t) = Ta + A_o \cdot \sin \omega t \qquad (2)$$

where $T(0,t)$ = Surface temperature at time, t

Ta = Average annual ground temperature

If the active layer is considered as a semi-infinite homogeneous medium, with the above boundary condition, ground temperature at any depth and time, T(z,t), is (after Carslaw & Jaeger, 1947):

$$T(z,t) = Ta + A_o e^{-z(\omega/2\alpha)^{\frac{1}{2}}} \cdot \sin\left[\omega t - (\omega/2\alpha)^{\frac{1}{2}} \cdot z\right] \qquad (3)$$

where α is thermal diffusivity, a measure of the temperature change resulting from input of a given amount of heat. Diffusivity is a function of the specific heat (C), density (ρ) and thermal conductivity (K) of the material: $\alpha = K/C\rho$.

Equation 3 indicates that temperature waves, conducted into the active layer and permafrost, attenuate exponentially with depth, and experience a linear lag in phase. The rate at which these processes occur is a function of thermal diffusivity.

2.212 Mass transfer

In addition to conductive transfer, heat is transported, in porous media such as the active layer, via three distinct mass transfer mechanisms (Harlan, 1971). These are: vapour transfer via unfilled pore spaces, liquid transfer through pore spaces under positive hydraulic gradients (e.g. supra permafrost ground water), and liquid transfer, under free energy gradients, via

water films adsorbed on particle surfaces, for example, movement towards freezing fronts (Harlan, op cit.).

In theory, freezing point depression allows mass transfer at temperatures below 0°C (Williams, 1964). Zero curtain (Muller, 1947) evidence, however, suggests that, at Timmins 4, the major part (if not all) of the soil moisture does indeed freeze at 0°C (Nicholson & Thom, 1973). Thus, heat transfer in ground below this temperature, in the Schefferville area, may be considered to occur almost entirely by conduction.

On the other hand, in unfrozen ground, heat transfer by suprapermafrost groundwater, appears to be very important at Timmins 4 (Nicholson & Thom, op cit). Mass transfer is also thought to be responsible for the development of especially deep active layers, and to explain, in large part, the presence of taliks, bodies of perennially unfrozen material, beneath major valleys.

2.22 Thickness of the active layer

Variations in active layer development are mainly a function of the surface boundary condition, and the thermal properties of the ground beneath. The lower boundary of the active layer, corresponding in most instances to the upper surface of the permafrost, occurs where the maximum annual ground temperature is equal to 0°C. In general, active layer thicknesses decrease

with latitude, in response to a reduction in available degree-days of thawing (Brown, 1972b). Spatial variations, however, are also related to anomalies in the surface boundary condition, which result from the influence of environmental factors, in modifying the components of the surface energy balance (subsection 2.12).

The development of the active layer under different conditions is well documented (see, for example: Cook, 1956; Beckel, 1957; Brown, 1965; 1972a; 1972b; Bliss and Wein, 1971; French, 1970; Price, 1971).

2.23 Active layer in the Schefferville area

The spacing of sensors in most existing thermocables is inadequate for detailed studies of the active layer. However, active layer thicknesses of 2 to 4 m were inferred at Ferriman by Annersten (1964, Figure 4). He noted that active layer development was only two-thirds as great on a north-facing slope as on one with a westerly aspect. Thicknesses at Timmins 4 appear to be very variable, averaging about 3 m (Nicholson and Thom, 1973. Table I). Valley sites, affected by groundwater movement, however, have active layers up to 12 m thick. Elsewhere, the greatest development occurs on sparsely-vegetated ridge-tops, which have shallow snow covers and, paradoxically, the greatest frost penetration (Nicholson and Thom, op cit.).

2.3 PERENNIALLY FROZEN GROUND

2.31 Heat transfer

Under most conditions, particularly in the continuous permafrost region the base of the active layer corresponds to the upper boundary of the underlying perennially frozen ground, and is termed the permafrost table (Muller, 1947). The occurrence of talik zones, which constitute an exception in the Schefferville area, is discussed in section 2.5.

Heat transfer in permafrost occurs almost exclusively by conduction. The thermal regime in the upper part, like that of the active layer overlying it, includes a downward transmitted cyclical component, which attenuates rapidly with depth. At the level of zero annual amplitude (Muller, op cit.), z_a, such fluctuations are considered to be negligible. The thermal regime within perennially frozen ground may be described by the Fourier heat conduction law (e.g. Gold and Lachenbruch, 1973). In its one-dimensional form, this important relationship is expressed:

$$q^* = -K.G \qquad (4a)$$

$$\text{or} \quad G = -q^*.K \qquad (4b)$$

where q^* = Terrestrial heat flow or geothermal flux (Wm^{-2})

K = Thermal conductivity: a measure of energy transfer under a given thermal gradient ($Wm^{-1}K^{-1}$)

G = Thermal gradient (= dT/dz)

Thus, gradient varies directly with heat flow, and indirectly with conductivity. By convention, upward heat flow is considered negative, and vice versa.

Without invalidating the steady-state assumption, a more realistic approximation for naturally-occurring geological conditions may be obtained by replacing the single homogeneous layer by a series of such layers. If the magnitude of the terrestrial heat flux is regarded as constant, the gradient then changes inversely with conductivity, such that:

$$q^* = K_1.G_1 = K_2.G_2 = ... = K_n.G_n \qquad (5)$$

where K_n is the conductivity of the n th layer, and G_n the gradient passing through it.

Under steady-state conditions, providing the geothermal flux and variations in conductivity are known and heat flow is essentially vertical, ground temperature is a function only of distance below the level of zero annual amptitude, z_a:

$$T(z) = \frac{q^*}{K} . \quad \Delta z - T(z_a) \qquad (6)$$

where $T(z)$ = Temperature at depth, z

$T(z_a)$ = Temperature at level of zero annual amplitude, z_a

$\Delta z = z - z_a$

This relationship is incorporated into a model, for modelling the ground thermal regime, which is developed in Chapter 4.

2.32 Thickness of permafrost

Under steady-state conditions, and assuming vertical heat flow, the increase in temperature with depth is easily quantified, so that the thickness of the perennially frozen layer can be readily determined. Graphically, the base occurs where a plotted depth-temperature profile intersects the $0^{o}C$ line (see Figure 4). The depth to the base of permafrost, z_p, may also be calculated directly. Thus, rearranging equation 6, and placing $T(z)$ equal to zero:

$$z_p = \frac{K}{q^*} \cdot T(z_a) + z_a \qquad (7)$$

The base of permafrost and its probable configuration are discussed more fully below.

2.4 BASE OF PERMAFROST

2.41 Depth to the lower boundary

The base of permafrost corresponds to the $0^{o}C$ isotherm at depth.

In theory, its position is determined by the relative influence of the geothermal flux, q*, the temperature at the level of zero annual amplitude and ground thermal properties. For practical purposes, the geothermal flux may be assumed constant and, in this case, according to equation 7, the depth to the lower boundary is effectively a function only of the thermal conductivity, and of variations in $T(z_a)$.

The position of the boundary varies spatially in response to these variations, and to some degree also it responds slowly to temporal changes in the surface boundary condition (sub-section 2.61). In both cases, these effects are accompanied by a sizeable phase lag with depth, and are reduced exponentially by attenuation (Kudryavtsev, 1965).

2.42 Configuration of the base of permafrost

The form of the permafrost base in the continuous zone has been modelled by Lachenbruch (1968a, Figure 5), but in the discontinuous zone its configuration is largely conjectural. Only at the southern edge (Johnston et al., 1963; Brown, 1973), near to the ocean (Misener, 1955; Lachenbruch, 1957a; Lachenbruch, Greene and Marshall, 1966), and in parts of the Mackenzie River Valley (Johnston and Brown, 1964; Smith, 1972), has it been possible to approximate the lower boundary in more than one dimension, from measured ground temperatures. On the other

hand, the number of isolated measurements of permafrost thickness is now fairly large (Judge, 1973a, Figure 3).

Only a few thermocables penetrate the permafrost base in the Schefferville area, so that its overall configuration here is also essentially unknown. Extrapolated permafrost depths of approximately 75 m and greater than 100 m have been suggested for the Ferriman Ridge and Timmins 4 sites, respectively, by Annersten (1964) and Nicholson and Thom (1973). There is also evidence to suggest that the lateral margins of permafrost bodies at Timmins 4 are steeply inclined (Nicholson and Thom, op cit.).

In the present study, it is assumed, as a basis for discussion, that the configuration of the base of permafrost in the Schefferville area, is similar to that proposed for the continuous zone by Lachenbruch (1968a, Figure 5). It is seen as a low-amplitude mirror image of the surface relief, modified by the influence of the surface drainage pattern.

2.5 TALIK ZONES

The development of especially deep active layers in valley sites at Timmins 4 has been noted in sub-section 2.23. These are generally associated with areas of deep snow accumulation. However, when ground water movement is also significant, a sufficiently

large temperature anomaly may be created as to result in the formation and preservation of a zone of perennially unfrozen material. Such zones are termed taliks, and usually located between the active layer and permafrost table. Nicholson and Thom (1973, Figure 6) have given a section across the main talik zone at Timmins 4.

2.6 DISTURBANCES TO THE THERMAL REGIME

In the preceding sections, and, for the most part, in the pages which follow, it is convenient to assume a steady-state, one-dimensional conduction model as an approximation for the ground thermal regime. With the limited data available, this approach is generally adequate. At the same time it is constructive to consider two forms of disturbance to the ground thermal regime, with which such a model is unable to deal satisfactorily: temporal changes in the surface boundary condition; and, lateral heat flow. Both topics have already been treated more comprehensively than is possible here, (e.g. by Gold & Lachenbruch, 1973), and need be discussed only briefly.

2.61 Temporal changes in the surface boundary condition

Changes in mean surface temperature, due to climatic fluctuations (Birch, 1948; Jessop, 1971), or surface disturbance (e.g. Linell, 1973), cause variations in the thermal regime as the steady-state equilibrium is restored. The effects of

positive and negative temperature changes on the underlying profile, termed degradation and aggradation, are shown in Figure 5. In terms of simple conduction theory, the restored profile, following a change in surface temperature from $-T_o$ to $(-T_o + \Delta T)$, has the form:

$$T(z) = \frac{q^*}{K} \cdot z - T_o + \Delta T \qquad (8)$$

where $z \geq z_a$. Temperature variations such as these lead eventually to aggradation or degradation at the base of permafrost by an amount equal to $\Delta T/G$.

Annersten (1964) contended that there was evidence for active degradation of the permafrost at Ferriman. More recent data from this site, and information from the Timmins area, do not support this view (Nicholson & Thom, 1973).

2.62 Lateral heat flow

Non-vertical heat flow due to lateral variations in the surface boundary condition is a more fundamental problem. According to the theory of potential flow, the effect of a positive temperature anomaly, in this instance a generally warmer zone within an area which is generally colder, is to cause a conductive, often non-vertical, flow of heat between the two, from warmer to colder.

At Timmins 4, positive surface temperature anomalies are generally related to the insulating effects of deep snow

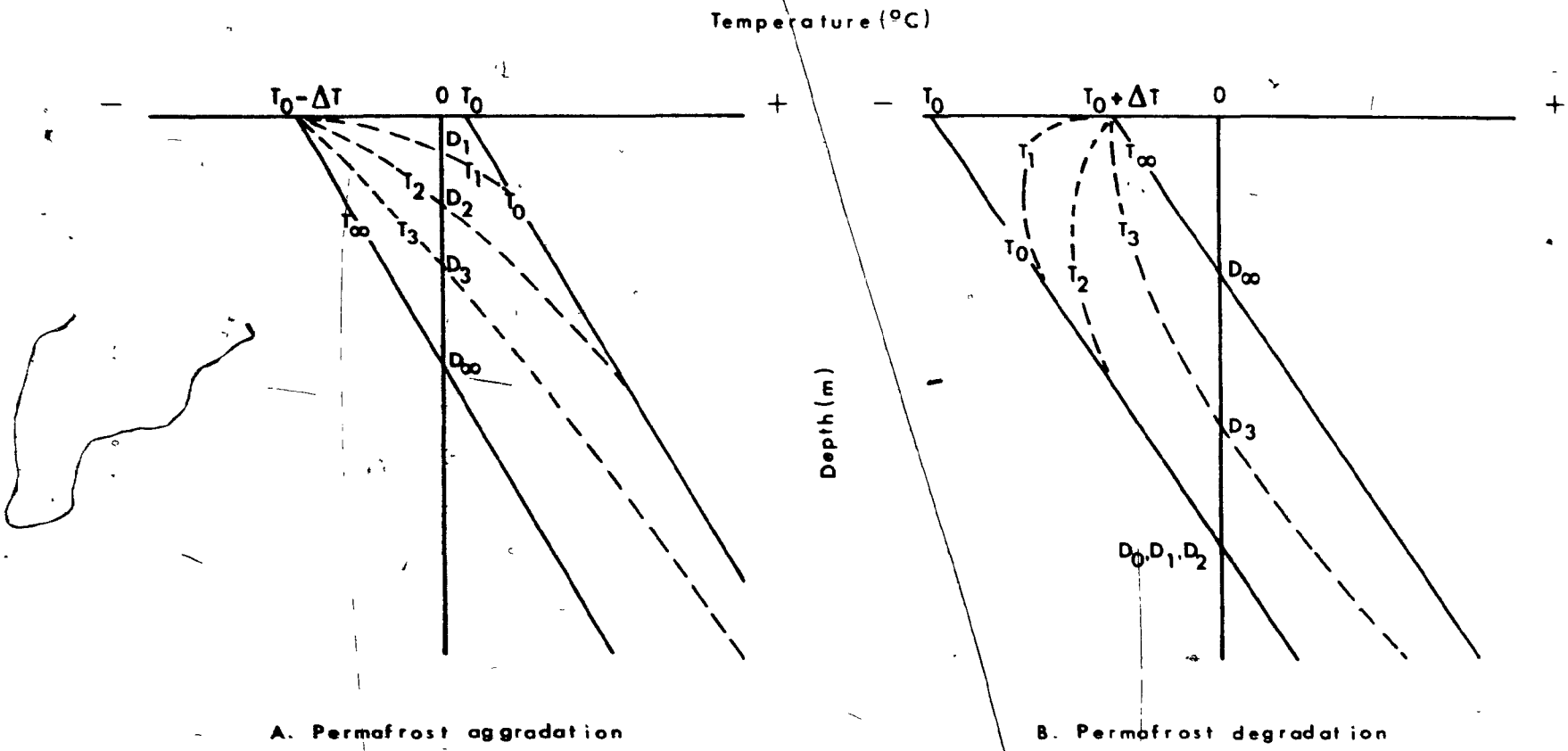

Figure 5: Aggradation and degradation of permafrost (after Lachenbruch, 1968a. Figures 2 and 3). Following an increase or decrease in surface temperature from T_o to $T_o \pm \Delta T$, the ground temperature equilibrium is regained via a series of intermediate curves, e.g. T_1, T_2, T_3, resulting in corresponding changes in permafrost thickness (D_1 to D_∞).

(Granberg, 1973). Such accumulations of snow are confined to valley sites, where the size of the anomaly may also be influenced by the effects of mass transfer, via suprapermafrost groundwater. This situation has been illustrated in a section across the site, Timmins 4 by Nicholson and Thom (1973, Figure 6). The approximately vertical isotherms and associated horizontal heat flow lines should be noted.

Negative surface temperature anomalies may be caused by relief, but are generally of negligible magnitude unless the scale of the relief is extremely large (Lachenbruch, 1968b). In the Schefferville area, negative anomalies do appear, superficially, to be related to relief, but, in fact, are generally a function of variations in snow distribution (sub-section 2.121).

CHAPTER 3

COLLECTION OF GROUND TEMPERATURE AND ENVIRONMENTAL FACTOR DATA

3.1 SAMPLING DESIGN

Sampling design is normally the first stage in data collection for any project. However, in this case, the major financial investment involved in drilling (thousands of dollars per hole) meant that existing installations (thermocables) had to be utilized in collection of ground temperature data. Ideally, some form of random sampling design should be employed. Unfortunately, the thermocable sites at Timmins 4 are randomly located only insofar as an attempt was made, during their installation, to sample as many apparently contrasting ground temperature conditions as possible. This was logical at the time but forms a complication as far as data collection for the present study is concerned. The environmental factors were sampled around sites where temperature data were available. The factors were evaluated at more than one scale where feasible.

3.2 GROUND TEMPERATURE

Twenty-six thermocables were installed, to depths of 10m to 110m, at the Timmins 4 site, between 1968 and 1972 (Nicholson and Thom, 1973). Temperature data from twenty-one of these are included in the present analysis. The remaining five cables, installed for a

permafrost amelioration project, are not strictly comparable and have been omitted. The locations of cables 1 to 20 and 25 are shown in Figure 3.

3.21 Collection of data

Temperature sensors of two types have been employed in thermocable construction at Timmins 4. Cables 1 to 17, installed in 1968 and 1970, contain copper-constantan thermocouples, which are read using a Honeywell potentiometer (Thom, 1970). Published (1938) calibration tables are available for conversion to degrees Fahrenheit, but to avoid introducing unnecessary inaccuracy during further conversion to degrees Celsius for use in this study, a computer program was written which permits direct conversion from the raw EMF data. This makes use of a fourth-order minimax polynomial function, after Shirtliffe (1971). An accuracy of $\pm$ 0.1°C is claimed for means of series of thermocouples readings from the Timmins 4 site (Nicholson and Thom, 1973).

Thermistors have been used in thermocables installed since 1970 (Nicholson and Thom, op cit.). Resistance measurements are made using a modified Wheatstone bridge, developed by the Earth Physics Branch, Ottawa, and converted to degree Celsius, by means of tables generated using a curve fitting program, written by Dr. A. Jessop, of the same Branch. Nicholson and Thom (op cit.) claim an accuracy of up to $\pm$ 0.01°C for thermistors

TABLE II

MEASURED AVERAGE ANNUAL GROUND TEMPERATURES, TIMMINS 4

Cable No.	$T_{1.5m}$	$T_{2.5m}$	T_{5m}	$T_{7.5m}$	T_{10m}	$T_{12.5m}$	T_{15m}	T_{20m}	T_{25m}	T_{30m}
1	-0.841	-0.757	-0.496	-0.238	-0.192	-0.139	-0.108	-0.077	+0.058	+0.144
2	-1.377	-1.144	-0.850	-0.612	-0.526	-0.461	-0.402	-0.349	-0.318	-0.288
3	-2.255	-1.800	-1.299	-1.217	-1.208	-1.152	-1.021	-0.940	-0.814	-0.739
4	-0.002	-0.063	-0.242	-0.378	-0.478	-0.538	-0.571	-0.593	-0.597	-0.583
5	+0.798	+0.749	+0.659	+0.578	+0.428	+0.329	+0.176	-0.039	-0.194	-0.284
6	-2.839	-2.483	-2.122	-1.978	-1.836	-1.766	-1.578	-1.431	-1.254	-1.145
7	-1.637	-1.494	-1.329	-1.299	-1.228	-1.147	-1.116	-1.042	-0.905	-0.824
8	+0.640	+0.531	+0.225	-0.052	-0.178	-0.262	-0.298	-0.318	-0.321	-0.323
9	+1.251	+0.851	+0.442	+0.158	-0.051	-0.129	-0.199	-0.280	-0.323	-0.347
10	+0.708	+0.669	+0.766	+0.862	+0.928	+0.982	+0.912	+0.818	+0.744	+0.711
11	+1.026	+1.034	+1.140	+1.169	+1.140	+1.082	+1.030	+0.910	+0.808	+0.739
12	-1.568	-1.576	-1.284	-0.998	-0.766	-0.615	-0.510	-0.428	-0.372	-0.270
13	+0.930	+0.908	+0.844	+0.784	+0.708	+0.628	+0.546	+0.419	+0.308	+0.242
14	-2.280	-2.236	-2.159	-2.051	-1.950	-1.836	-1.720	-1.525	-1.340	-1.175
15	+0.229	+0.172	+0.105	+0.059	-0.030	-0.127	-0.160	-0.490	-0.642	-0.728
16	-5.000	-4.428	-3.778	-3.247	-2.798	-2.469	-2.169	-1.855	-1.635	-1.496
17	+0.363	+0.294	+0.111	+0.024	-0.066	-0.143	-0.218	-0.288	-0.339	-0.309
18	+0.240	-0.860	-2.190	-1.395	-0.710	-0.555	-0.343	-0.288	-0.162	-0.095
19	-0.890	-1.500	-2.095	-1.918	-1.899	-1.782	-1.658	-1.359	-1.229	-1.242
20	+0.030	-0.970	-2.008	-2.316	-2.116	-1.982	-1.690	-1.495	-1.290	-1.090
25	-4.000	-3.740	-2.830	-2.560	-2.380	-2.228	-2.071	-1.805	-1.565	-1.295

installed in thermocables at the Timmins 4 site.

3.22 Compilation of temperature variables

All thermocables at Timmins 4 have been read on at least a monthly basis since installation (Nicholson and Thom, 1973). Mean annual temperatures were compiled from these data using the means of monthly means for individual sensors in each cable. The original measurement depths vary but data for ten standard depths, from 1.5m to 30m, were obtained by interpolation (see Table II). In the case of a number of very shallow thermocables, it was necessary to extrapolate with respect to neighbouring deeper cables, so as to ensure that a full 30m profile was available for use in the analysis.

3.3 SNOW

Attempts to make use of the well-documented relationship between ground temperature and snow as a basis for permafrost prediction in the Schefferville area have been hampered, until recently, by the difficulties associated with accurate mapping of the cover, over sufficiently large areas. Granberg (1972, 1973) has pioneered two methods by which this may be accomplished. One, a model relating snow accumulation to terrain roughness, provided snow data for the prediction model developed by Nicholson and Granberg (1973); the other approach, production of large-scale snow maps from sequential aerial photography, taken at intervals

through the melt period, is employed here.

3.31 Preparation of a snow map from sequence melt photography

Figure 6 shows the maximum or "peak" snow accumulation pattern for the Timmins 4 site, during winter 1971-72. This map was compiled by superimposing snow boundaries from aerial photographs taken on a series of flights during the 1972 and 1973 melt season. The first map of this type was produced, from oblique photographs, by Granberg (1972, Figure 24). The present map (Figure 6) differs in that it is the first to be compiled using vertical photography. Implicit in production of both maps is the assumption that, due to the generally cloudy climatic conditions during the snowmelt (i.e. minimum of direct solar radiation), snowmelt is relatively uniform (Granberg, 1973).

3.311 Aerial Photography.

Information concerning the five aerial photography flights over the Timmins area is summarized in Table III. On each occasion, a de Havilland Beaver aircraft was used, flying at an altitude of approximately 3050m (10,000 ft) above the terrain, i.e., about 3660m (12,000 ft) above sea level. Photographs were taken through a hole in the floor of the aircraft, using a hand-held Bronica S2, 6cm x 6cm format, camera loaded with Kodak Tri-X Professional film. With this arrangement, an area of approximately 13.4 square

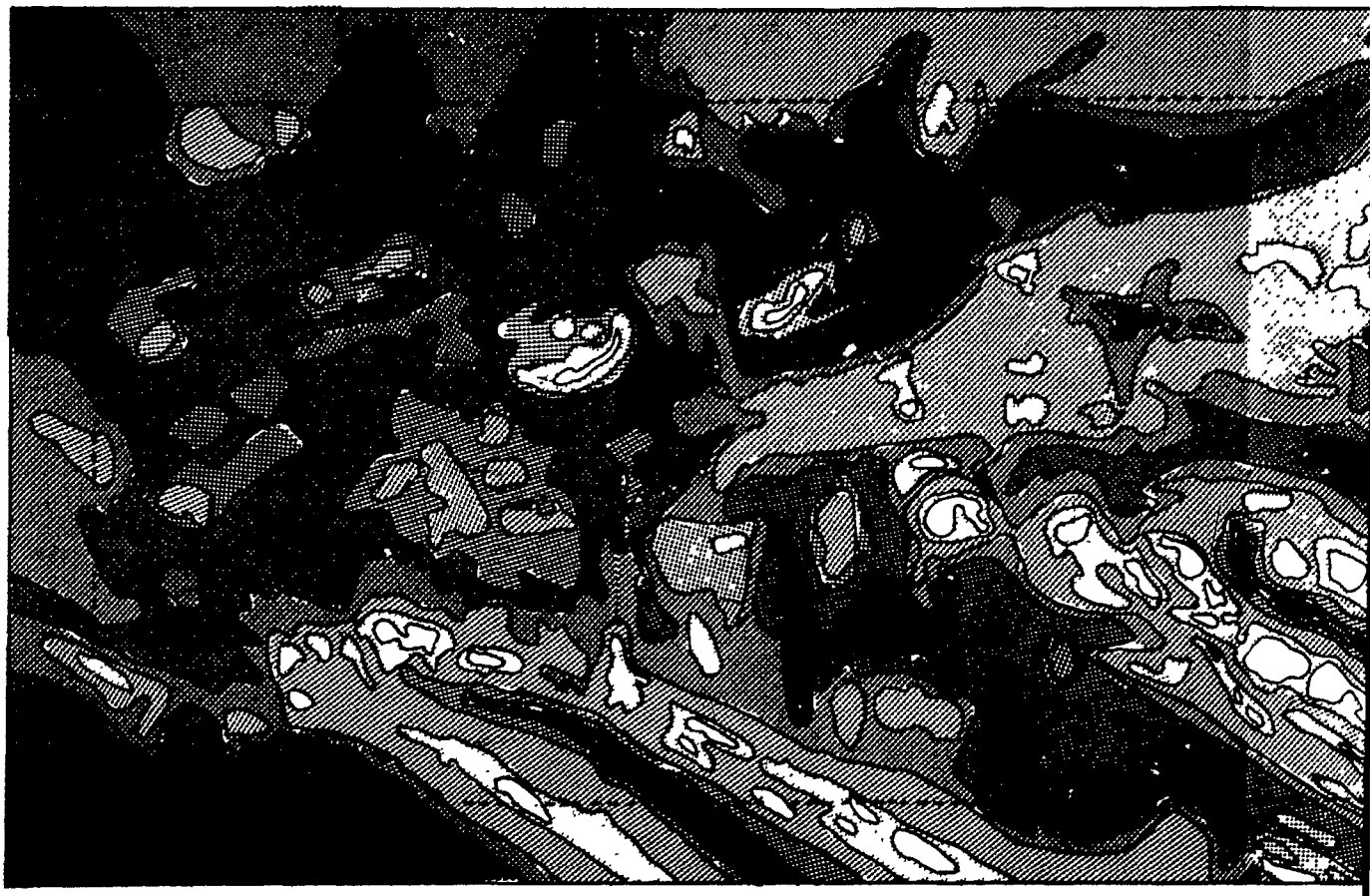

FIGURE 6

SNOW DEPTH MAP FOR TIMMINS 4 : WINTER 1971-72

< 2 cm	48 – 100 cm
2 – 16 cm	100 – 123 cm
16 – 48 cm	> 123 cm

0 — 100 m

kilometers, i.e. 3660m by 3660m, is included in each frame. The time interval between exposures was chosen so as to provide an overlap of approximately 60 percent between frames, to allow stereoscopic viewing. Photomosaics of the frames used in compilation of Figure 6 are reproduced here as Plates 1 to 5.

Aircraft availability and access problems, during the latter part of the 1972 melt season curtailed the photography program. This necessitated a further flight in 1973, which allowed the later portion of the melt sequence to be monitored.

3.312 Production of snow cover map.

A Ryker, model L-1, vertical sketchmaster was used to transfer snow boundaries from individual photographs to a copy of the 1:1200 scale topographic plan (Figure 2), which was used as a base map. Some enlargement of the imagery was necessary due to scale differences between photographs from different flights, and between the photographs and base map. Thermocable shacks, roads and surface drainage features were employed as ground control during rectification. Nonetheless difficulty was experienced close to the edge of the individual photographs due to distortion in these areas. The whole procedure took approximately one week.

3.313 Quantifying the mapping classes.

Values were assigned to snow depth categories on the map, using a

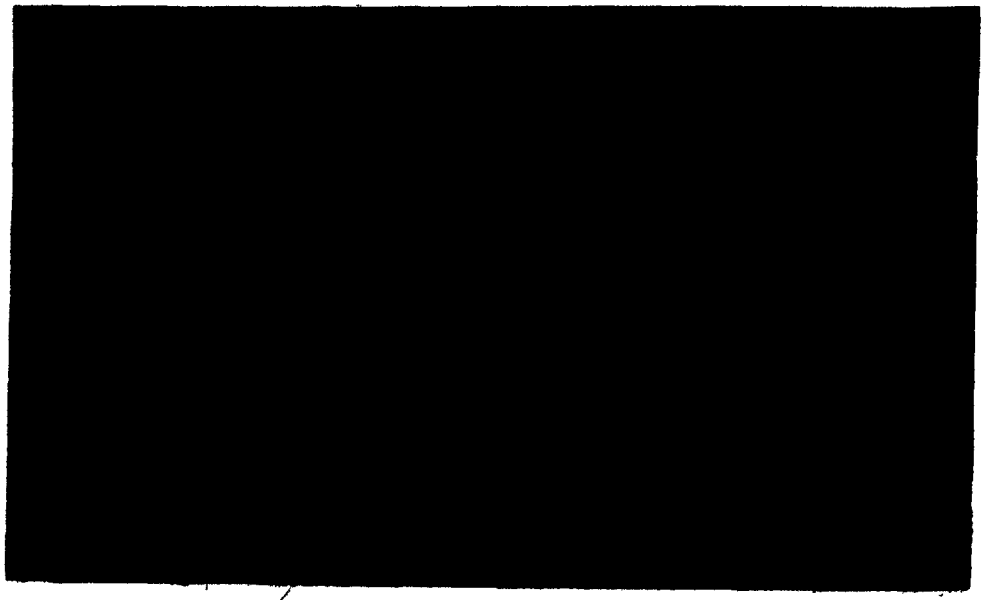

Plate 1: Snow distribution at Timmins 4, 27 April 1972

Plate 2: Snow distribution at Timmins 4, 16 May 1972

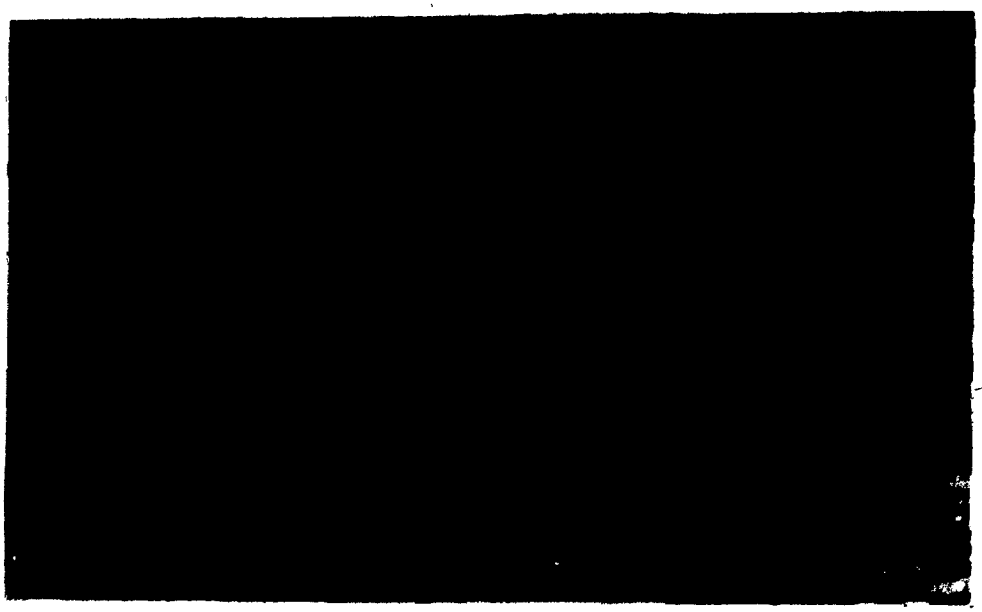

Plate 3: Snow distribution at Timmins 4, 30 May 1972

Plate 4: Snow distribution at Timmins 4, 6 June 1972

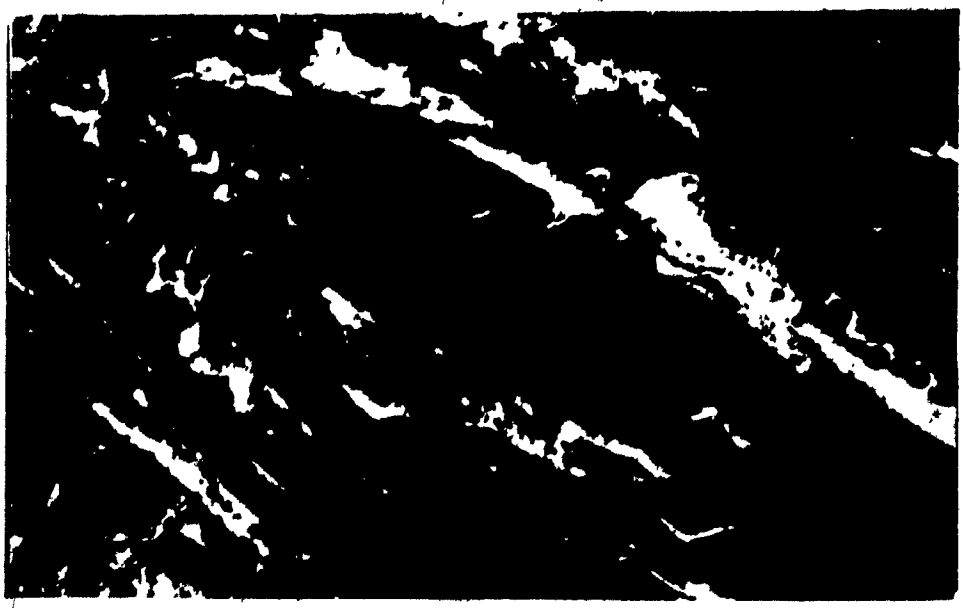

Plate 5: Snow distribution at Timmins 4, 18 May 1973

variant on the procedure adopted by Granberg (1972). For flights 1 to 4, in 1972, each isoline on the completed map was assumed to have a value equivalent to the mean of "peak" snow readings (taken as April 15th, 1972), on the Timmins 4 snow course (Figure 3), for the stakes melted out prior to that particular flight. A somewhat different approach was required for the additional flight in 1973. In this instance, the value assumed is the mean of 1972 peak values for all stakes in the area melted bare prior to the flight in 1973. Values obtained in this way, together with intermediate values assigned to the areas between isolines, are listed in Table III. The procedure is illustrated graphically in Figure 7, while peak and melt period readings of the Timmins 4 snowcourse are given in Appendix I.

3.32 Accuracy of the Timmins 4 snow map

A subjective comparison between Figure 6 and snow maps compiled previously for this site from sequence melt photographs (e.g. Granberg, 1972, Figure 24), suggest that the overall snow distribution pattern usually varies little from year to year, despite wide variations in total snow fall. This would seem to confirm the general validity of the present approach.

It is more difficult to arrive at an estimate of the absolute accuracy of values assigned to individual depth

TABLE III

TIMMINS 4 SNOW DEPTH CATEGORIES

Flight No.	Date	Category Number	Value assigned (cm)
		1	0
1	27 April 1972	2	2
		3	9
2	16 May 1972	4	16
		5	32
3	30 May 1972	6	48
		7	74
4	6 June 1972	8	100
		9	112
5	18 May 1973	10	123
		11	135

TABLE IV

COMPARISON OF ASSIGNED AND OBSERVED SNOW DEPTHS

Snow map category	Assigned mean depth for map category (cm)	Observed mean depth from stakes within category (cm)
1	0	17
3	9	38
5	32	45
7	74	74
9	112	106
11	135	132

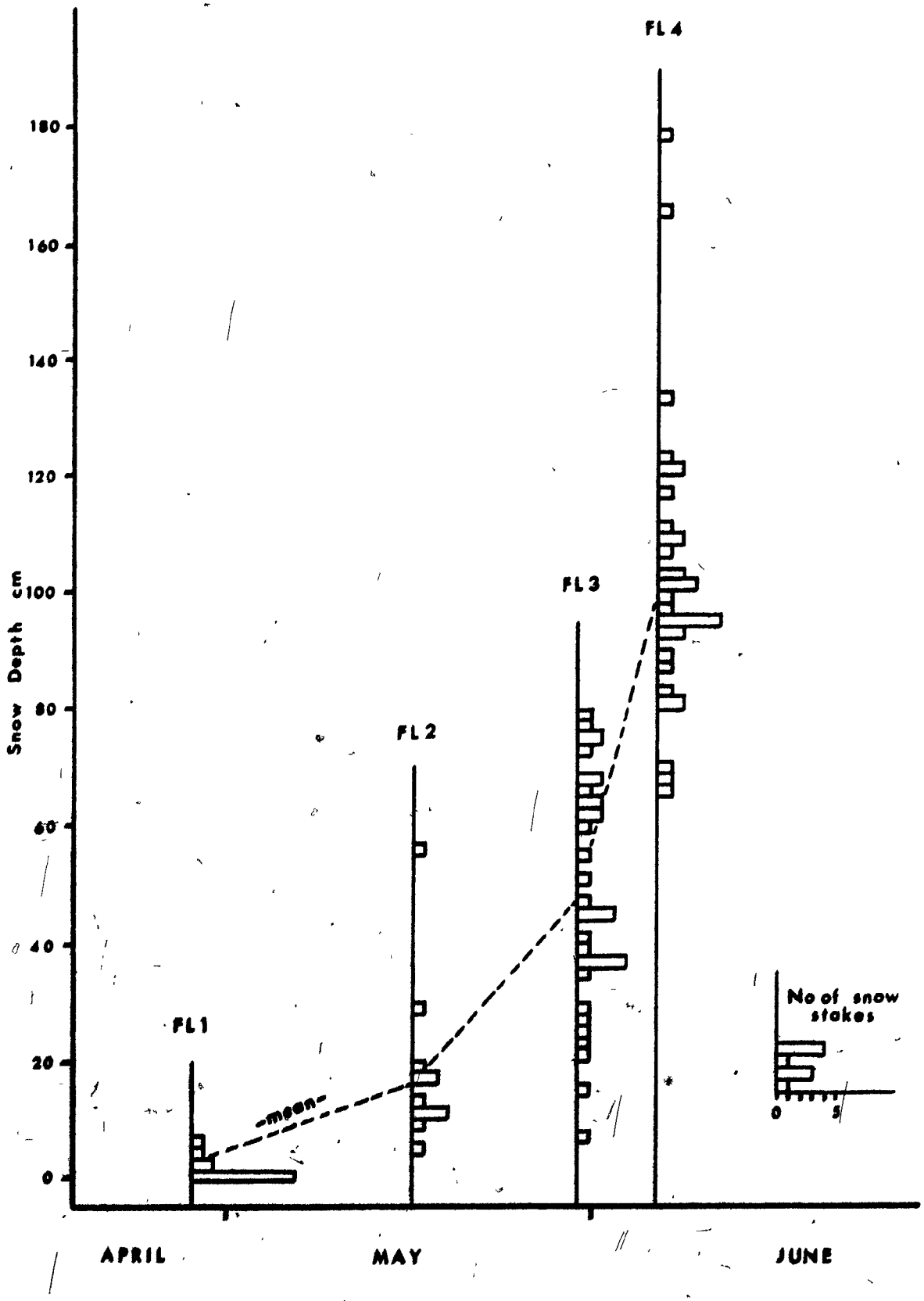

Figure 7: Snow depths on 15 April, 1972 (Peak snow) for stakes melted bare between flights.

categories on the snow map (Table III). One approach is to compare the values obtained from the map with mean peak snow depths for actual sites. Such a comparison is presented in Table IV.

Table IV shows that computed and observed peak snow depths correspond most closely in the deeper depth categories. This is encouraging since the w/a values, i.e. the snow depths which correspond to a mean annual ground temperature of 0°C (sub-section 2.231), fall within this depth range.

For categories 1 and 3, and to some extent category 5, the correspondence is not as good (Table IV). This is believed to be due to the fact that these categories include only a small number of snow stakes, so that the influence of isolated deep snow sites, as well as plotting errors during construction of the map and real errors inherent in the method, is proportionally much greater.

3.33 Compilation of the snow depth variables

Variables representative of average peak snow depth were compiled for each thermocable site, and for circles of increasing radius around the cable-head. The procedure adopted is similar, in a number of respects, to that employed by Nicholson and Granberg (1973).

3.331 Collection of data.

The snow depth map produced for Timmins 4 (Figure 6) was sampled at forty-one points around each thermocable site. Sampling points were arranged, six metres apart, in an orthogonal cross centered on the thermocable and aligned parallel to the map grid, which is also parallel to the terrain (Figure 3). This sampling design, which is illustrated in Figure 8, is intended to ensure that variations is snow depth, both parallel and perpendicular to the topography, are monitored. An integer value was recorded at each sampling point. This corresponds to the depth category within which the point falls on the snow map.

3.332 Compilation of variables.

Average peak snow variables were compiled for circles of differing radii about each thermocable site using cross data collected as described above. First, the cable-head integer value was converted directly to an equivalent snow depth in centimetres. Mean values were then computed for each 6 m interval, in sequence outwards from the cable head to 60 m, using the four values recorded for the interval together with all those closer to the cable. Taking the 18 m mean snow depth variable as an example, the sum of all values recorded for the 18 m, 12 m and 6 m intervals as well as the cable-head, was divided by thirteen: the number of sampling points (see Figure 8). Eleven snow depth variables, representing average snow conditions over circles of radii 5 m,

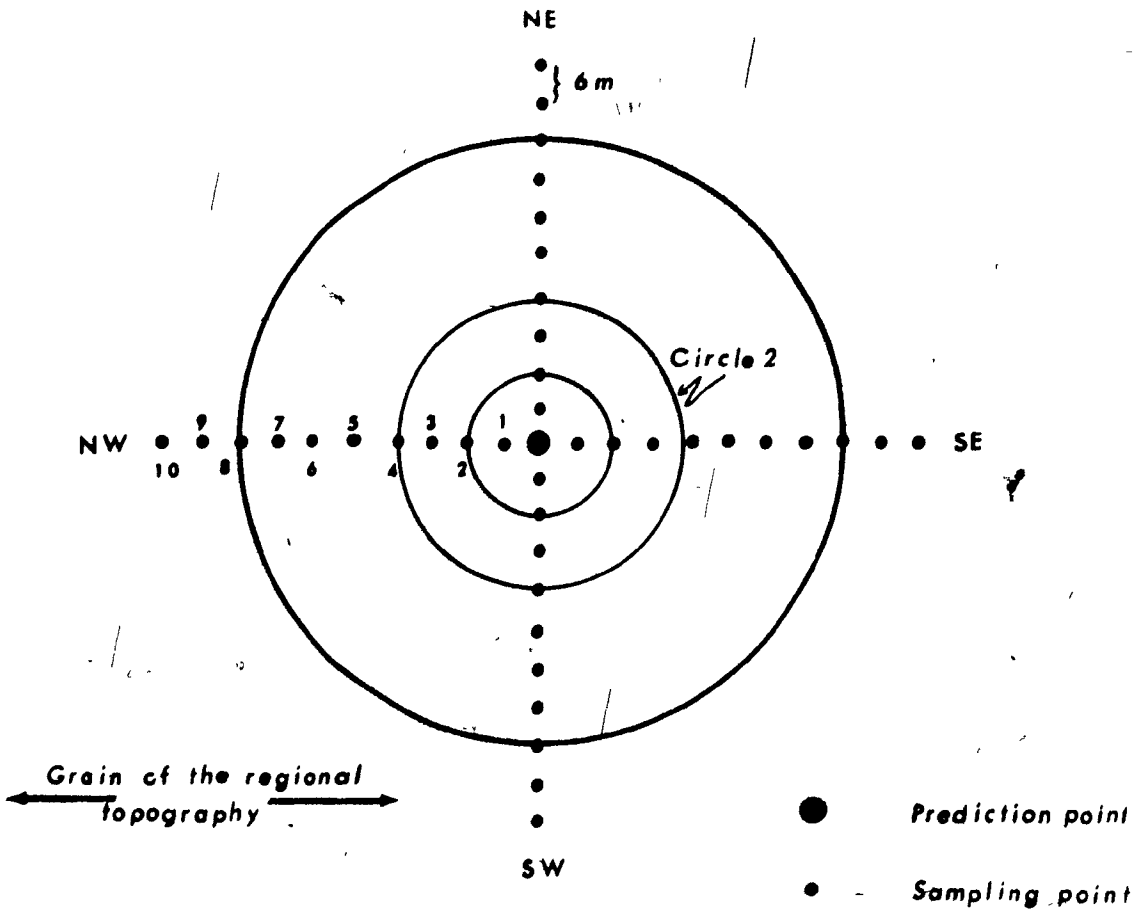

Figure 8: Sampling grid adopted for collection of snow and other environmental factor data. Mean snow depth over any circle around the prediction point is computed as the mean of all values falling within this circle. Thus, for circle 2 the mean depth is:

$$\bar{S} = \frac{SCH + \sum_{j=1}^{4} (NE_j + SE_j + SW_j + NW_j)}{n}$$

where n is the number of sampling points included (=17).

7.5m, 10m, 12.5m, 15m, 20m, 25m, 30m, 40m, 50m, and 60m, were then obtained by interpolating linearly between values computed for the different intervals. Figure 9 shows the plots of mean snow depth versus circle radius for each cable location, from which the interpolated values were obtained.

3.34 Discussion

It will be apparent that the computational procedure, described above, weights sampled snow depth values equally regardless of their distance from the cable-head. However, each set of four points at varying distances from the cable may be considered to represent the area of a ring around the cable. The area of each ring increases in proportion to the square of its distance from the cable. Thus, the snow variables compiled here, in effect, bias the mean towards those values nearest the cable. Theoretically, this is not undesirable since it produces a weighting which approaches a solid angular weighting. Lachenbruch (1957b) indicates that this should be the true situation for the influence of a surface thermal disturbance on a point at depth. To further evaluate this problem, variables were also compiled which weighted the snow depths according to ring area. The resulting correlations with ground temperature, though slightly lower in all cases, were significant at the same high level. The original variables were, therefore, retained.

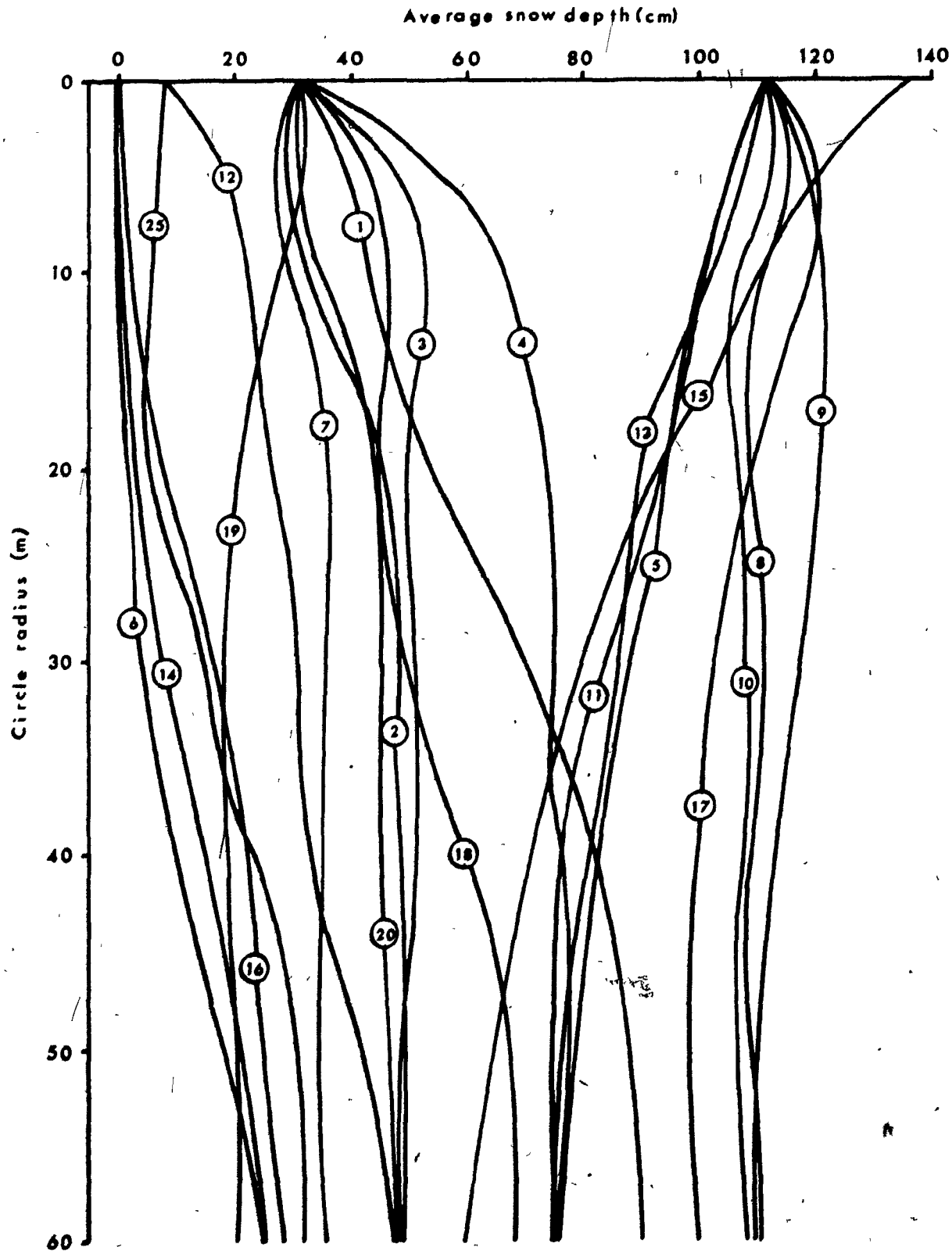

Figure 9: Average snow depth versus circle radius for thermocables at Timmins 4

3.4 RELIEF VARIABLES

In the Schefferville area, topography and the occurrence of permafrost appear, superficially at least, to be closely related. To test this hypothesis, seven different indices of relief were evaluated using data collected from the 1:1200 topographic plan of Timmins 4 (Figure 2). For each thermocable, the site elevation was obtained by interpolating between contours on Figure 2, a procedure which provides an accuracy of at least ± 2.5m (the contour interval). However, it is likely that an accuracy of ± 0.3m or better, is obtained in most instances. An index of topographic shape was computed as the difference between site elevation, and the mean elevation of the surrounding terrain. The latter was computed, by analogy with compilation of snow variables (see Figure 8), over circles of radii 20m and 30m, centered on the cable-head. Thus, a hill or ridge site has a high positive convexity index, while the reverse is true of valley sites. Slope and aspect variables were compiled with reference to an assumed plane passing through the cable-head, and intersecting the terrain at some distance up and down slope. This variable was also compiled at two scales, with respect to planes of lengths 20m and 30m.

3.5 VEGETATION VARIABLES

In collection of vegetation data, an attempt was made to derive a series of variables representative of the percentage coverage

of different vegetation types around each thermocable. Five classes of vegetation were considered:

i Bare ground
ii Moss
iii Lichen
iv Vascular plants
v Brush, i.e. Betula spp.

The percentage coverage of each class within a series of one metre quadrats, located at 3 m intervals outwards from the cable-head (in four directions, along the arms of a cross, located orthogonally to the terrain), was recorded for each thermocable site. This sampling design is very similar to that adopted in collection of snow data and is shown in Figure 8. Mean values for circles of radii 6 m and 12 m were then compiled using a procedure analogous to that employed in deriving the snow depth variables (sub-section 3.23). Lastly, a further vegetation variable was synthesized by the addition of the percentages of bare ground and lichen for the 12 m circle.

3.6 GROUND THERMAL PROPERTIES

The thermal characteristics of the lithological units which comprise the Knob Lake Group are not well documented. Diffusivity values have been quoted by both Annersten (1964) and Nicholson and Thom (1973), while Yap (1972) has considered conductivity changes with temperature. However, all these

studies were concerned with the properties of iron-rich, generally ore-grade, material. Thermal conductivity data are required for all major units within the Knob Lake Group, both iron-rich and iron-poor, if even simple steady-state conduction models are to be developed.

It is fortunate, therefore, that it was recently possible to have thermal conductivity determinations made on samples of the main rock types present in the Schefferville area, by Dr. A. Judge of the Earth Physics Branch, Ottawa (personal communication). Dr. Judge kindly consented to carry out this work on a series of samples submitted by the author. It should be noted that in this region leaching of silica and iron enrichment have been very important in formation of soft iron ores. Slight variations in the amount of leaching and enrichment result in a wide variety of rock types, each having slightly different thermal properties, depending on its relative iron and silica content. It is believed that the samples, which were collected with the assistance of Jim Orth, a geologist with IOCC, are representative, insofar as this was practical.

3.61 Conductivity data

The thermal conductivity, K, determinations, made by Dr. Judge, are presented in Table V. For each rock type, an unfrozen K value was obtained using a modified "divided-bar" apparatus of the type illustrated by Judge, 1973b (Figure 14). The corresp-

TABLE V

THERMAL CONDUCTIVITY DETERMINATIONS, KNOB LAKE GROUP

(Dr. A. Judge, personal communication)

Rock type	Sample Location	Rock conductivity -unfrozen ($Wm^{-1}K^{-1}$)	Rock conductivity -frozen ($Wm^{-1}K^{-1}$)	Mean ($Wm^{-1}K^{-1}$)
Lower Lean Chert	Barney	6.36	6.36	6.36
Upper Red Cherty Iron Formation	Barney	7.16	7.53	7.35
Pink Grey Cherty Iron Formation	Goodream	5.97	6.10	6.04
Lower Red Cherty Iron Formation*		6.56	6.81	6.67
Lower Iron Formation	Timmins 4	4.03	5.18	4.61
Silicate-Carbonate Iron Formation	Burnt Creek Mine	1.89	2.29	2.09
Ruth Slate	Timmins 4	3.18	4.08	3.63
Wishart Quarzite	Barney	5.84	5.90	5.87
Fleming Chert Breccia	Knob Lake Ridge	6.05	6.08	6.07
Denault Dolomite	Knob Lake Ridge	4.98	4.98	4.98
Attikamagen Slate	Schefferville (townsite)	2.22	2.22	2.22
Blue Ore	Timmins 1 Mine	6.92	7.86	7.39
Red Ore	Redmond 1 Mine	4.73	5.73	5.23
Yellow Ore	Burnt Creek Mine	6.89	8.34	7.62

* Determination not made, K value estimated as mean of URC and PGC values.

onding frozen K values were computed indirectly, by assuming a "geometric" model for the conductivity of a porous medium (Woodside and Messmer, 1961).

3.62 Compilation of conductivity variables

Harmonic mean conductivities were computed for the geological units present within ten depth intervals beneath each site, i.e. between the surface and each of the standard depths, listed in Table II. The harmonic mean weights each lithological unit according to its intersected thickness within the interval of interest, thus:

$$\overline{Kz} = \sum_{i=1}^{n} \frac{K_i \cdot \Delta z_i}{z} \qquad (9)$$

where, $\overline{Kz}$ is the mean conductivity for the depth interval between the surface and depth z, and K_i and Δz_i are the thermal conductivity and thickness, respectively, of the i th lithological unit.

In compiling conductivity variables for the present analysis, use was made of the average of the frozen and unfrozen K values for each rock type (Table V). It was then unnecessary to consider temporal variations in the proportions of frozen and unfrozen ground, which result from changes in active layer thickness. Additionally, if a definite frozen or unfrozen value

was used to develop relationships, it would not be possible to use these later for prediction without prejudging the prediction. The thickness of each rock type intersected beneath different thermocable sites was estimated from a geological interpretation, compiled for the Timmins 4 site, by the author. This interpretation is based on the most recent Iron Ore Company 1:1200 scale surface geology plan, and information on the probable geometry of the Timmins 4 (Elross 1) ore-body, derived from Stubbins et al. (1960, Table 3). No allowance was made for the presence of overburden, due to a lack of definite information and the indication that it is thin over much of the site.

3.63 Validity of the conductivity variables

In absolute terms, the thermal conductivity determinations presented in Table V are believed to be accurate to within ±5 percent (A. Judge, personal communications). However, the accuracy of the conductivity variables compiled therefrom may be questioned on three counts:

i. With only one determination per rock unit, in most instances, it is likely that this value may not be fully representative of the different rock types as a whole.

ii. In the absence of accurate plans and sections, it is difficult to judge the validity of the geological interpretation used as a basis for compilation of the conductivity variables.

iii. For practical reasons, a single harmonic mean value was used, when in reality there is considerable geological variation, even within a single lithological unit.

It is difficult to gauge either the relative importance of these factors, or the extent of their influence. However, it is probable that the first and third are less important than the second.

3.7 GROUNDWATER VARIABLES

There is evidence for supra-permafrost groundwater movement at Timmins 4, both in the morphology of thermocable profiles, and in the presence of talik zones beneath the major valleys. (Nicholson and Granberg, 1973 Figure 6). However, work has only recently begun to provide information on the magnitude and configuration of such flows (J. Lewis, personal communication). Observations by the author, of conditions where talik zones are intersected during open-pit mining operations, indicate that groundwater flows occur most importantly within steep-sided talik zones of limited lateral, though often considerable vertical, extent.

In the light of these observations, a series of 19 variables was compiled to represent the influence of groundwater at the different thermocable sites. As a simplification, it was assumed that this effect might be represented by some function

of discharge within or beneath the nearest drainage channel (talik), Q, and of distance from this channel, d. Discharge, in turn, was considered to be related to the area of the drainage basis located "upstream" from the cable. Each of the variables was an arithmetic combination of the two factors, for example: $Q.d$, Q/d, $Q.d^2$, Q/d^2, $Q.d^{\frac{1}{2}}$, $Q/d^{\frac{1}{2}}$ etc. It will be apparent that each variable, computed in this fashion, is a linear combination of the others. The variable giving the highest correlation with ground temperature is discussed in the next chapter.

CHAPTER 4

QUANTIFYING THE RELATIONSHIP BETWEEN GROUND TEMPERATURE AND THE ENVIRONMENTAL FACTORS

4.1 INTRODUCTION

The environmental parameters may be grouped according to the manner in which they affect ground temperatures. One set, most importantly relief, snow cover and vegetation, modifies the thermal regime via the micro-climatic fluxes which control surface temperature. The other set determines the temperature distribution with a given surface boundary condition (ground thermal properties, which affect conduction, and groundwater movement influencing mass transfer effects). This chapter is concerned with a quantitative assessment of the relationship between the environmental parameters and average annual ground temperature at different depths. This will be accomplished by means of an examination of the linear correlation coefficients which describe the different relationships.

It is impossible to make statistically-valid inferences based on these results, for reasons both of small sample size and of non-normality of the different variable distributions. However, the general conclusions which can be drawn do facilitate comparison with previous results, and provide the basis for a later evaluation of multiple regression equations.

4.2 EXPECTED AND OBSERVED CORRELATIONS WITH GROUND TEMPERATURE

Linear correlation coefficients were computed to describe the relationships between ground temperature at all levels and the various environmental factors. These results are given in Table VI, and a discussion of the data is presented in the following sections.

4.21 Correlations with relief

Ground temperature conditions often seem to be closely related to relief (sub-section 1.21), and the relief variables considered here, as expected, exhibit negative correlations with ground temperature (Table VI). For example, the coefficients with elevation increase with depth, whereas those with site convexity show the opposite trend. The indication is, therefore, that elevation is a large-scale surface influence variable, affecting deeper temperatures, while the convexity variable chosen is more important on a small scale, since it is most closely correlated with shallow temperatures. Below 7.5m depth, the correlations with elevation are all significant at the 99 percent level or better.

The values of the coefficients with slope and aspect are all low or very low. This is contrary to what might be expected from the literature (e.g. Brown, 1969), but is probably due to the fact that the Timmins 4 site does not exhibit great var-

TABLE VI

LINEAR CORRELATION COEFFICIENTS BETWEEN GROUND TEMPERATURE AND THE ENVIRONMENTAL PARAMETERS

	$T_{1.5m}$	$T_{2.5m}$	T_{5m}	$T_{7.5m}$	T_{10m}	$T_{12.5m}$	T_{15m}	T_{20m}	T_{25m}	T_{30m}
Relief variables										
ELEV	-0.235	-0.306	-0.411	-0.523	-0.611	-0.640	-0.670	-0.711	-0.752	-0.782
SLOPE40	-0.191	-0.126	-0.059	-0.034	-0.011	-0.039	-0.057	-0.073	-0.097	-0.120
SLOPE60	-0.166	-0.130	-0.110	-0.079	-0.037	-0.060	-0.075	-0.086	-0.107	-0.123
ASPECT	-0.120	-0.139	-0.144	-0.098	-0.049	-0.060	-0.077	-0.079	-0.081	-0.098
CONVEX20	-0.641	-0.657	-0.657	-0.634	-0.599	-0.599	-0.587	-0.541	-0.484	-0.444
CONVEX30	-0.725	-0.741	-0.723	-0.690	-0.633	-0.637	-0.621	-0.568	-0.503	-0.454
Snow variables										
SNOWCH	+0.799	+0.859	+0.869	+0.848	+0.817	+0.799	+0.786	+0.741	+0.682	+0.625
SNOW5	+0.831	+0.887	+0.885	+0.865	+0.836	+0.818	+0.803	+0.763	+0.709	+0.656
SNOW7.5	+0.836	+0.891	+0.885	+0.865	+0.836	+0.817	+0.803	+0.763	+0.710	+0.658
SNOW10	+0.838	+0.892	+0.883	+0.861	+0.832	+0.812	+0.797	+0.756	+0.703	+0.651
SNOW12.5	+0.839	+0.892	+0.880	+0.856	+0.827	+0.807	+0.792	+0.750	+0.696	+0.644
SNOW15	+0.846	+0.900	+0.889	+0.863	+0.832	+0.814	+0.799	+0.759	+0.707	+0.657
SNOW20	+0.851	+0.905	+0.895	+0.869	+0.838	+0.820	+0.807	+0.771	+0.724	+0.678
SNOW25	+0.842	+0.896	+0.887	+0.863	+0.837	+0.819	+0.807	+0.775	+0.733	+0.692
SNOW30	+0.823	+0.877	+0.871	+0.851	+0.832	+0.814	+0.802	+0.773	+0.737	+0.701
SNOW40	+0.796	+0.848	+0.842	+0.834	+0.828	+0.811	+0.800	+0.778	+0.753	+0.727
SNOW50	+0.773	+0.819	+0.811	+0.812	+0.819	+0.804	+0.794	+0.779	+0.761	+0.743
SNOW60	+0.758	+0.803	+0.796	+0.800	+0.811	+0.799	+0.791	+0.782	+0.770	+0.759
Vegetation variables										
BARE6	-0.550	-0.441	-0.278	-0.309	-0.371	-0.389	-0.407	-0.427	-0.423	-0.427
MOSS6	+0.602	+0.661	+0.695	+0.700	+0.699	+0.686	+0.690	+0.656	+0.609	+0.564
LICHEN6	+0.102	-0.076	-0.295	-0.252	-0.161	-0.133	-0.113	-0.068	-0.036	+0.003
VASCVEG6	+0.643	+0.674	+0.674	+0.651	+0.610	+0.612	+0.616	+0.604	+0.575	+0.540
BRUSH6	+0.592	+0.630	+0.652	+0.635	+0.604	+0.605	+0.607	+0.600	+0.580	+0.568

continued/....

TABLE VI (Continued)

	$T_{1.5m}$	$T_{2.5m}$	T_{5m}	$T_{7.5m}$	T_{10m}	$T_{12.5m}$	T_{15m}	T_{20m}	T_{25m}	T_{30m}
Vegetation variables										
BARE12	-0.536	-0.420	-0.239	-0.258	-0.309	-0.327	-0.344	-0.361	-0.361	-0.364
MOSS12	+0.649	+0.690	+0.700	+0.698	+0.693	+0.684	+0.690	+0.657	+0.609	+0.564
LICHEN12	+0.070	-0.108	-0.333	-0.290	-0.200	-0.171	-0.151	-0.102	-0.063	-0.020
VASCVEG12	+0.646	+0.675	+0.660	+0.614	+0.554	-0.549	-0.548	+0.521	+0.482	+0.436
BRUSH12	+0.556	+0.603	+0.628	+0.587	+0.522	+0.520	+0.512	+0.492	+0.466	+0.448
TOT BL12	-0.687	-0.745	-0.745	-0.721	-0.683	-0.675	-0.678	-0.643	-0.596	-0.550
Geological variables										
GEOL2.5	+0.639	+0.672	+0.683	+0.655	+0.577	+0.612	+0.611	+0.634	+0.638	+0.637
GEOL5	+0.639	+0.672	+0.683	+0.655	+0.577	+0.612	+0.611	+0.634	+0.638	+0.637
GEOL7.5	+0.639	+0.672	+0.683	+0.655	+0.577	+0.612	+0.611	+0.634	+0.638	+0.637
GEOL10	+0.639	+0.672	+0.683	+0.655	+0.577	+0.612	+0.611	+0.634	+0.638	+0.637
GEOL12.5	+0.639	+0.672	+0.683	+0.655	+0.577	+0.612	+0.611	+0.634	+0.638	+0.637
GEOL15	+0.644	+0.676	+0.687	+0.659	+0.581	+0.616	+0.616	+0.640	+0.643	+0.642
GEOL20	+0.645	+0.675	+0.685	+0.659	+0.584	+0.617	+0.620	+0.645	+0.649	+0.648
GEOL25	+0.638	+0.674	+0.693	+0.673	+0.600	+0.635	+0.636	+0.662	+0.666	+0.663
GEOL30	+0.631	+0.671	+0.696	+0.680	+0.610	+0.644	+0.645	+0.671	+0.675	+0.671
Groundwater variables										
GWATER1	-0.400	-0.339	-0.208	-0.278	-0.410	-0.386	-0.381	-0.384	-0.383	-0.375
GWATER2	+0.152	+0.236	+0.340	+0.376	+0.388	+0.396	+0.416	+0.429	+0.443	+0.442
GWATER3	+0.349	+0.408	+0.473	+0.504	+0.535	+0.533	+0.548	+0.555	+0.552	+0.542
GWATER4	+0.334	+0.390	+0.458	+0.483	+0.504	+0.506	+0.524	+0.541	+0.541	+0.533
GWATER5	+0.362	+0.404	+0.434	+0.471	+0.508	+0.506	+0.510	+0.517	+0.510	+0.500
GWATER6	+0.359	+0.412	+0.470	+0.500	+0.525	+0.523	+0.538	+0.543	+0.535	+0.520

iation in either slope angle or aspect, and is therefore not ideal for reflecting the influence of these factors. Analysis presented later, as well as personal observation, indicates that relief is strongly correlated with snow distribution, which suggests that the relationship between relief and ground temperature may be an essentially indirect one.

4.22 Correlations with snow depth

The relationship between ground temperature and peak snow depth at sites in the Schefferville area is well documented. In general, the correlations given in Table VI are in good agreement with the results of earlier studies. Ground temperature, at all depths, is highly correlated with snow depth ($r > 0.7$, in almost all cases), while the coefficients, without exception, are significant at the 99.9 percent level (Table VI).

It was also expected that shallow temperatures would correlate best with snow depth over circles of relatively small radius and temperatures at greater depth with snow depth over larger areas, as described by Nicholson and Granberg (1973). Table VI shows that between the surface and 15m depth the highest correlations are with average snow depth over a 20m radius circle. Below 15m, temperature correlates best with the snow cover over a 60m circle. Thus, the relationship applies in a general way, as would be expected from first principles. There is no suggestion, however, of a specific ratio between the depth of the temperature

data and size of the snow area.

4.23 Correlations with vegetation

Subjective observations in the Schefferville area suggest that there is a strong correspondence between different vegetative cover types and ground temperature conditions. The coefficients listed in Table VI confirm this view, suggesting that the influence of vegetation is felt on two levels. On a small scale, the different cover types form insulating layers at the surface, the effectiveness of which is a function of their thickness and density. On a large scale, vegetation is a reflection of the impact of other environmental factors, notably relief and snow depth. In considering the muitiple regression results later, an attempt is made to determine the relative importance of these two facets.

With the exception of the bare ground and lichen variables, correlations with vegetation are positive (i.e. greater vegetation development correlates with higher temperatures), fairly high ($r > 0.5$, in most cases) and significant at the 98.5 percent level or better (Table VI). Although the coefficients are fairly uniform, there is a trend for a decrease with ground temperature at greater depths. In general, for any given depth, the highest positive correlations are with the variable which represents percentage moss cover.

The lichen and bare ground variables have lower but

negative correlations with ground temperature as would be expected. A synthetic variable, representing percentage bare ground and lichen combined, gives the highest correlation with ground temperature of any of the variables considered.

4.24 Correlations with thermal conductivity and other geological variables

Geology and rock type, per se, are only indirectly related to ground temperature distribution, via their influence on topography and relief (sub-section 1.21). However, when a similar surface temperature and terrestrial heat flux prevail, the occurrence of low ground temperatures could be expected to coincide with high thermal conductivity zones, and vice versa. This suggests a negative correlation between the two variables. While this relationship holds for individual thermocable sites, the values presented in Table VI indicate that for Timmins 4 as a whole, these two variables are positively correlated. Uniformly high coefficients ($r > 0.6$) describe the relationships between temperature at different depths, and conductivity for each of the depth increments considered. Moreover, there is a trend for the highest correlations with temperature at a given depth to be with mean conductivity over the larger increments considered (Table VI). All correlations are significant at better than the 99.0 percent level.

It will be shown later that the apparent discrepancy between expected and observed correlations with thermal conductivity can be explained in terms of the overwhelming importance of snow depth, which exerts a much stronger influence than conductivity on the distribution of ground temperatures. Thus, the Timmins 4 ore-body, which is composed of high conductivity material, is also situated beneath a valley which has a deep snow cover. Conversely, the ridges at this site are composed of relatively unleached material, of lower conductivity, yet have a shallow snow cover. The observed positive correlations may, for this reason, be viewed essentially as false correlations.

4.25 Correlations with groundwater

In general, supra-permafrost groundwater has a warming influence on ground temperatures in permafrost. In unfrozen valley sites at Timmins 4, however, it may have the opposite effect, maintaining temperatures at 0 to 0.5°C, when the existence of deep winter snow suggests they should be considerably warmer (Nicholson and Granberg, 1973). This qualification notwithstanding, a positive correlation was expected between the two variables.

In fact, with one exception, the groundwater variables considered are positively correlated with ground temperature (Table VI). The values of the coefficients decrease consistently with depth, and about half the correlations are significant at the 99.0 percent level or better. Unfortunately, collection of data

for use in compilation of the groundwater variables is both tedious and time-consuming. In addition, in some types of terrain it is almost impossible to delineate either the drainage basins or channels involved. This is especially true within the undulating, poorly-drained lower part of the Timmins 4 site.

For these reasons, it was decided to omit the groundwater variables from further analysis. This is quite logical if an attempt is later to be made to develop a predictive procedure which has application on a reasonably large scale, and would, thus, involve compilation at a large number of prediction points.

4.3 MODELLING THE SHALLOW GROUND THERMAL REGIME

4.31 Previous studies

With the exception of a number of somewhat rigidly theoretical approaches, having engineering application (e.g. Lachenbruch, 1957a, 1959; Brown, W.G., 1963; Hwang, Murray and Brooker, 1972), few studies have been concerned specifically with modelling the ground thermal regime within the permafrost region. A review of the literature indicates that studies are limited, by the availability of measured ground temperature information, to only two small areas within the North American permafrost zone, where it has been feasible to collect such data.

Positive temperature anomalies, related to the presence of surface water bodies, complicate the regime in one of these areas, the Mackenzie Delta, N.W.T., and predictive models must include a correction for such effects (Brown, W.G. et al, 1964; Smith, 1972). Thus, for example, the steady state temperature at time, t, for any point (x,y,z), beneath a river channel, may be computed (after Smith, op cit., Equation 2) as:

$$T(x,y,z,t) = \theta(x,y,z,t) + \left[T(x,y,0,t) + Gg.z\right] \quad (10)$$

where θ is a disturbance factor, described by Lachenbruch (1957a Equation 28), and the second term is the undisturbed profile for the area (see section 2.3), Gg being the geothermal gradient. A related study employs a finite difference approach to model temporal changes in ground temperature, and thus permafrost distribution, which occur as a result of channel migration (Smith and Hwang, 1973).

Until recently, application of simple conduction models was not practical in the Schefferville area, due to a lack of available information on subsurface thermal properties. Instead, it was found more profitable to make use of the well-documented relationship between ground temperature and winter snow depth as a basis for development of empirical predictive procedures. Most recently, Nicholson and Granberg (1973) have related mean annual ground temperature, T, at depth, D (in metres), to average snow depth over a circle of radius, twice D, about the cable-head,

as follows:

$$T = aS - w + 0.01D \qquad (11)$$

where a and w are constants, such that $0.028 < a < 0.035$, $2.2 < w < 2.7$, and $68 < w/a < 78$. The term w/a is the snow depth, in centimetres, which corresponds to a temperature of 0°C, and 0.01D is a correction for the geothermal gradient (Nicholson and Granberg, op cit.). Similar equations have been used by Nicholson (1974), to predict the distribution of ground temperatures along cross-sections through Timmins 4, and by Granberg (1973), in conjunction with a computer mapping program, to produce a near-surface (1.5m) temperature map for the site.

4.32 Present approach.

The analysis and discussion in section 4.2 show that ground temperature, at least at shallow depths, is significantly correlated with a number of environmental parameters. This confirms the largely qualitative conclusions previously described in the literature review in Chapter 2, and provides a basis for derivation of an improved procedure for modelling the distribution of ground temperatures in this area.

As a working hypothesis, it is proposed that the accuracy of the model developed by Nicholson and Granberg, and described in the previous sub-section, might be improved, in terms of variance explained, if the influence of environmental

parameters, other than snow depth, was also to be included. To this end, a revised model is formulated, such that:

$$T = f(X_1, X_2, X_3 .. X_n) \qquad (12)$$

where, T is mean ground temperature at any shallow depth of interest, X_1 is a variable for snow depth, and X_2, X_3 .. X_n are variables, representative of environmental factors such as, relief, vegetation, geology and ground water. Singly, or in combination, these latter are considered potentially of value in providing increased explanation of variations in the ground thermal regime. The observed interactions amongst these variables, which have been summarized by Brown (1970, Table I), strongly suggests that a multi-variate approach is required.

4.33 Step-wise multiple regression

This type of analysis provides a statistical technique whereby the extent to which the variance in a dependent variable (in this case, ground temperature) is explained by a set of independent variables (the environmental parameters), may be assessed. Step-wise multiple regression provides a least squares solution and is a variant on linear multiple regression. It differs from the latter in its ability to indicate the particular combination of independent variables which gives the highest explanation of the variance in a dependent variable. It is intended that the results of the analysis should later form the basis for derivation of

improved semi-empirical equations for modelling the ground thermal regime.

4.331 Procedure

In step-wise multiple regression, the equation which provides greatest explanation of the variance in a dependent variable, is built up recursively. That is to say independent variables are introduced, in turn, and in such a way that, at each "step", the variable included is the one which gives the greatest increase in explanation (i.e. reduction in residual sums of squares), when combined with those already entered.

In all, ten separate analyses were performed. For each analysis, ground temperature at one of the standard depths, given in Table II, was used as the dependent variable.

4.332 Choice of input variables

Environmental variables evaluated as possible predictors of ground temperature distribution are described in Chapter 3. Most of these were compiled at more than one scale. However, the matrix of correlation coefficients, presented in Table VI, indicates a consistency, in most cases, in the scale at which the greatest correlation is obtained with each of the ten temperature variables. It was desirable to reduce the number of variables introduced into the analysis for two reasons. Firstly, this reduces computational time and avoids storage problems with the

original large number of variables. Secondly, unnecessary duplication is avoided (e.g. where inclusion of two almost identical variables would result in the immediate elimination of one, as a linear combination of the other). Thus, when a variable had been evaluated at more than one scale, only the one giving the highest correlation with ground temperature was included in the multiple regression.

Only in the case of the snow variables was this procedure not strictly adhered to. It was considered justified in this instance, for the following reasons, to assume operation of the "2R" relationship between snow depth and ground temperature, described by Nicholson and Granberg (see sub-section 4.31). Most importantly, there is a consistent trend in the data given in Table VI, albeit not a precise one, for snow depth over areas of increasing size to correlate best with ground temperature at increasing depths. In addition, all the snow-temperature relationships considered show an equally high level of correlation, and are significant at the 99.9 percent level. The range in temperature-snow coefficients at any given depth is very small (< 0.03).

A listing of variables considered for inclusion in the step-wise multiple regression analyses is presented in Table VII.

TABLE VII

VARIABLES COMPILED FOR INCLUSION IN THE MULTIPLE REGRESSION ANALYSIS

Variable name	Representative of:
Temperature variables	
$T_{1.5m}$	Mean annual temperature at 1.5m
$T_{2.5m}$	" " " " 2.5m
T_{5m}	" " " " 5m
$T_{7.5m}$	" " " " 7.5m
T_{10m}	" " " " 10m
$T_{12.5m}$	" " " " 12.5m
T_{15m}	" " " " 15m
T_{20m}	" " " " 20m
T_{25m}	" " " " 25m
T_{30m}	" " " " 30m
Relief variables	
ELEV	Site elevation
SLOPE40	Slope of 40m slope segment through site
SLOPE60	" " 60m " " " "
ASPECT	Site aspect
CONVEX20	Convexity index for circle of radius 20m
CONVEX30	" " " " " " 30m
Snow variables	
SNOWCH	Mean cable head snow depth
SNOW5	Mean snow depth for 5m radius circle
SNOW7.5	" " " " 7.5m " "
SNOW10	" " " " 10m " "
SNOW12.5	" " " " 12.5m " "
SNOW15	" " " " 15m " "
SNOW20	" " " " 20m " "
SNOW25	" " " " 25m " "
SNOW30	" " " " 30m " "
SNOW40	" " " " 40m " "
SNOW50	" " " " 50m " "
SNOW60	" " " " 60m " "
Vegetation variables	
BARE6	Percentage cover of bare ground:6m circle
MOSS6	" " " moss : " "
LICHEN6	" " " lichen : " "
VASCVEG6	" " "vascular plants: "
BRUSH6	" " " brush : " "

Continued/....

TABLE VII (Continued)

Variable Name	Representative of:
Vegetation variables	
BARE12	Percentage cover of bare ground: 12m circle
MOSS12	Percentage cover of moss: 12m circle
LICHEN12	" " lichen: " "
VASCVEG12	" " vascular plants: " "
BRUSH12	" " brush : " "
TOTBL12	" " bare ground and lichen: " "
Geological variables	
GEOL5	Mean conductivity: surface to 5m
GEOL7.5	" " : " " 7.5m
GEOL10	" " : " " 10m
GEOL12.5	" " : " " 12.5m
GEOL15	" " : " " 15m
GEOL20	" " : " " 20m
GEOL25	" " : " " 25m
GEOL30	" " : " " 30m
Groundwater variables	
GWATER1	Influence of groundwater : A. Log d
GWATER2	" " " $A/d^{\frac{1}{2}}$
GWATER3	" " " Log A.d
GWATER4	" " " A/2d
GWATER5	" " " A^2/d
GWATER6	" " " A/d

4.333 Computational details

The multiple regression analyses were carried out on the IBM 360/75 computer at McGill University, using an SPSS (Statistical Package for the Social Sciences) package program. A program of this type was chosen, in preference to one written specifically for the study, both for its economy in computing time, and for the peripheral information, such as normalised and partial correlation coefficients, which it is possible to output at the same time.

Full details of the program and computational procedure are included in the SPSS handbook (Nie, Bent and Hull, 1970. Chapter 15). Special note should be taken of the method by which the variables to be entered into the regression equation were chosen. Two factors are taken into consideration. The variable introduced, at each "step", is the one which, firstly, has the highest F statistic (a measure of the significance of its normalized regression coefficient, were it to be included), and, secondly, whose tolerance (a measure of the extent to which it is a linear combination of variables already entered) is greatest.

4.34 Discussion of the regression results

The results of the ten step-wise multiple regression analyses are summarized in Table VIII. In each instance, the dependent (ground temperature) variable is listed, the order of introduction of

TABLE VIII

MULTIPLE REGRESSION RESULTS

Dependent Variable	Independent variable	Multiple R	R^2 x 100	Change in R^2 x 100
$T_{1.5m}$	SNOWCH	0.7988	63.81	63.81
	GEOL20	0.8735	76.30	12.49
	BARE6	0.9032	81.58	5.28
	BRUSH6	0.9151	83.74	2.16
	CON30	0.9177	84.22	0.48
	ELEV	0.9205	84.73	0.51
	VASCVEG6	0.9209	84.81	0.08
	MOSS12	0.9219	84.98	0.17
$T_{2.5m}$	SNOW5	0.8872	78.72	78.72
	GEOL30	0.9331	87.06	8.34
	VASCVEG6	0.9410	88.55	1.49
	BRUSH6	0.9441	89.14	0.59
	BARE6	0.9492	90.09	0.95
	CON30	0.9517	90.58	0.49
	ELEV	0.9525	90.73	0.15
T_{5m}	SNOW10	0.8827	77.92	77.92
	GEOL30	0.9304	86.57	8.65
	ELEV	0.9497	90.19	3.62
	VASCVEG6	0.9576	91.71	1.52
	BARE6	0.9696	94.00	2.29
	MOSS12	0.9730	94.68	0.68
	CON30	0.9735	94.77	0.09
	BRUSH6	0.9736	94.78	0.01
$T_{7.5m}$	SNOW15	0.8633	74.53	74.53
	ELEV	0.9532	90.87	16.34
	GEOL30	0.9598	92.13	1.26
	VASCVEG6	0.9645	93.04	0.91
	BARE6	0.9718	94.43	1.39
	CON30	0.9735	94.77	0.34
	MOSS12	0.9743	94.92	0.15
	BRUSH6	0.9743	94.93	0.01
T_{10m}	SNOW20	0.8376	70.15	70.15
	ELEV	0.9661	93.33	23.18
	BRUSH6	0.9685	93.81	0.48
	VASCVEG6	0.9713	94.35	0.54
	GEOL30	0.9722	94.52	0.17
	CON30	0.9724	94.55	0.03
	MOSS12	0.9724	94.56	0.01

Continued/....

TABLE VIII (Continued)

Dependent Variable	Independent variable	Multiple R	R^2 x 100	Change in R^2 x 100
$T_{12.5m}$	SNOW25	0.8191	64.10	67.10
	ELEV	0.9598	92.13	25.03
	CON30	0.9655	93.22	1.09
	VASC6	0.9670	93.50	0.28
	BRUSH6	0.9691	93.91	0.41
	MOSS12	0.9692	93.94	0.03
	GEOL30	0.9692	93.94	0.00
T_{15m}	SNOW30	0.8018	64.29	64.29
	ELEV	0.9571	91.61	27.32
	CON30	0.9671	93.53	1.92
	VASCVEG6	0.9702	94.12	0.59
	BRUSH6	0.9722	94.53	0.41
	MOSS12	0.9733	94.73	0.20
	GEOL30	0.9740	94.86	0.13
T_{20m}	SNOW40	0.7792	60.72	60.72
	ELEV	0.9457	89.43	28.71
	VASCVEG6	0.9618	92.51	3.08
	CON30	0.9659	93.30	0.79
	BRUSH6	0.9675	93.61	0.31
	GEOL30	0.9684	93.78	0.17
	MOSS12	0.9720	94.48	0.70
	BARE6	0.9726	94.60	0.12
T_{25m}	SNOW50	0.7610	57.91	57.91
	ELEV	0.9431	88.94	31.03
	VASCVEG6	0.9601	92.18	3.24
	GEOL30	0.9646	93.04	0.86
	MOSS12	0.9675	93.61	0.57
	BRUSH6	0.9704	94.17	0.56
	BARE6	0.9715	94.38	0.21
	CON30	0.9718	94.43	0.05
T_{30m}	SNOW60	0.7589	57.59	57.59
	ELEV	0.9504	90.33	32.74
	VASCVEG6	0.9615	92.44	2.11
	GEOL30	0.9665	93.41	0.97
	BARE6	0.9686	93.81	0.40
	BRUSH6	0.9713	94.33	0.52
	MOSS12	0.9726	94.59	0.26
	CON30	0.9729	94.65	0.06

independent variables is indicated and a list of the resulting multiple correlation coefficients given. The percentage explanation of the variance in ground temperature at each depth, and changes therein, following introduction of new independent variables, are also shown. The results appear to confirm, in part, the conclusions reached from a consideration of the linear correlations.

Two trends are immediately apparent: snow depth provides by far the greatest explanation of the variance in ground temperature at all depths considered ($R^2 > 0.6$), while the next most important variable is either thermal conductivity or elevation (Table VIII). The importance of ground thermal properties was to be expected, but it is surprising that this variable provides the greatest explanation at shallow depth. This may be due to the fact that at deeper depths other factors mask its importance. Linear correlations between elevation and ground temperature below 10m are high ($r > 0.6$), but there is no obvious physical explanation for a relationship as strong as that implied in the multiple regression results. Over the range in elevation at Timmins 4, the normal decrease in temperature with altitude is far too small to have the required influence. Moreover, elevation does not appear to correlate highly with any of the other variables evaluated, a fact which is confirmed by consideration of the partial correlation coefficients. It is tentatively suggested,

therefore, that elevation reflects the influence of one or more variables which were not evaluated here. Some type of groundwater variable, or one representing average snow depth over very large areas of influence seems most likely (Nicholson, 1974).

The influence of different vegetation variables also varies, though only the variable representative of vascular plant coverage consistently provides greater than a one percent increase in explanation. The importance of the others varies with depth. The low explanation due to the moss variable should be noted, since linear correlations with this variable were high (Table VI). Reference to the pertinent partial correlation coefficients suggests that this situation is a function of more significant correlation between percentage moss cover and peak snow depth.

No other major trends are apparent in the regression results (Table VII) and the addition of other variables rarely produces any real increase in explanation. For example, of the relief variables, only relief shape enters into the regressions and this variable generally contributes less than one percent in explanation.

In summary, peak snow depth, followed by either thermal conductivity (in the active layer) or elevation (beneath the active layer), is most important in explaining variations in the distribution of ground temperatures, down to a depth of 30m.

Snow alone explains 60 to 65 percent of the variance in ground temperature, and the inclusion of the second variable raises this figure to between 85 and 90 percent.

4.4 DERIVATION OF PREDICTIVE EQUATIONS

This section is concerned with compilation of optimum equations for modelling the distribution of shallow ground temperatures, as a function of the environmental parameters earlier described. Use is made of the relationships disclosed by the multiple regression analyses.

4.41 Equations for shallow ground temperature prediction

The multiple regression results given in Table VIII indicate that equations which include all possible independent variables provide a very high explanation of the variance in ground temperature, at a given shallow depth. This is to be expected since, in such cases, a large number of environmental factors are employed to explain variations in ground temperature within a sample of only twenty-one sites. The results show, in addition, that by far the greatest proportion of the explanation obtained is due only to the two most important variables in each instance: snow, and either conductivity or elevation, according to depth (Table VIII). The inclusion of additional variables provides little or no increase in explanation. Thus, it was decided to include only the first two variables when compiling the improved

equations.

In the event, two separate sets of equations were derived from the multiple regression results. Equations for computing ground temperature using only snow were first compiled (Table IX). These allow an initial comparison with the Nicholson-Granberg model (sub-section 4.31), and also provide an indication of the increase in explanation, which is attributable to the inclusion of the second variable.

The improved, or Optimum Predictive Equations are presented in Table X. Since only two independent variables are included in each instance, these equations are believed to be consistent, insofar as this is possible, with the guide-lines, proposed by Ezekiel and Fox (1959) regarding the validity of multiple correlation coefficients, in terms of sample size and number of variables.

To facilitate comparison between sets of equations, scatter diagrams have been plotted showing measured and predicted temperatures, as computed for each depth using the two sets of equations. These plots are included here as figures 10a and 10b. The computed temperature values are presented in Tables XI and XII, respectively.

TABLE IX

EQUATIONS COMPILED USING THE SNOW VARIABLE ALONE

Regression Equation	w/a	Multiple R	R^2 x 100	S.E. (^oC)
$T_{1.5m}$ = 0.02832 . SNOWCH - 2.40811	85	0.7988	63.81	1.071
$T_{2.5m}$ = 0.02935 . SNOW5 - 2.58561	88	0.8872	78.72	0.729
T_{5m} = 0.02764 . SNOW10 - 2.50399	90	0.8827	77.92	0.665
$T_{7.5m}$ = 0.02596 . SNOW15 - 2.31621	89	0.8633	74.53	0.647
T_{10m} = 0.02298 . SNOW20 - 2.03021	88	0.8376	70.15	0.608
$T_{12.5m}$ = 0.02243 . SNOW25 - 1.99598	89	0.8191	67.10	0.610
T_{15m} = 0.02075 . SNOW30 - 1.85142	89	0.8018	64.29	0.572
T_{20m} = 0.01875 . SNOW40 - 1.70764	91	0.7792	60.72	0.511
T_{25m} = 0.01721 . SNOW50 - 1.59432	92	0.7610	57.91	0.464
T_{30m} = 0.01622 . SNOW60 - 1.49960	93	0.7589	57.59	0.423

TABLE X

OPTIMUM PREDICTIVE EQUATIONS

Multiple Regression Equation	Multiple R	R^2 x 100	S.E. (^oC)
$T_{1.5m}$ = 0.02283 . SNOWCH + 0.40866 . GEOL20 - 4.56637	0.8735	76.23	0.891
$T_{2.5m}$ = 0.02421 . SNOW5 + 0.30816 . GEOL30 - 4.14649	0.9331	87.06	0.584
T_{5m} = 0.02233 . SNOW10 + 0.28586 . GEOL30 - 3.89833	0.9304	86.57	0.532
$T_{7.5m}$ = 0.02418 . SNOW15 - 0.03388 . ELEV + 24.02806	0.9535	90.87	0.398
T_{10m} = 0.02078 . SNOW20 - 0.03519 . ELEV + 25.35165	0.9661	93.33	0.295
$T_{12.5m}$ = 0.01989 . SNOW25 - 0.03500 . ELEV + 25.26180	0.9598	92.13	0.306
T_{15m} = 0.01800 . SNOW30 - 0.03302 . ELEV + 23.88169	0.9571	91.61	0.285
T_{20m} = 0.01545 . SNOW40 - 0.02918 . ELEV + 21.09076	0.9457	89.44	0.272
T_{25m} = 0.01339 . SNOW50 - 0.02692 . ELEV + 19.48747	0.9431	88.94	0.244
T_{30m} = 0.01210 . SNOW60 - 0.02538 . ELEV + 18.41532	0.9504	90.33	0.207

4.411 Equations compiled from snow alone

These equations, presented in Table IX, may be summarized in a simple linear regression of the following form (after Nicholson and Granberg, 1973):

$$T = aS - w \qquad (13)$$

where T is ground temperature at depth z ($z \leq 30m$), and S is mean snow depth for a circle, of radius twice z, about the cable-head. The results of the present analysis, suggest that the values of the constants, a and w, fall within the following limits: $0.016 < a < 0.029$, $1.50 < w < 2.59$, and $85 < w/a < 93$.

Table VIII shows that both explanation of the variance in ground temperature, R^2, and standard error of estimate decrease fairly consistently with depth. The snow depth, corresponding to a ground temperature of $0^{\circ}C$, w/a, averages approximately 89cm.

Comparison with previous equations

Two types of equation describing the relationship between snow depth and ground temperature are described in the literature. Krinsley (1963) and Mackay and Mackay (1974) report a logarithmic relationship between snow and minimum temperatures at very shallow depths. These authors attempted no correlations with mean temperature. The equations derived here, for prediction of mean annual temperatures at greater depths, closely resemble those

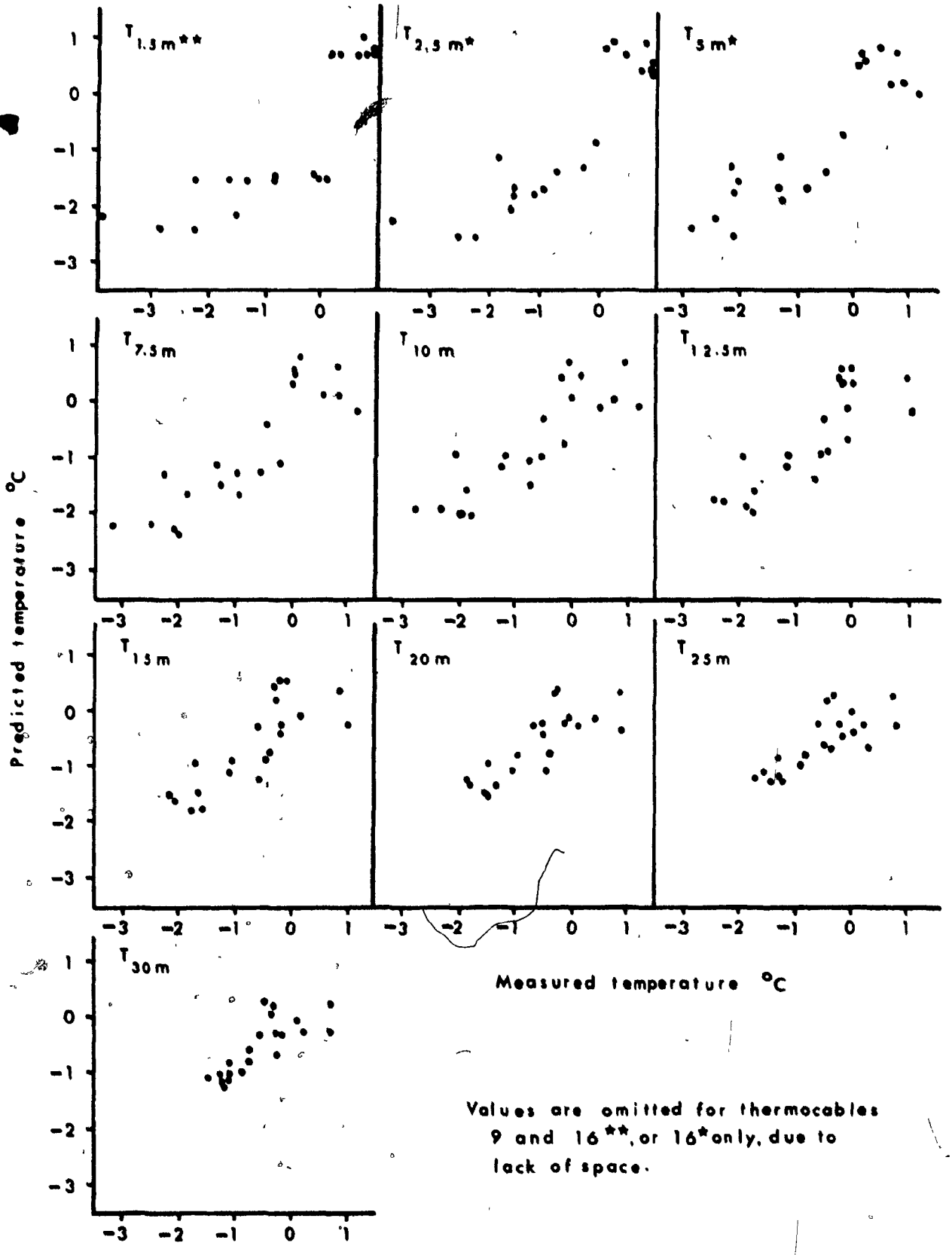

Figure 10a: Measured ground temperatures versus temperatures predicted using equations containing only the snow depth variable.

TABLE XI

TEMPERATURES PREDICTED USING THE SNOW VARIABLE ALONE

Cable No.	$T_{1.5m}$	$T_{2.5m}$	T_{5m}	$T_{7.5m}$	T_{10m}	$T_{12.5m}$	T_{15m}	T_{20m}	T_{25m}	T_{30m}
1	-1.502	-1.394	-1.329	-1.083	-0.769	-0.619	-0.401	-0.181	-0.080	-0.040
2	-1.502	-1.814	-1.631	-1.270	-0.927	-0.883	-0.866	-0.796	-0.730	-0.668
3	-1.502	-1.142	-1.039	-0.982	-0.897	-0.897	-0.866	-0.768	-0.777	-0.723
4	-1.502	-0.889	-0.663	-0.483	-0.330	-0.296	-0.289	-0.281	-0.267	-0.285
5	+0.764	+0.473	+0.238	+0.189	+0.146	+0.063	-0.040	-0.174	-0.230	-0.286
6	-2.408	-2.586	-2.498	-2.303	-2.003	-1.949	-1.758	-1.515	-1.259	-1.089
7	-1.502	-1.814	-1.686	-1.436	-1.185	-1.171	-1.088	-1.038	-0.999	-0.932
8	+0.764	+0.769	+0.583	+0.532	+0.491	+0.487	+0.458	+0.332	+0.280	+0.268
9	+0.764	+0.907	+0.854	+0.835	+0.737	+0.689	+0.589	+0.392	+0.283	+0.276
10	+1.075	+1.036	+0.799	+0.638	+0.511	+0.469	+0.388	+0.308	+0.268	+0.260
11	+0.764	+0.473	+0.017	-0.084	-0.045	-0.134	-0.231	-0.343	-0.345	-0.280
12	-2.153	-2.046	-1.888	-1.675	-1.410	-1.341	-1.200	-1.010	-0.837	-0.687
13	+0.764	+0.473	+0.246	+0.124	+0.022	-0.029	-0.050	-0.187	-0.276	-0.270
14	-2.408	-2.586	-2.476	-2.275	-1.966	-1.884	-1.702	-1.471	-1.267	-1.089
15	+0.764	+0.872	+0.564	+0.355	+0.102	-0.092	-0.225	-0.412	-0.484	-0.530
16	-2.408	-2.586	-2.432	-2.186	-1.853	-1.716	-1.488	-1.284	-1.143	-1.044
17	+0.764	+0.977	+0.774	+0.643	+0.498	+0.355	+0.288	+0.177	+0.103	+0.100
18	-1.502	-1.297	-1.213	-1.132	-0.996	-0.933	-0.789	-0.596	-0.434	-0.371
19	-1.502	-1.646	-1.722	-1.688	-1.545	-1.563	-1.476	-1.333	-1.231	-1.159
20	-1.502	-1.646	-1.526	-1.244	-0.962	-0.931	-0.918	-0.928	-0.875	-0.796
25	-2.153	-2.234	-2.357	-2.184	-1.876	-1.772	-1.553	-1.318	-1.097	-1.000

proposed by Nicholson and Granberg (1973). Most importantly, a simple linear regression appears adequately to describe the relationship in both instances. The two sets of Schefferville equations are also morphologically similar; the major discrepancy being in the values derived for the expression w/a: the snow depth corresponding to a temperature of 0°C. Values are considerably higher in the present study (90cm compared to 75cm), due, it is believed, to differences in both the snow data period, and the method of compilation, used by Nicholson and Granberg.

4.412 Optimum predictive equations

The equations compiled for predicting shallow ground temperatures in terms of snow depth, and either thermal conductivity or elevation, are presented in Table X. These fall into two groups, according to the identity of the second variable. The three shallowest equations include the thermal conductivity variable, and exhibit relatively high standard errors of estimate (> 0.5°C). This is partly related to the large range in temperatures at shallow depths, and partly to the observed lower correlation coefficients. The remaining equations may be summarized, as follows:

$$T = aS - bE + c \qquad (14)$$

where T = average annual temperature (°C), at depth, z, S =

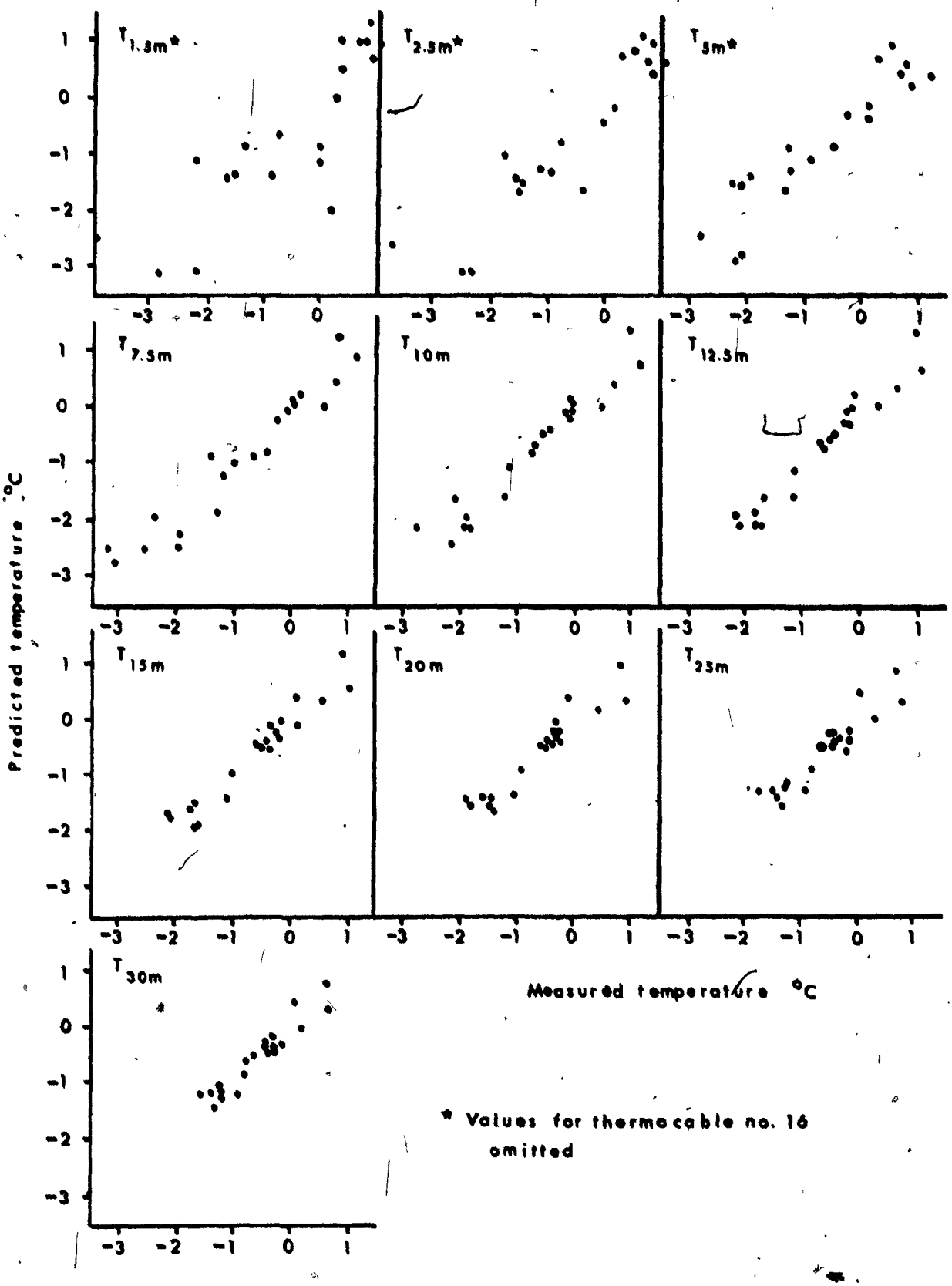

Figure 10b: Measured ground temperatures versus temperatures predicted using the Optimum equations.

TABLE XII

TEMPERATURES PREDICTED USING THE OPTIMUM PREDICTIVE EQUATIONS

Cable No.	$T_{1.5m}$	$T_{2.5m}$	T_{5m}	$T_{7.5m}$	T_{10m}	$T_{12.5m}$	T_{15m}	T_{20m}	T_{25m}	T_{30m}
1	-0.689	-0.790	-0.838	-0.207	+0.142	+0.283	+0.416	+0.494	+0.530	+0.490
2	-0.816	-1.232	-1.084	-0.828	-0.466	-0.422	-0.425	-0.394	-0.353	-0.303
3	-1.110	-0.900	-0.809	-1.180	-1.082	-1.074	-0.976	-0.904	-0.882	-0.809
4	-0.816	-0.470	-0.302	-0.675	-0.527	-0.499	-0.488	-0.467	-0.453	-0.450
5	+1.011	+0.653	+0.425	+0.044	0.000	-0.084	-0.181	-0.299	-0.350	-0.383
6	-3.083	-3.028	-2.857	-2.431	-2.103	-2.028	-1.823	-1.537	-1.273	-1.098
7	-1.396	-1.670	-1.670	-1.820	-1.567	-1.540	-1.432	-1.313	-1.227	-1.127
8	+1.011	+0.898	+0.706	+0.015	-0.063	-0.081	-0.101	-0.193	-0.240	-0.240
9	+1.011	+1.012	+0.923	+0.286	+0.074	+0.013	-0.068	-0.214	-0.303	-0.295
10	+1.262	+1.118	+0.595	+1.274	+1.393	+1.332	+1.186	+0.979	+0.850	+0.791
11	+1.011	+0.653	+0.425	+0.968	+0.783	+0.691	+0.549	+0.354	+0.291	+0.311
12	-1.341	-1.424	-1.287	-0.968	-0.655	-0.582	-0.483	-0.365	-0.248	-0.140
13	+0.716	+0.432	+0.227	+0.501	+0.425	+0.368	+0.313	+0.135	+0.025	+0.016
14	-3.083	-3.028	-2.844	-2.272	-1.931	-1.832	-1.643	-1.386	-1.173	-0.997
15	-0.001	-0.176	-0.386	+0.181	-0.060	-0.242	-0.362	-0.513	-0.564	-0.580
16	-3.659	-3.462	-3.206	-2.459	-2.108	-1.960	-1.719	-1.462	-1.290	-1.164
17	+0.541	+0.716	+0.374	+0.087	-0.078	-0.220	-0.269	-0.389	-0.394	-0.381
18	-1.952	-1.663	-1.538	-0.884	-0.721	-0.658	-0.539	-0.388	-0.271	-0.221
19	-1.368	-1.510	-1.540	-2.201	-2.044	-2.038	-1.910	-1.680	-1.523	-1.405
20	-1.110	-1.316	-1.401	-1.859	-1.591	-1.552	-1.496	-1.409	-1.303	-1.188
25	-2.477	-2.552	-2.462	-2.476	-2.150	-2.031	-1.795	-1.508	-1.270	-1.147

average peak snow depth (cm) over a circle radius twice z, where $7.5 \leq z \leq 30$, E = site elevation (m), and a, b and c are constants such that: $0.012 < a < 0.024$, $0.025 < b < 0.035$, and $18.42 < c < 25.35$. The standard error of estimate for these equations decreases with depth, from 0.4°C at 7.5m to 0.2°C at 30m. Percentage explanation of the variance in ground temperatures, R^2, averages about 90 percent for all depths (Table X).

4.42 Comparison between the two sets of equations

It is clear, from a comparison of the respective computed temperature values (Tables XI and XII), scatter diagrams (Figures 10a, b), multiple correlation coefficients and standard errors, that the optimum equations (Table X) are superior to those compiled using only snow (Table IX), for reconstructing measured shallow temperature conditions. Since these equations form part of the prediction model presented in a later section, it is valuable here to consider the predictive ability of the equations for different types of thermal regime; especially for frozen as opposed to unfrozen ground. To this end, the thermocable sites have been grouped according to thermal regime (as implied in the form of their shallow temperature profiles). Measured and predicted 30m profiles are plotted for comparison in Figure 11a and b.

TABLE XIII

CLASSIFICATION OF THERMOCABLE SITES ACCORDING TO TEMPERATURE PROFILE MORPHOLOGY

Class	Thermal condition	Sites included
I	Frozen	1, 2, 3, 6, 7, 12, 14, 16, 18, 19, 20, 25
II	Unfrozen	10, 11, 13
IIIA	Intermediate	8, 9, 17
IIIB	Intermediate	4, 5, 15

TABLE XIV

COMPARISON OF OBSERVED AND PREDICTED PERMAFROST THICKNESSES

Cable No.	Observed depth (m)	Predicted depth (m)	Cable No.	Observed depth (m)	Predicted depth (m)
1	22	30	12	55	50
2	88	80	14	120	100
3	122	115	15	112	80
4	113	95	16	100	80
5	106	110	17	110	120
6	120	120	18	50	40
7	110	120	19	133	135
8	110	120	20	114	120
9	110	120	25	110	115

4.421 Classification of sites

A division of the thermocable sites into three classes - frozen, unfrozen and intermediate - is presented in Table XIII. This classification is based on that suggested by Annersten (1962), for sites in the Ferriman Ridge area.

Profiles in classes I (frozen) and II (unfrozen) show steady temperature increases and decreases, respectively, with depth, in the zone subject to seasonal temperature fluctuation (Figure 11a, 11b). A wider range of thermal conditions is included within the intermediate class. Profiles belonging to Class IIIA are characterized by an initial temperature decrease, but then exhibit very little change with increasing depth (Figure 11b). Class IIIB profiles are similar, in form, to those included in Class I, except that they cross the 0°C line from positive to negative, at depth (Figure 11b). These latter two sub-classes are believed to represent deep active layer or lateral heat flow and talik conditions, respectively (Nicholson and Thom, 1973).

4.422 Reconstruction of measured profiles

Frozen sites

Although the shape of Class I profiles is generally well reproduced, most are predicted up to 0.5°C too cold, when only snow is used (Figure 11a). The size of the average residual is

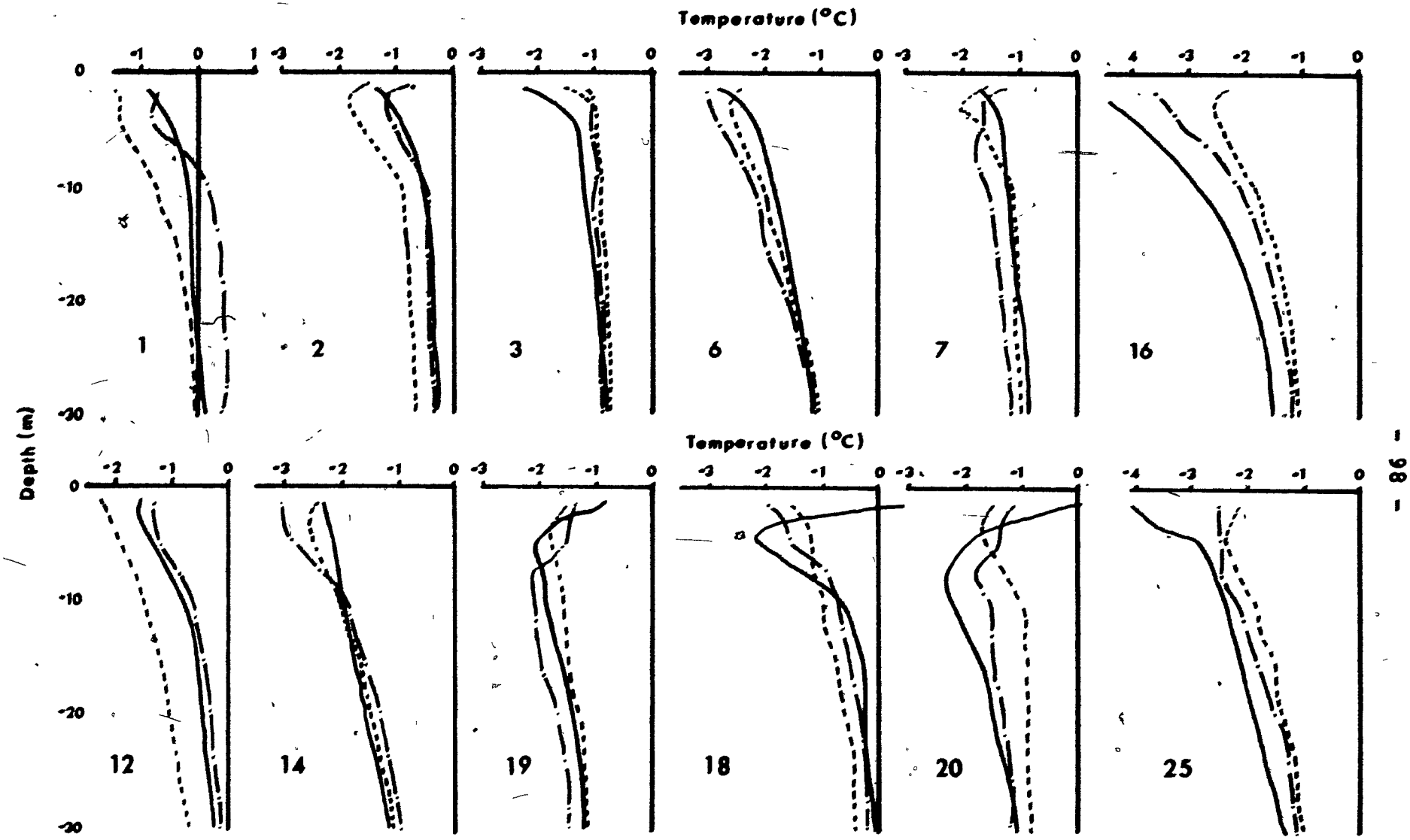

Figure 11a: Measured and predicted temperature profiles, Timmins 4. Part I Frozen sites. For Legend, see Part II (p. 99).

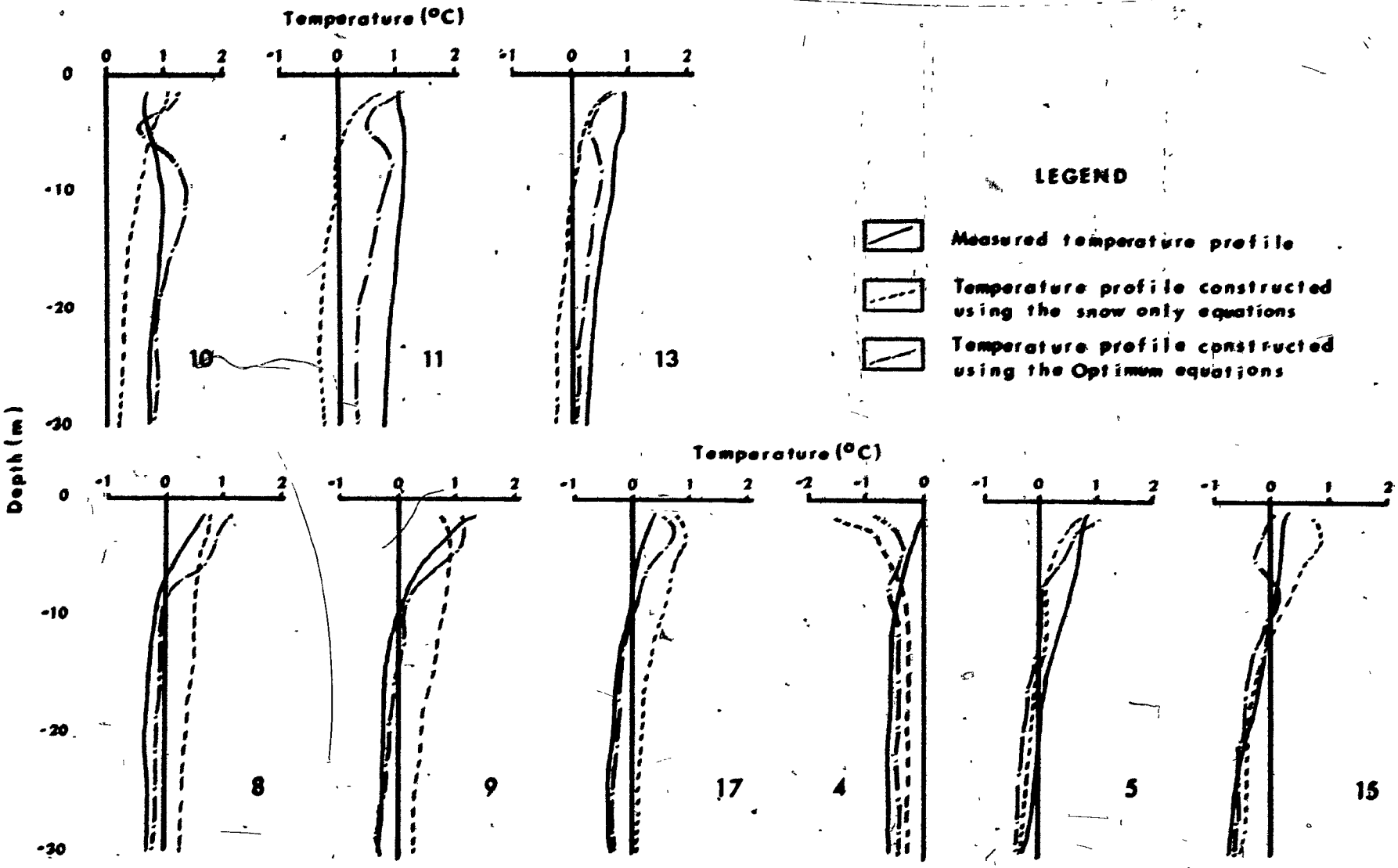

Figure 11b: Measured and predicted temperature profiles, Timmins 4. Part II Unfrozen sites, and Part III Intermediate sites.

reduced, to better than 0.3°C, when the optimum equations are employed.

Unfrozen sites

Neither set of equations really adequately reproduces the profiles included in Class II (Figure 10b). Using only snow, reconstruction of profile shape is not good and temperatures are predicted 0.5°C to 1.0°C too cold. The presence of a deep active layer or talik (see Class IIIA) is projected at sites 11 and 13. Although the size of the residuals is reduced when the optimum equations are employed, the profiles for thermocables 11 and 13 are even then not well produced. The improved profile for site 10 corresponds well at depth (below 20m).

Intermediate sites

Profiles at the deep active layer sites (8, 9, 17) are predicted approximately 0.5°C too warm, and their shape corresponds only fairly well with observed conditions, when snow alone is used (Figure 11b). Prediction is better in both respects when the optimum equations, including thermal conductivity and elevation, are used. The thermal regime at site 4, subject to lateral heat flow effects, is well predicted, by both sets of equations as are the Class IIIB profiles, although the predicted thickness of the talik zone at site 5 is underestimated.

4.423 Summary

The preceding discussion indicates that the shallow ground thermal regime may be modelled, with considerable accuracy, as a function of snow, and thermal conductivity or elevation, using the optimum equations presented in Table X. Although, overall, the standard error of estimate averages 0.41°C and explanation 87.6 percent, the validity of the model does appear to vary spatially. The ground thermal regime is most poorly reproduced in unfrozen areas. Fortunately, these areas are not of paramount importance in projecting the distribution of permafrost.

CHAPTER 5

MODELLING THE DISTRIBUTION OF GROUND TEMPERATURES

This chapter describes the development of a model for predicting ground temperatures. The model was developed and tested at the Timmins 4 site, and most of the chapter is concerned with details of its derivation and application at this site. Brief consideration is also given to the extent to which the model is applicable at the Ferriman Ridge permafrost site.

5.1 PREVIOUS APPROACHES TO PREDICTION

An important second objective of the study is to make use of the relationship between environmental factors and ground temperature in the development of a technique for modelling the distribution of ground temperatures in three dimensions, on a reasonably large scale (i.e. for areas of a few square kilometres). Prediction is not a simple task, since the Schefferville area lies in the discontinuous zone where permafrost distribution is very variable over short distances. Direct observation of the presence of frozen ground is especially difficult because of the deep active layers in this zone. However, a review of the literature suggests that both direct and indirect methods may be useful near Schefferville and in other areas. Ground temperature data usually constitute the only really reliable indication of the presence or absence of frozen ground, and their availability determines the extent to

to which direct and indirect approaches can be employed in prediction.

5.11 Indirect methods

If temperature data are limited, or unavailable, an indirect approach has to be adopted. This involves relating the spatial distribution of frozen, and/or unfrozen, ground to the occurrence of more readily surveyed environmental parameters. Factors previously employed in this fashion include: air temperature (Brown, 1966a), relief (Bonnlander and Major-Marothy, 1964; Ives, 1961; Johnston, Brown and Pickersgill, 1963; Dingman and Koutz, 1974), vegetation (Bonnlander and Major-Marothy, op cit.; Ives, op cit.; Gill, 1973) and snow (Annersten, 1964).

Permafrost thicknesses may be projected similarly, if temperature data are available as control (Bonnlander and Major-Marothy op cit.; Annersten, op cit.). If this approach is not feasible, the position of the base of permafrost may be approximated, using simple conduction models of the type described by Judge (1973c).

5.12 Direct methods

Thermocable measurements allow the vertical distribution of frozen and unfrozen ground to be monitored directly at discrete points. In areas with good geological control, geophysical techniques, particularly bore-hole logging, may give almost as reliable a

result (Séguin and Garg, 1974). In either event, with a reasonable density of points, an approximation for the three-dimensional geometry of permafrost may then be obtained by interpolation. This procedure can be considered analogous to delineation of an ore body from bore-hole information. Vertical cross-sections showing the two-dimensional distribution of ground temperatures have been produced in both the Mackenzie Delta area (Brown et al., 1963; Mackay, 1967; Smith, 1972), and the Schefferville area (Annersten, 1964; Thom, 1969; 1970; Nicholson and Thom, 1973; Nicholson, 1974). Thom (1970) and Séguin (1974a, Figure 6) have attempted to provide three-dimensional predictions by the addition of basal plans.

5.2 DEVELOPMENT OF THE PREDICTIVE MODEL

5.21 Theoretical Basis of the Model

This model considers the ground divisible into two layers for prediction purposes. Near surface temperatures can be predicted by quantification of the relationship between ground temperature and the environmental parameters, as described in Section 4.4. Below a certain level, however, small scale variations in the surface environmental parameters become less important, the theoretical surface area significantly affecting temperature variations becomes larger and, for practical reasons, the volume of measured temperature data for deriving the relationship becomes smaller. The exponential increase in coverage required

for quantifying environmental parameters which occurs with increasing depth, and simultaneous decrease in the volume of available temperature data, mean that there is a cut-off point beyond which the first method of modelling is no longer practical. It is this cut-off level which forms the boundary between the two layers. Within the lower layer, it is assumed that heat transfer occurs entirely by conduction. Prediction in this zone is by means of a simple heat flow model for downward extrapolation of the temperatures predicted at the base of the upper layer. In the first instance, it is assumed that one dimensional vertical heat transfer prevails in this lower zone. At a later stage, empirical allowance is made for lateral heat flow effects.

The level of zero annual amplitude, z_a, occurs at a depth of approximately 25 to 30m in the Schefferville area (Annersten, 1964; Nicholson & Thom, 1973). By coincidence 30m is also the greatest depth for which it was possible to derive an optimum equation for empirical prediction of ground temperatures using environmental parameters (see Section 4.31). Thus, 30m was a natural choice for the boundary between the two layers in the model. This level, z_a, is the shallowest level at which it can be confidently expected that significant annual temperature variations are absent.

For the first stage of modelling, simple one-dimensional vertical heat flow was assumed below the 30m level. Restating

Equation 6 (sub-section 2.31), the temperature of the ground at any depth z, such that $z \geq z_a$, is computed as follows:

$$T(z) = \frac{q^*}{K} \cdot \Delta z + T(z_a) \qquad (15)$$

where q* is terrestrial heat flow, Δz is the depth increment considered (i.e. between z_a and z), and K is the thermal conductivity for this interval.

In practice, the thermal regime in the Timmins area is complicated by the presence of non-vertical heat flows. Problems which arise as a result are considered in sub-section 5.23, together with a proposed simple empirical correction. For the moment, it is convenient to retain the simpler picture, of uniform vertical heat transfer.

In the compilation of a large scale prediction, temperature profiles were computed at points 60m apart on the square grid shown in Figure 3. Temperature profiles were produced using the computed relationship between ground temperature and environmental parameters to predict temperatures in the upper layer, and then extrapolating these values downwards into the lower zone using a simple conductive heat flow model. The three-dimensional distribution of ground temperatures and permafrost was then obtained by interpolating between the temperature profiles.

5.22 Input Data

5.221 Terrestrial Heat Flux

A value of -50.2 mWm^{-2} (1.25 cal $cm^{-2}s^{-1}$) was assumed for q*, the terrestrial heat flux. No determinations for q* are presently available from interior New Quebec-Labrador (Judge, 1973c, Figure 2), so that it was necessary to make an estimate as to the probable magnitude of this flux. The above value was chosen for two reasons. Firstly, it is consistent with observed temperature conditions in two thermocables, within frozen ground at Timmins 4, for which good geological control is available (numbers 19 and 20). It also falls within the range of previous determinations from the Churchill structural province, of which the Labrador Trough forms a part (Judge, op cit.). At an early stage in the analysis, values of 33.5 mWm^{-2} and 41.9 mWm^{-2} for q* were also considered and tested but ground temperatures projected using these values were not found to be as consistent with observed conditions.

5.222 Environmental parameters

Snow depth, thermal conductivity and elevation variables were next compiled for use with the optimum predictive equations (Table X). These variables were evaluated at each of the 133 points on the Timmins 4 prediction grid (Figure 3).

Data from Figure 6, the Timmins 4 snow map, were used in compilation of snow depth variables, as described in sub-

section 3.332, while elevations were obtained by interpolating between contours on a topographic map of the site (Figure 2). Finally, mean thermal conductivities were computed for depth increments of interest beneath each site. Use was made of Equation 9, the conductivity determinations for individual lithological units given in Table V, and unit thicknesses from the Timmins 4 geological interpretation prepared by the author (see sub-section 3.62).

5.23 Compilation procedure

5.231 Construction of ground temperature profiles

Depth-temperature profiles were constructed in two stages. Firstly, mean annual temperatures were computed for ten standard depths, down to 30m, using the optimum predictive equations, listed in Table X, and the input data described above. The temperature profiles were then extended downwards, at 10m intervals, from 30m to 150m, using Equation 15. In each instance the predicted 30m temperature was substituted for $T(z_a)$, and new Δz and K values were computed. "Frozen" thermal conductivity values (Table V) were employed in all cases, except where the presence of unfrozen ground was definitely indicated (by the occurrence of a predicted positive 30m temperature), when the corresponding "unfrozen" values were used.

5.232 Interpolation

Vertical sections, showing the distribution of ground temperatures were produced by manual linear interpolation between predicted profiles. Unfortunately, with an interval of 60m between profiles, it is not always possible to provide an unambiguous solution, by interpolation alone. This problem was especially acute in compilation of sections across the site, where considerable variation in both relief and snow cover thickness occurs within very short distances, causing anomalies in the distribution of ground temperatures. Difficulties of this type were minimized by taking observed relief and snow variations into account and also by interpolating with reference to temperatures in nearby measured thermocable profiles.

5.24 Comparison between measured and predicted ground temperature sections

Although, the main features of permafrost occurrence at Timmins 4 are now reasonably well known (Nicholson and Thom, 1973), direct comparison between measured and predicted three-dimensional distributions would require complicated procedures. Instead of attempting such a comparison directly, it is proposed to draw conclusions, regarding the validity of the model, based on a consideration of ground temperature sections, compiled using the different procedures. Longitudinal profiles and cross-sections, constructed for this purpose, are shown in Figures 12 and 13.

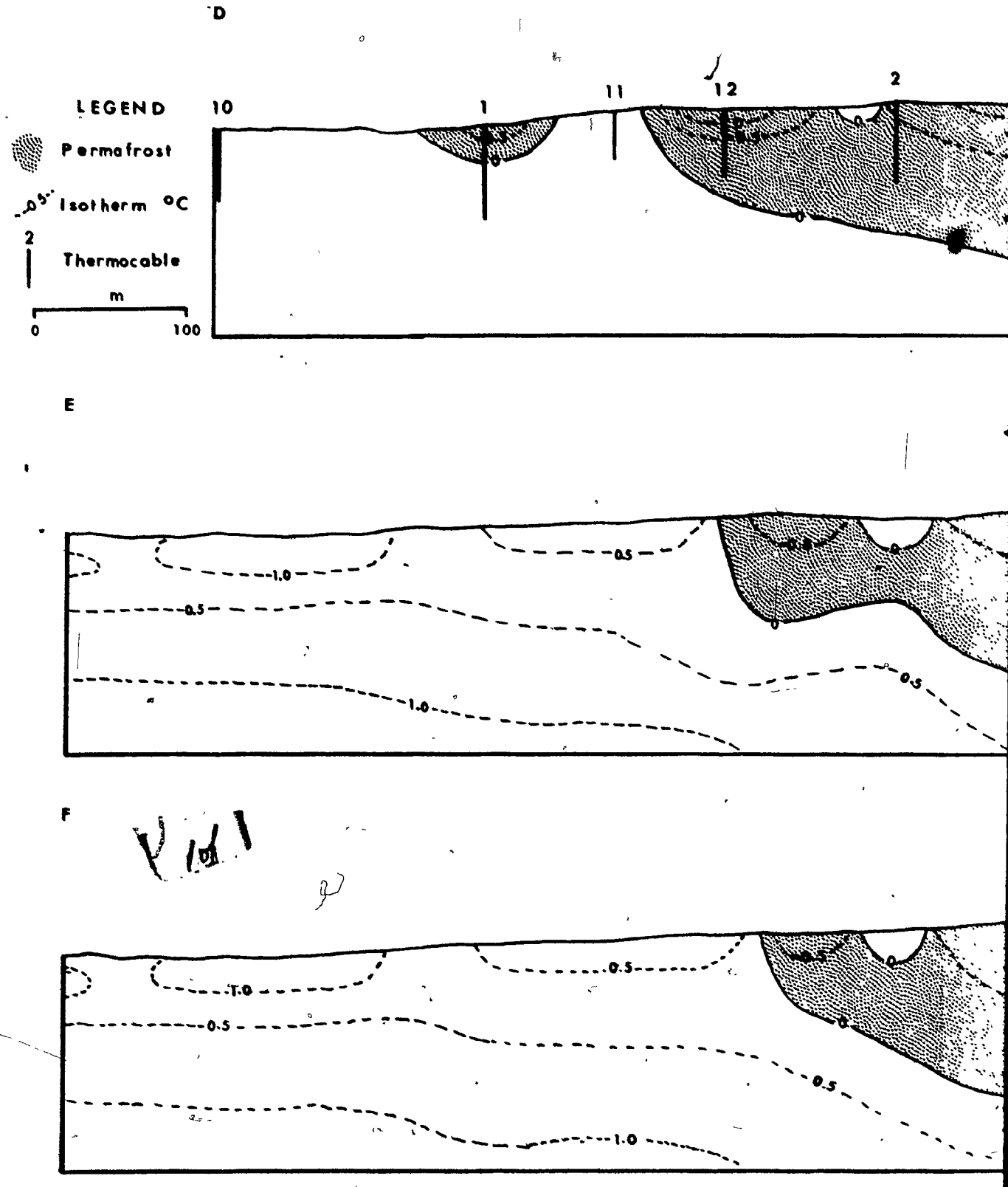

Figure 12: Comparison of measured and predicted longitudinal temperat

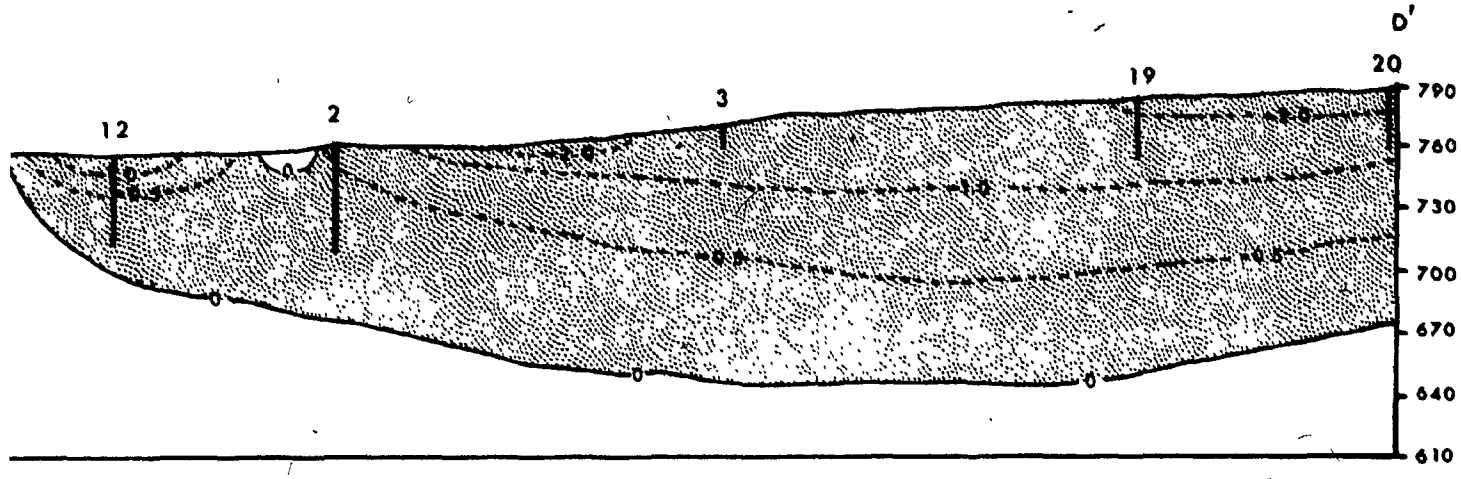

Figure 12a

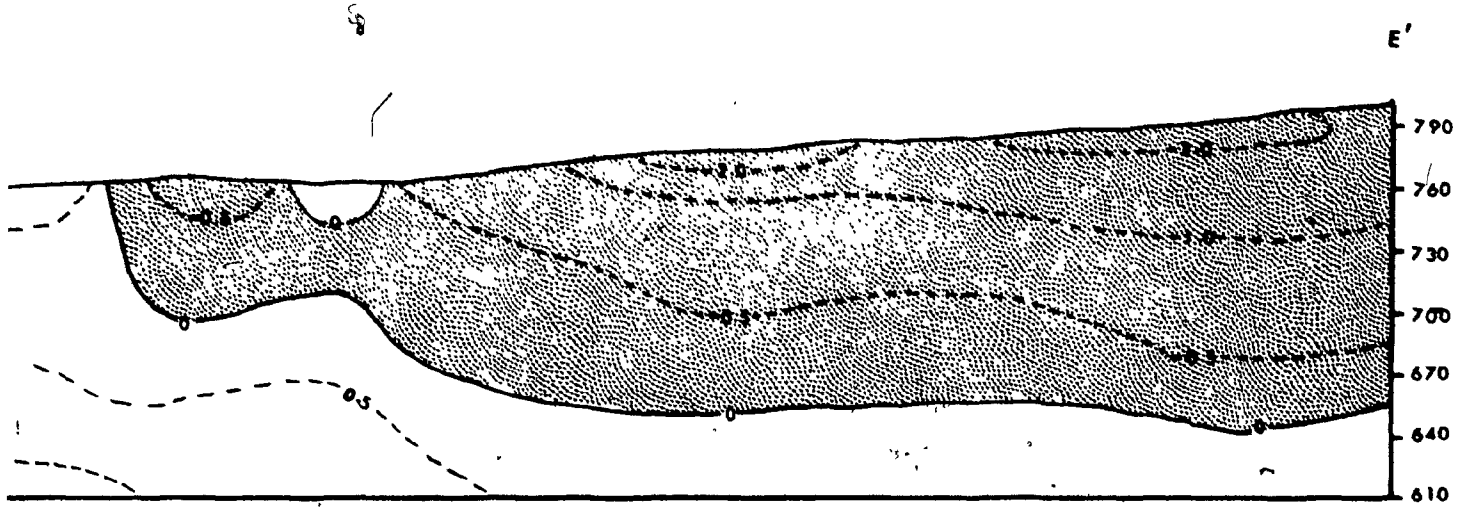

Figure 12b

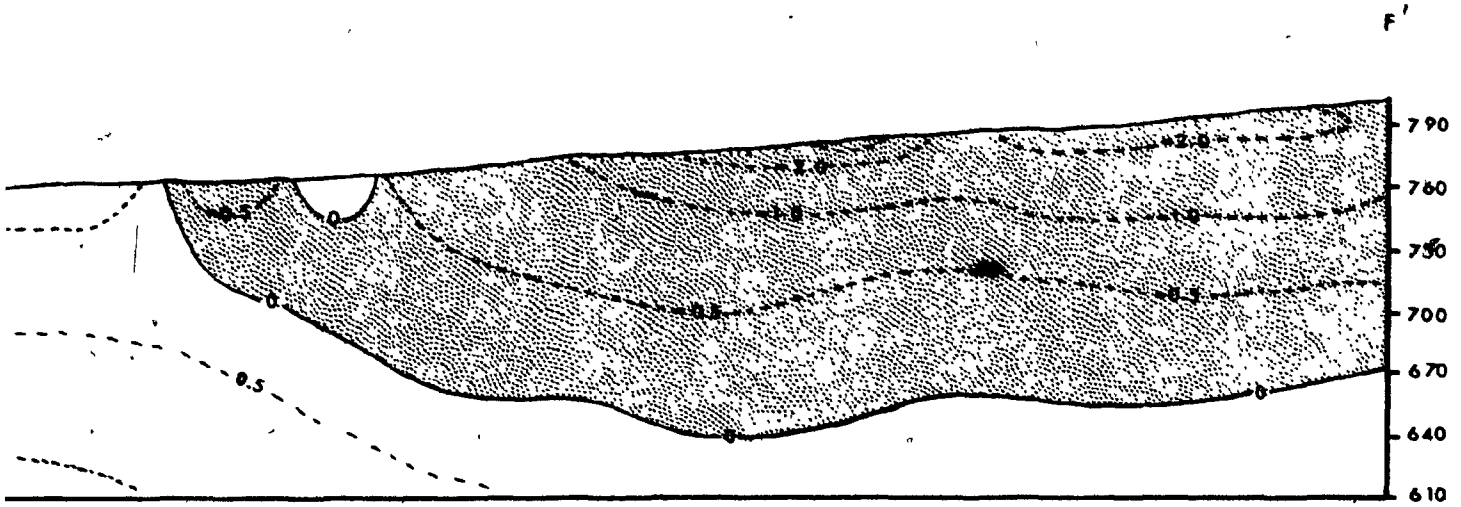

Figure 12c

icted longitudinal temperature profiles, Timmins 4.

1 20f2

5.241 Measured sections

Sections A-A' and B-B' (Figures 12a, 13a) were redrawn, based on those compiled by Nicholson and Thom (1973, Figures 5 and 6), but using the mean temperature values listed in Table II. In addition, profile A-A' was extended southwards to incorporate data from two new thermocables, numbers 19 and 20. The isotherm pattern and inferred distribution of permafrost are essentially the same as those given by Nicholson and Thom. The locations of the two sections are indicated in Figure 3.

5.242 Predicted sections

The corresponding predicted sections, C-C' and D-D' (Figures 12b and 13b, respectively), were constructed from temperature profiles compiled for the line of prediction points, situated closest to the measured sections. The location of these sections is also shown in Figure 3 (they correspond to profile 2+00NE and section 124 on the IOCC survey grid). Although the positions of sections A-A' and C-C' correspond closely, there is a slight discrepancy in the relative positions of the cross-sections (B-B' and D-D'), due to the configuration of the prediction grid. Examination of the predicted temperature distribution on either side of the measured section, however, suggests that no significant changes in thermal regime are involved.

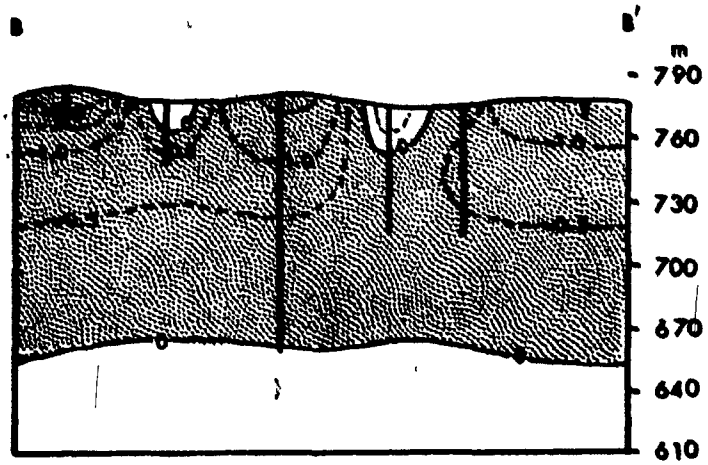

Figure 13a.

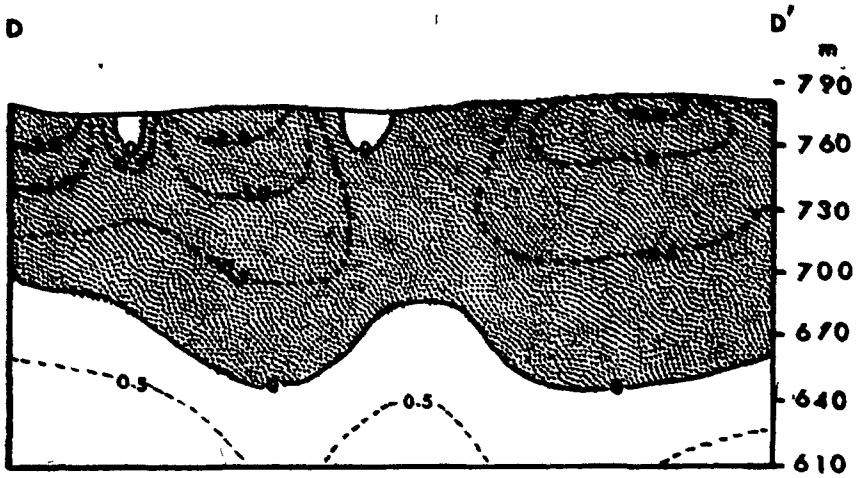

Figure 13b

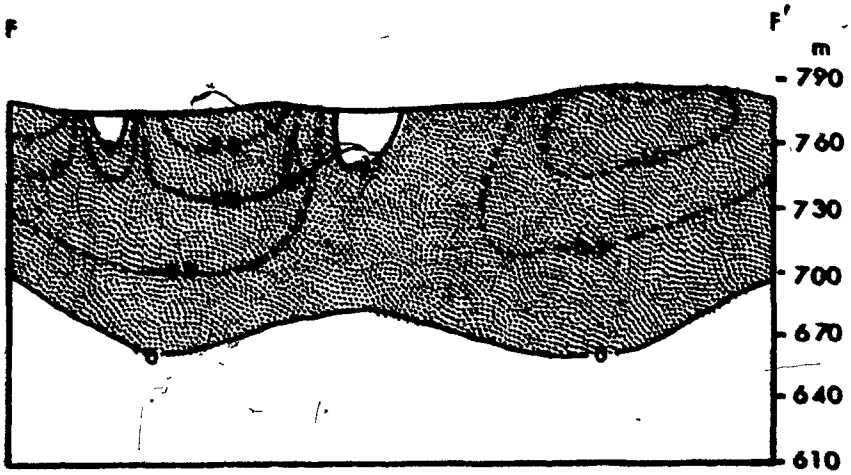

Figure 13c

Figure 13: Comparison of measured and predicted ground temperature cross-sections, Timmins 4. For legend, see Figure 12.

5.243 Comparison

There is good agreement between the longitudinal profiles, A-A' and C-C' (Figures 12a and 12b), as regards both the isotherm pattern and the proposed distribution of permafrost. Frozen ground appears to extend, in both cases, to a depth of approximately 140m to 150m. It is unfortunate that there is no deep temperature control in the areas of deepest permafrost to confirm this prediction.

The correlation between the cross-sections, B-B' and D-D', is not as good. Although the general pattern of isotherms is similar, individual isotherms and the base of permafrost in the predicted section, D-D', show considerably greater relief than the measured section B-B' would suggest is actually present (Figure 13). This discrepancy is most apparent beneath the major valley, there being reasonable agreement under the ridges. An explanation and suggested correction are given below.

5.25 Improvements in the basic model

5.251 Problems with the one-dimensional model

The relatively low accuracy with which the model is able to reconstruct the ground thermal regime, beneath valley sites, is noticeable (e.g. Figure 13b). To a great extent, this deficiency appears to reflect the presence of non-vertical heat transfers, set up between the generally warmer valleys and somewhat cooler

ridge areas, in response to lateral variations in near-surface ground temperature (see sub-section 2.62).

Use of the one-dimensional conduction model implies, firstly, that temperatures increase steadily with depth, under the influence of the terrestrial heat flux q*, and secondly, it assumes, tacitly, that there is, in effect, a semi-infinite uniform upper boundary at a depth of 30m (z_a). Unfortunately, observed temperature data, and sections constructed therefrom (e.g. Figure 13a), indicate that neither condition is strictly fulfilled at the Timmins 4 site. Ground temperatures at the 30m level show considerable lateral variation (Table II), and, especially in the vicinity of valley and deep snow areas, the thermal regime is rarely consistent with a one-dimensional model. In practice, near the 30m level, there is often either no vertical temperature gradient, or temperatures decrease with increasing depth, due to lateral heat flow effects. When employed as a basis for construction of deep ground temperature profiles, the resulting predicted values give rise to the anomalous predicted isotherm distribution (Figure 13b).

5.252 Proposed modification to allow for lateral heat flow effects

The influence of lateral heat flow may be approximated by taking into account predicted temperatures at laterally-adjacent prediction points. By analogy with the snow cover-temperature relationship (section 3.3), it is proposed, as a first approximation, that

each of the predicted 30m values be replaced by an average 30m temperature compiled over a circle of radius twice the depth of interest. These new values will be entered, as before, in Equation 15, to predict a new temperature for each depth. As an illustration, in computing the temperature at 70m (i.e. 40m below z_a), the average temperature for a circle of radius 80m (i.e. twice 40m) would be substituted for $T(z_a)$ in Equation 15.

5.253 Improved Timmins 4 temperature sections

The longitudinal profile and cross-sections shown in Figures 12b and 13b have been redrawn using temperature profiles constructed as described above. For convenience in comparison with observed and previously predicted conditions, these new sections are reproduced as Figures 12c and 13c respectively.

In general, the pattern of isotherms, and implied heat flow distribution, remains similar in all three sets of sections. Moreover, the spatial distributions of frozen and unfrozen ground in each case appear to be in good agreement. However, the three-dimensional geometry and basal configuration of permafrost, inferred from measured temperatures (Figures 12a, 13a), albeit fairly approximate, do seem to be more accurately reproduced in the revised sections (Figures 12c, 13c), than in those compiled using the original model (Figures 12b, 13b).

Overall, the proposed correction leads to a reduction in predicted permafrost thicknesses beneath the ridges, and an increase under the valleys. Thus, there is a net reduction in the amplitude of relief on the base of permafrost and a general smoothing of the isotherms. Assuming that the observed sections (Figures 12a, 13a) constitute the most reasonable presently-available approximation for actual ground temperature conditions at Timmins 4, then it is tentatively concluded that the proposed correction makes possible the desired improvement in the accuracy of the original model. This being the case, a full-scale prediction was compiled, using the improved profiles, for the distribution of ground temperatures and permafrost at Timmins 4.

5.26 Problems resulting from the inclusion of elevation

A typical optimum predictive equation, that included the elevation variable, is:

$$T_{15m} = 0.018 \cdot SNOW30 - 0.033 \cdot ELEV + 23.88 \qquad (16)$$

By varying elevation, while holding snow depth constant, it can be shown that this equation indicates a change in ground temperature of approximately $3^{o}C$ per 100m (compared with the dry adiabatic lapse rate of $1^{o}C$ per 100m). Such a gradient is considerably greater than that occurring naturally at Timmins 4. Assuming vertical heat flow and a terrestrial heat flux, q*, of $-50.2\ mWm^{-2}$, it appears to indicate the presence of rock material

with a thermal conductivity of about 16$Wm^{-1}K^{-1}$. In fact, the range of conductivities observed at Timmins 4 is between 2.2 $Wm^{-1}K^{-1}$ and 7.4 $Wm^{-1}K^{-1}$ (Table V). This discrepancy, it is concluded, indicates that the inclusion of elevation has made the equations site specific.

An attempt was made to test this hypothesis, by applying the model at thermocable sites on Ferriman Ridge which is more than 60m higher than Timmins 4. Predicted temperatures were up to 2°C colder than measured. Since the Nicholson-Granberg model was found to apply at Ferriman (Nicholson and Granberg, 1973), it appears almost certain that the optimum predictive equations are indeed site-specific.

While it is possible that this situation limits application of the predictive equations to the Timmins 4 site, this is not necessarily the case. In the next chapter, the model will be tested at a new site in the Timmins mining area. Timmins 2 lies within the same elevation range as Timmins 4, but is otherwise quite dissimilar.

5.3 OCCURRENCE OF PERMAFROST AT TIMMINS 4

5.31 Present knowledge of ground temperature conditions

The following brief synthesis of the results of studies at the Timmins 4 site since 1968 is intended as a framework within which the distribution, projected by the model, may be discussed.

The spatial distribution of frozen ground has been approximated at different depths by Thom (1970), Granberg (1973, Figure 8) and Nicholson (1974, Figure 16). In addition, approximate indications as to its possible vertical development have been provided in measured sections (Thom, 1969; 1970; Nicholson and Thom, 1973), and in predicted sections by Nicholson (op cit.). Unfortunately, neither the exact position of the permafrost base, nor its configuration is known with certainty. Maximum thicknesses of 100m to greater than 130m have been inferred by different authors, from extrapolation of measured thermocable profiles (Thom, 1970; Nicholson and Thom, op cit.). Séguin (1974a) states that deep resistivity profiling suggests the lower permafrost boundary, in one part of the site, occurs at a depth of approximately 150m. Séguin and Garg (1974) report an approximate depth of 53m (175 ft) at thermocable No. 3 (see Figure 3, for location).

From these studies, it is concluded that permafrost is essentially continuous beneath the site, except for its northeastern sector. Vertical development is greatest beneath the ridges, and the frozen layer is thinner, sometimes with the presence of talik zones, under the main valleys. Frozen ground becomes increasingly discontinuous, both horizontally and vertically, towards the lower, northern part of the site, where it is restricted to small isolated areas with low winter snow accumulation.

5.32 Predicted distribution of permafrost and unfrozen ground

The occurrence of frozen and unfrozen ground, as predicted by the improved model, is illustrated in Figures 14 to 17. Permafrost underlies approximately sixty percent of the Timmins 4 site. It is continuous, with a maximum thickness of approximately 150m, beneath ridge and valley terrain in the upper, southeastern half of the site, and occurs also as a smaller, frozen body, to a maximum depth of about 50m, near its western corner. The northern part of the site, with the exception of a few scattered, shallow permafrost occurrences, is unfrozen, as are the lower portions of the major valleys. Talik zones underlie the upper parts of these valleys.

5.321 Vertical sections

Together the longitudinal profiles (Figure 12c, 14) and cross-sections (Figure 13c, 15a-d) allow an impression to be gained of the three-dimensional distribution of ground temperatures, and heat flow pattern, at Timmins 4. Heat transfer at depth, appears to be essentially vertical over most of the site. Temperatures increase steadily with depth beneath the ridges, under the influence of the terrestrial heat flux but, beneath the valleys, temperatures often decrease, initially, before taking on the more normal pattern with depth. In the intermediate areas, between ridge and valley, the presence of near-vertical isotherms suggests

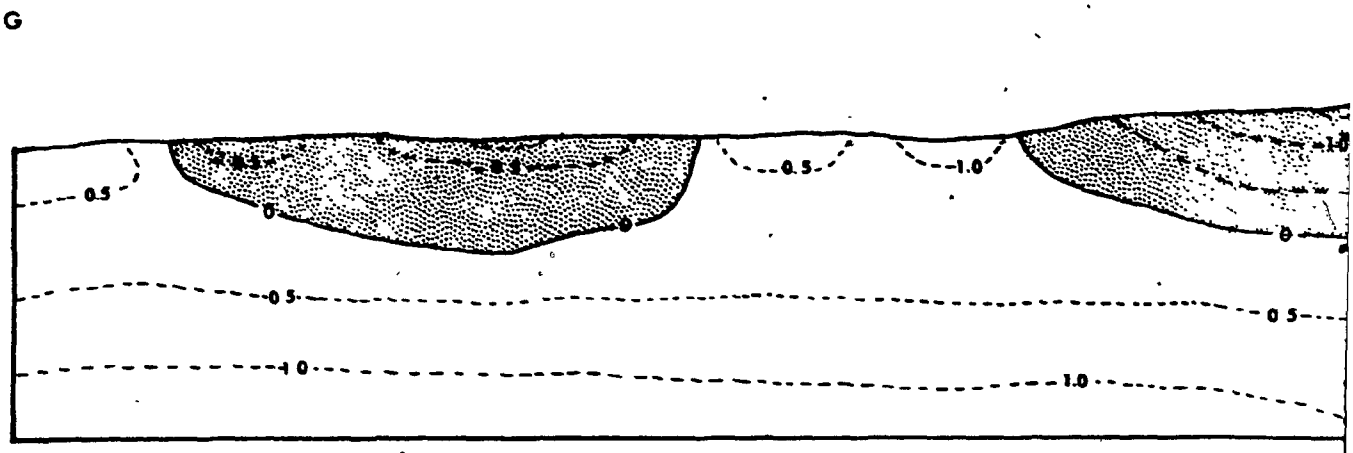

Figure 14: Predicted longitudinal temperature profile, Timmins 4.

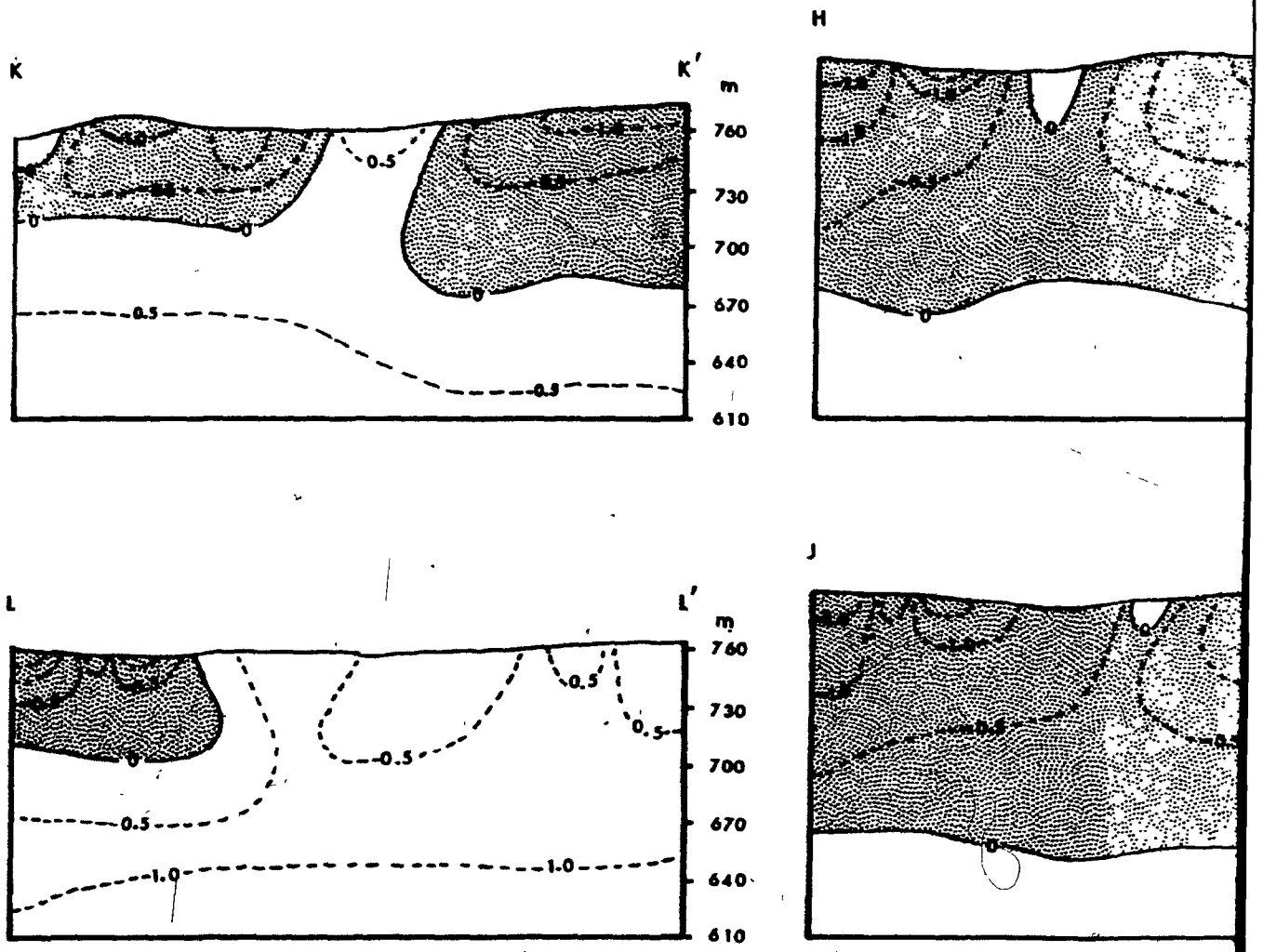

Figure 15: Predicted ground temperature cross-sections, Timmins 4.

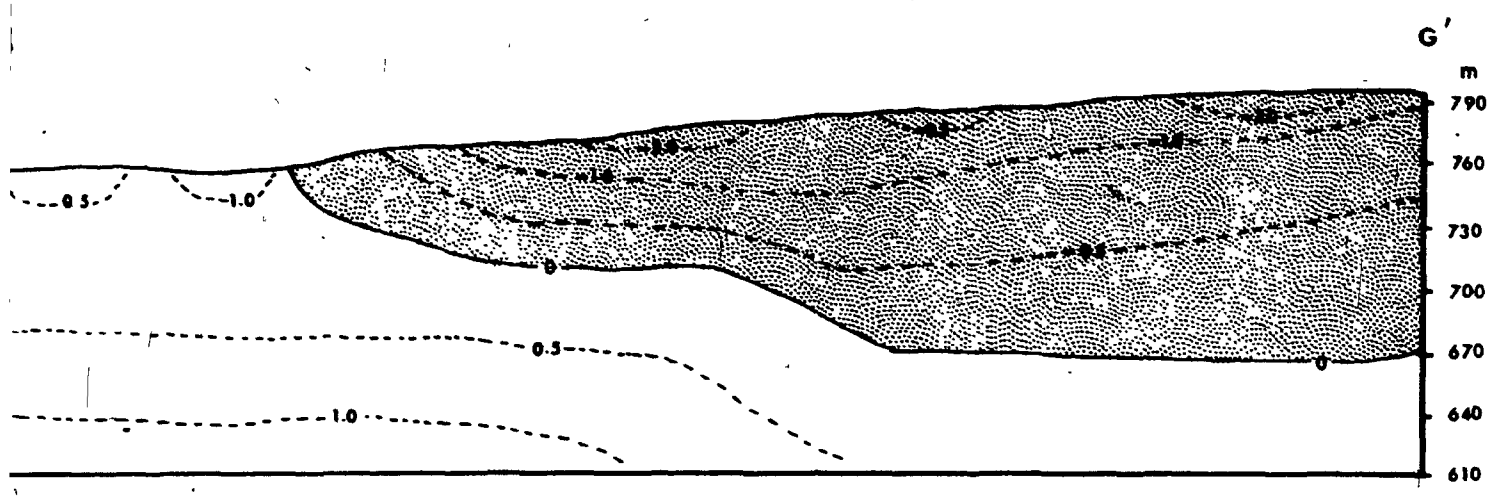

ature profile, Timmins 4.

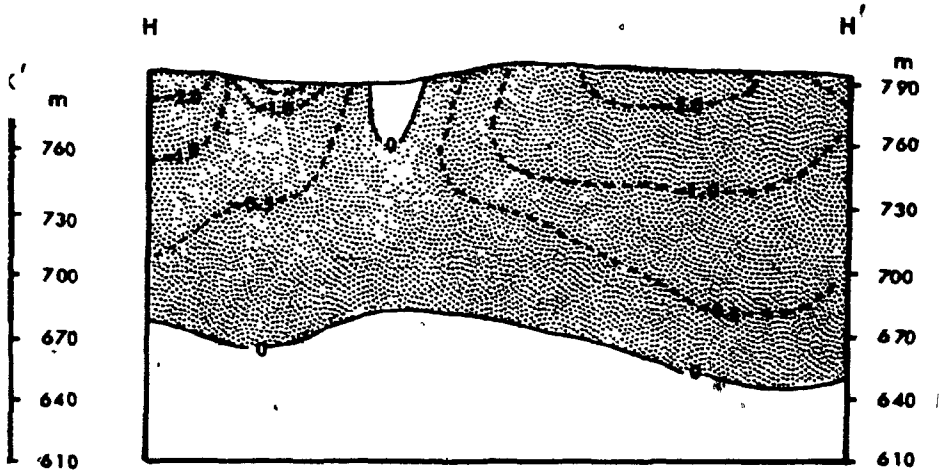

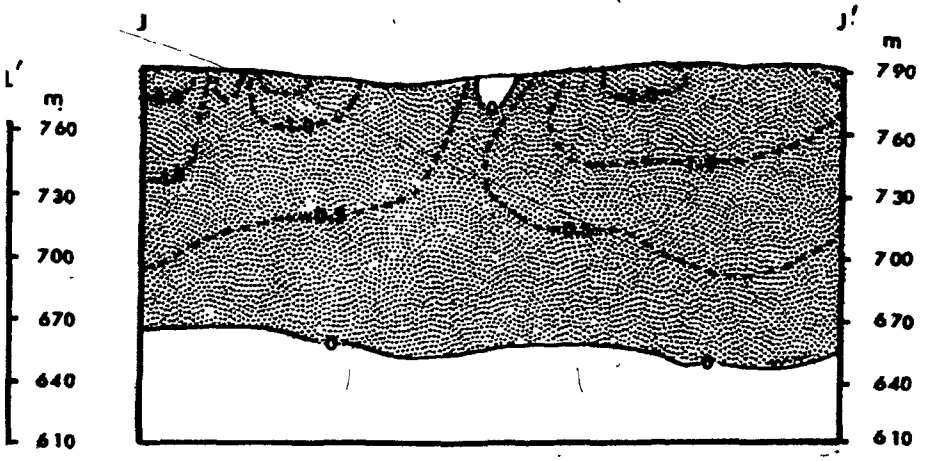

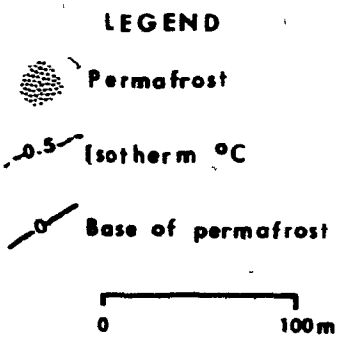

cross-sections, Timmins 4.

that horizontal heat flow is dominant. The overall heat flow pattern is, thus, one of net heat gain beneath the valleys, and net loss from the ridge areas.

5.322 Permafrost thicknesses

Figure 16 was compiled by contouring predicted permafrost thicknesses, as indicated by the position of the 0°C isotherm in each profile. Frozen ground occurs to a depth of about 150m beneath the ridge at the southern end of the site. Elsewhere the permafrost becomes thinner. In the north of the site, thicknesses range from 40 to 50m in the permafrost body near the western corner, to approximately 20m or less in small, isolated, masses within the otherwise unfrozen area. Absolute thicknesses are somewhat reduced in valley locations due to the presence of talik zones, which are up to 20m thick (see, for example, Figure 15b).

5.323 Base of Permafrost

The configuration of the permafrost base was defined by contouring basal elevations in each predicted profile. Figure 17 shows that the base of permafrost is a somewhat exaggerated mirror image of the surface relief. In general, it occurs at the greatest depths beneath the ridges, and is rather shallower under the valleys. The base of permafrost rises gradually northwestwards, along the axis of the site, from a minimum of about 630m (IOCC datum) in its southeast corner. The margins of individual permafrost bodies

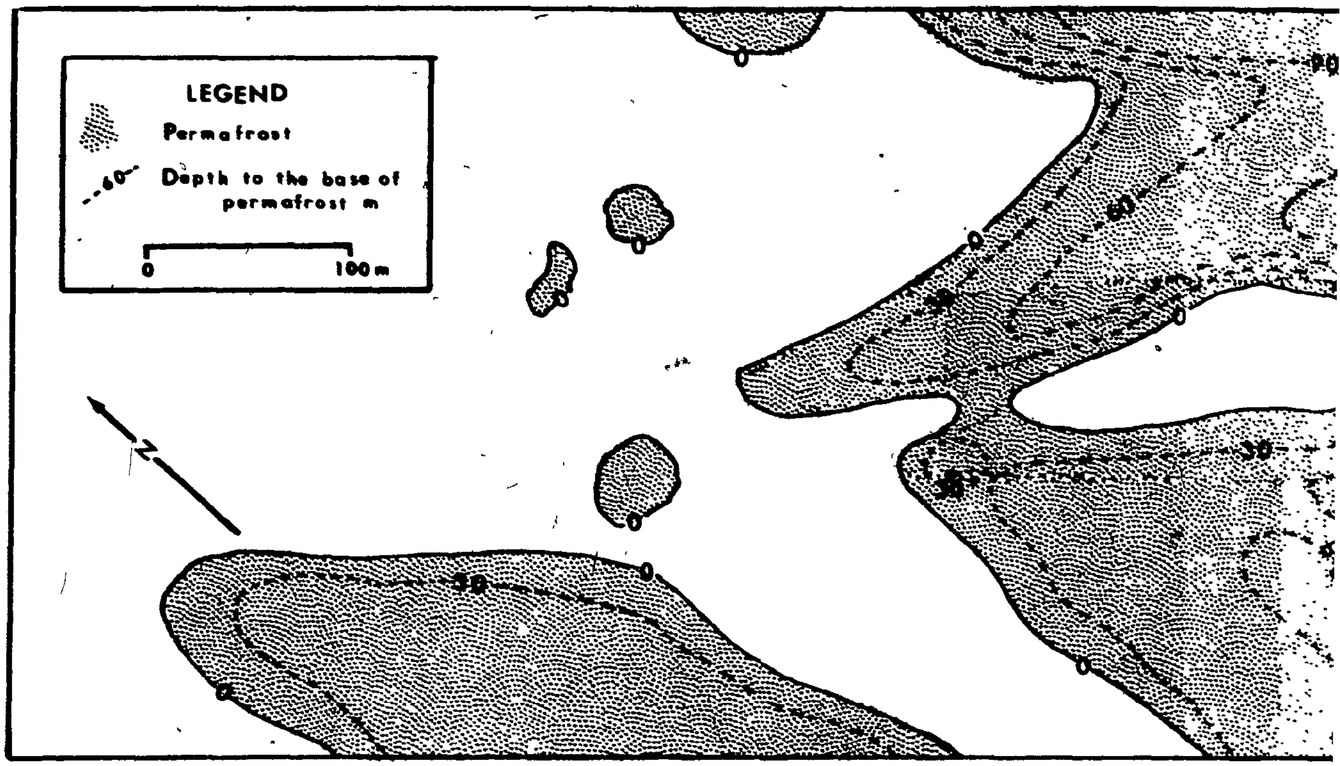

Figure 16 (Above): Permafrost depths, Timmins 4.   Figure 17 (Below)

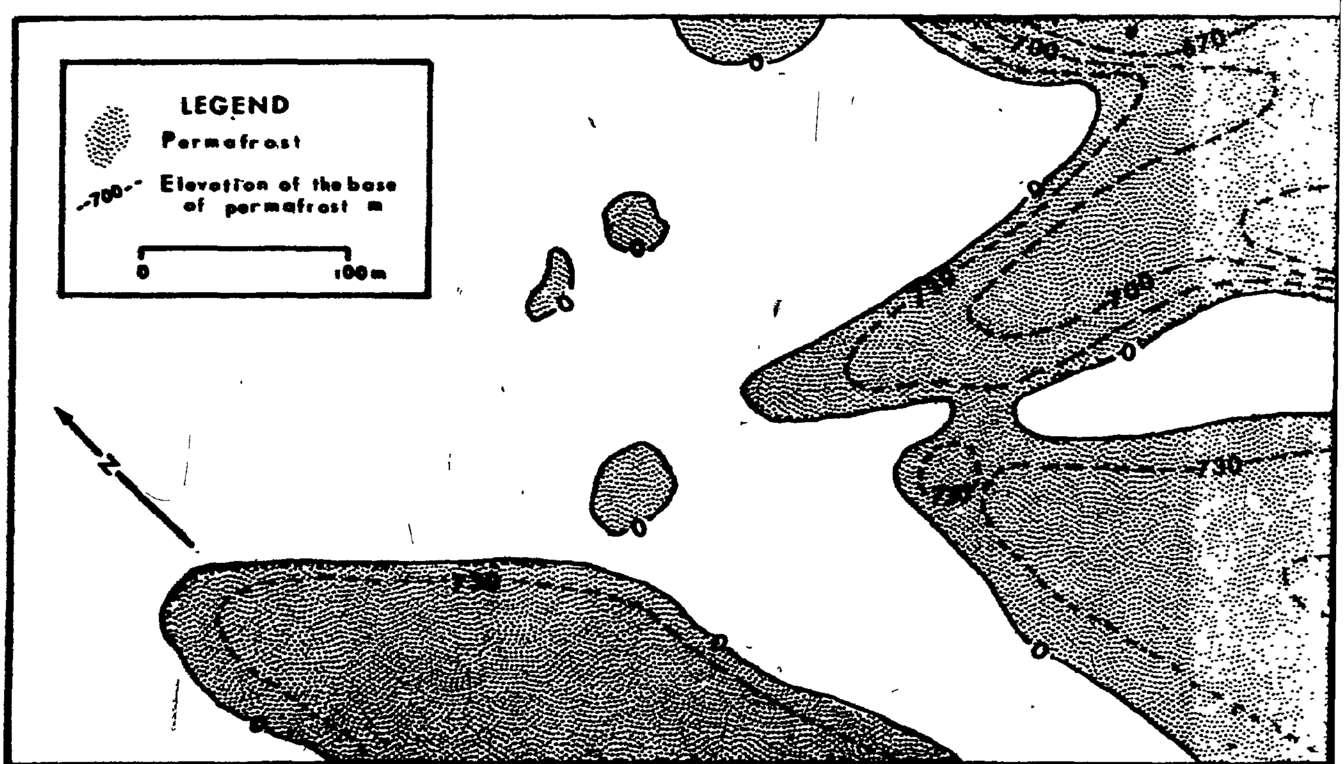

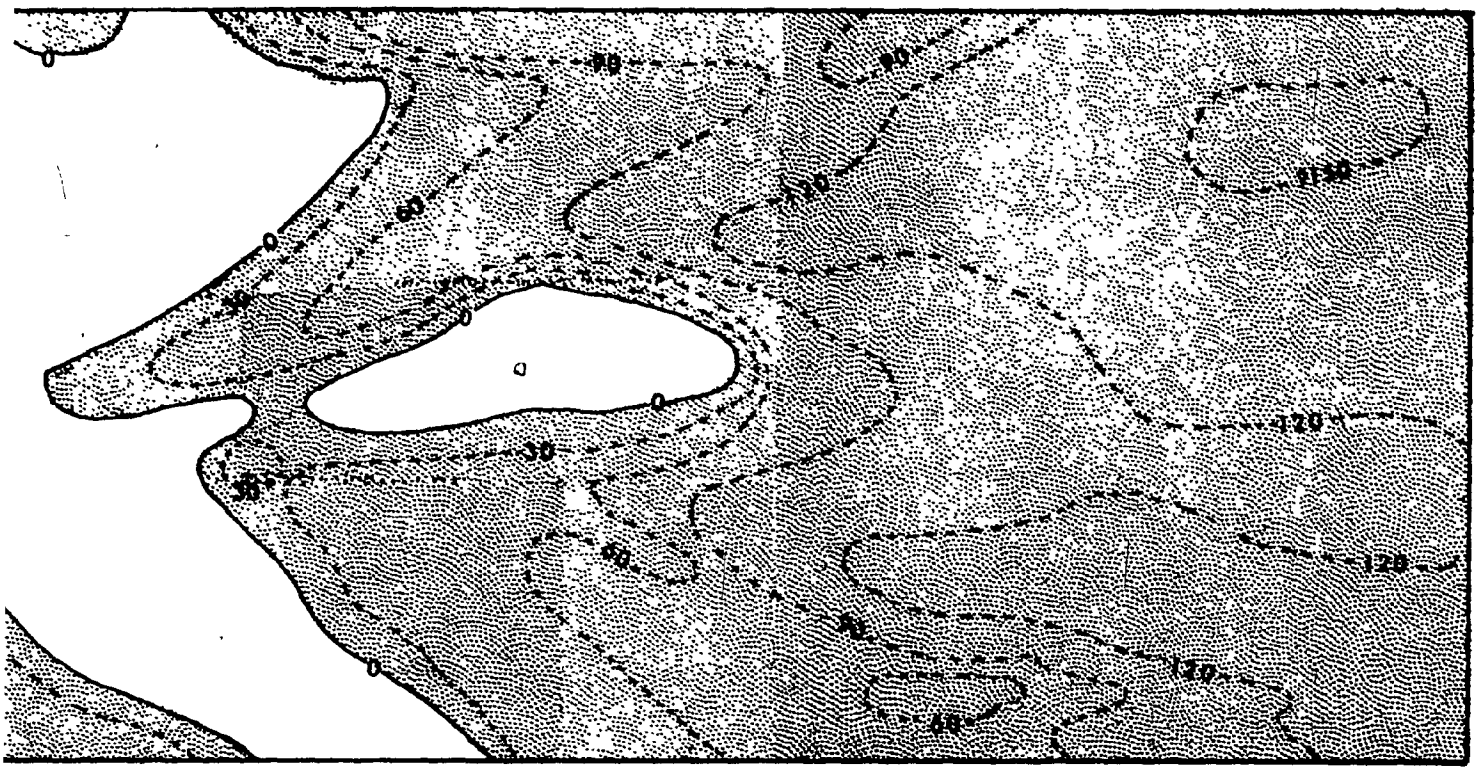

1 2 of 2

Timmins 4. Figure 17 (Below): Elevation of the base of permafrost, Timmins 4.

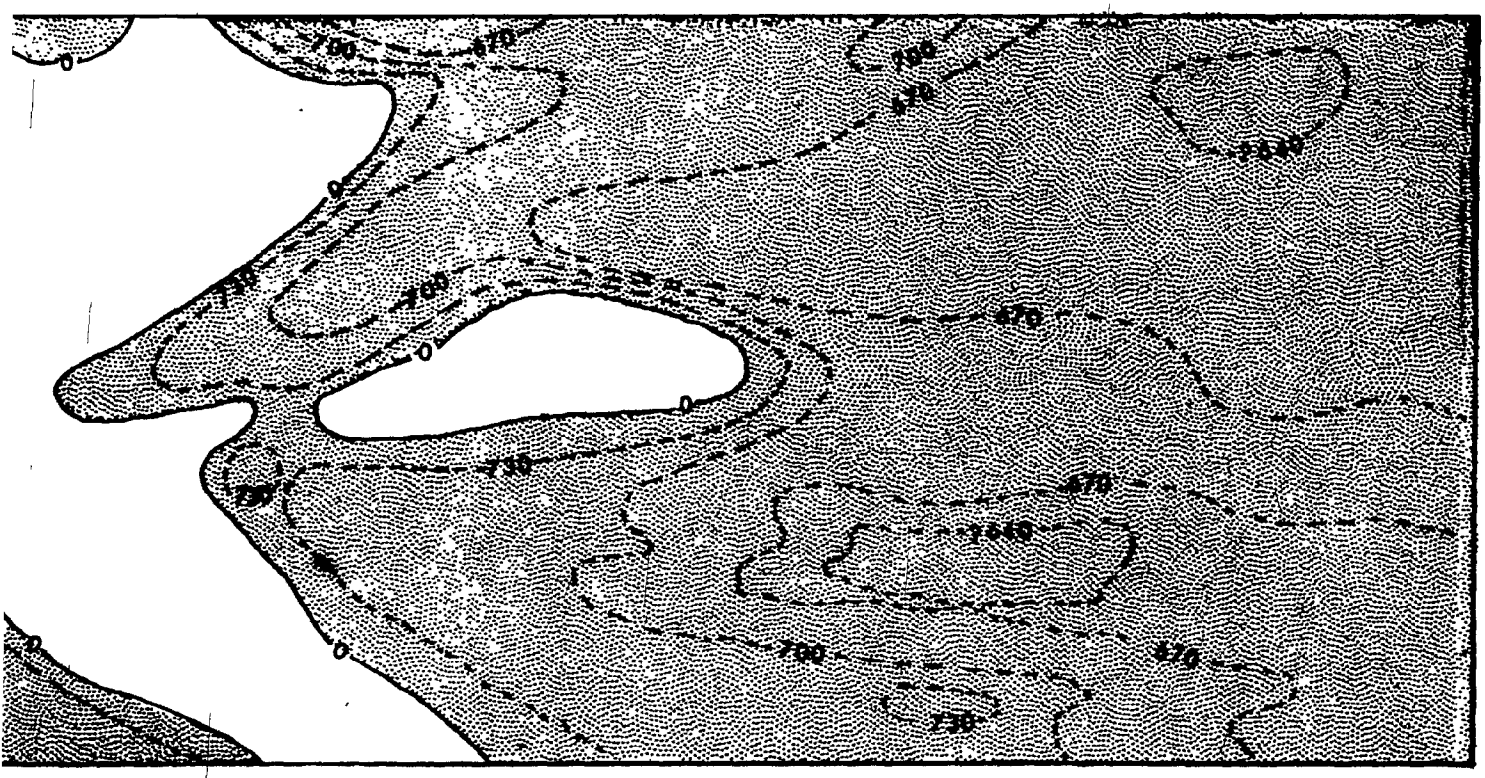

are apparently steeply inclined, rather than gradually wedging out, in agreement with Nicholson and Thom (1973).

5.324 Unfrozen areas

According to the prediction, about forty percent of the Timmins 4 site is unfrozen. These areas are delineated in Figure 16. Unfrozen ground also occurs as talik zones within the major valleys. The extent of such zones may be estimated from the vertical temperature sections (e.g. Figure 15).

5.33 Accuracy of the permafrost prediction

Comparison between measured and predicted ground temperature sections and profiles, suggests a close correspondence between the actual distribution of shallow ground temperature, and that projected here (sub-section 4.32). At the same time, the validity of the prediction varies spatially, such that the best fit is obtained in the frozen areas. It is least good where the ground is unfrozen. There is no apparent reason why these relationships should not be applied over the Timmins 4 site as a whole.

It is considerably more difficult to assess the accuracy with which permafrost thicknesses are predicted. A major problem is the absence of thermocables, penetrating the base of permafrost in the main permafrost area of Timmins 4, which would thereby indicate its position. Existing best estimates of the

thickness of frozen material at each thermocable site, obtained by extrapolation of measured profiles, are compared with predicted thicknesses in Table XIV. These data suggest that the model provides a reasonable estimate of permafrost thicknesses in the vicinity of the thermocables. If it is assumed that the accuracy of the input data used in compilation of the prediction is uniform across the site, then permafrost thicknesses can probably be considered to vary spatially with variations in predicted 30m ground temperature. This means that the prediction is subject to the same deficiencies as the predicted temperatures. Thus, projected permafrost conditions are probably closest to the actual situation beneath the ridges. In the valleys, where talik zones are present, the accuracy of prediction is lower due to the effects of circulating ground water and deep snow conditions.

In the final analysis, the validity of this assessment can only be tested by direct comparison, when the geometry of permafrost is defined in greater detail: either through additional temperature measurements or, as appears more likely, via direct observation when the Timmins 4 ore body is mined.

CHAPTER 6

OCCURRENCE OF PERMAFROST AT TIMMINS 2 - A TEST OF THE MODEL

It is virtually certain that many future mine sites in the Schefferville area will be underlain, at least in part, by perennially frozen ground. Potential mine sites are widely distributed and occur under a variety of natural conditions (Stubbins et al., 1960. Table 3.) Hence, it follows that predictive techniques, if they are to be of value in delineating permafrost zones, as an aid in mining, should have as wide an application as possible.

The model, presented in Chapter 5, seems to provide a reasonable estimate of permafrost development at the Timmins 4 Experimental Site (sub-section 5.33). Unfortunately, inclusion of the elevation variable has made the procedure site-specific to some degree. Until the full significance of elevation is established, allowing the specific relief characteristics of other sites to be introduced into the model, it is not feasible to employ the technique, without qualification, for permafrost prediction in the Schefferville region as a whole. It is not unreasonable, however, to suppose that the procedure might have application at sites in other parts of the Timmins mining area, which lie within the same elevation range as that found at the Timmins 4 site.

As a test of this hypothesis, an additional prediction was compiled for the site of the Timmins No. 2 mine. This is

described below.

6.1 THE TIMMINS 2 SITE

The location of Timmins No. 2 Mine is shown in Figure 1. It is situated approximately 1 km southeast of the Timmins 4 Experimental Site, and adjacent to the existing Timmins No. 1 Mine. The area chosen for detailed study corresponds approximately to the proposed ultimate open pit limits of the mine. Timmins 2 is situated at an elevation of between 750m and 775m (IOCC datum).

6.11 Physical Characteristics

The relief and surface drainage of the Timmins 2 site are shown in Figure 18. The northern part consists of a broad, upland ridge area, flanked by two narrow, southward-sloping channels. This area, which is bisected by a shallow valley, is generally well-drained. The southern portion of the site has more subdued, undulating relief and is relatively poorly-drained. The channels drain southwards across this area, via a series of ponds (mostly ephemeral) and streams, into Elross Creek (Figure 1). The Timmins 2 site has a generally southerly aspect.

Due to the close proximity of the Timmins 2 and Timmins 4 sites, it is reasonable to assume uniform climatic conditions, including snow melt. Similarly, the vegetation types, and their relation to relief are basically the same: the ridge areas have a lichen-bare ground assemblage while more sheltered, less well-

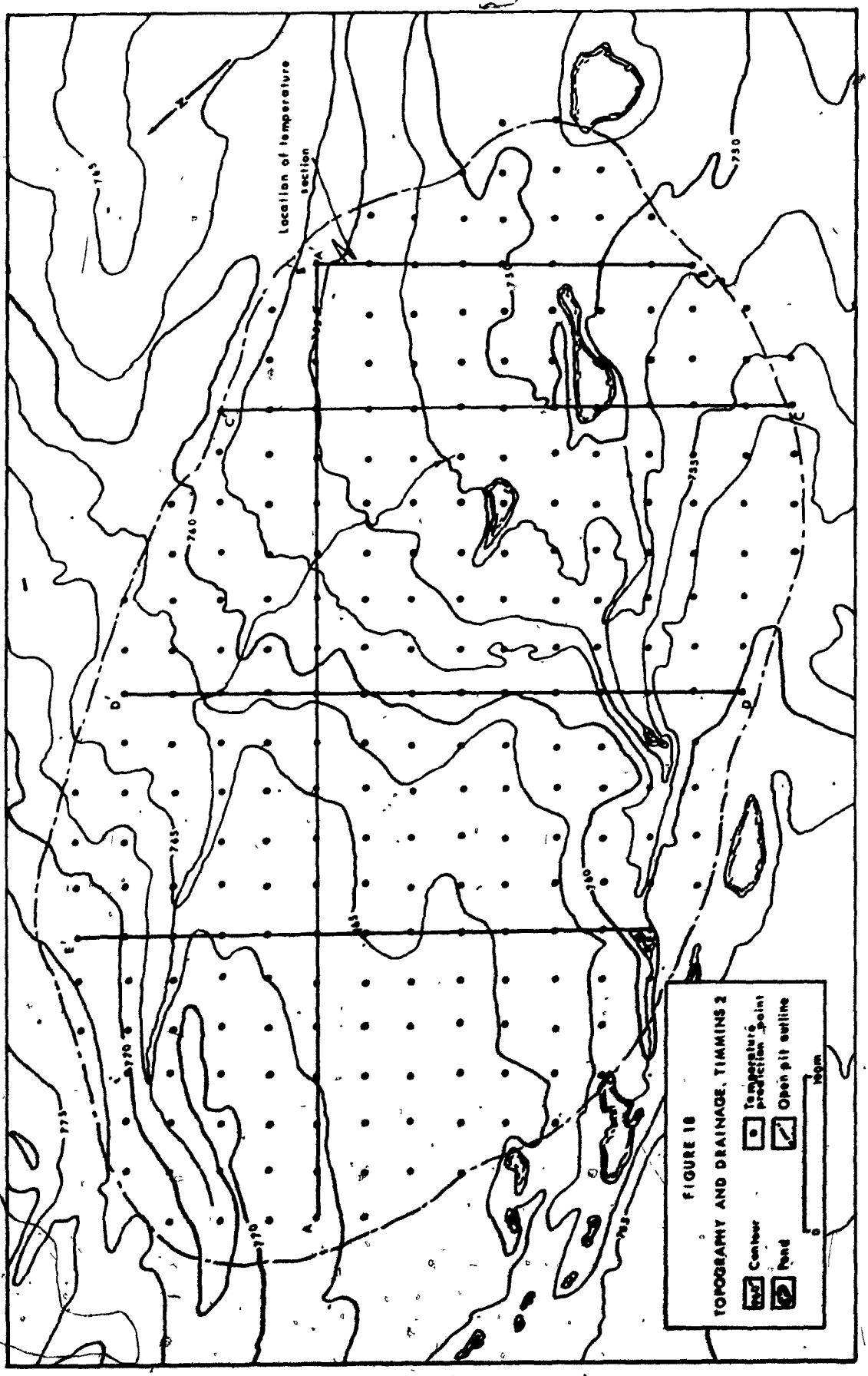

FIGURE 18

TOPOGRAPHY AND DRAINAGE, TIMMINS 2

drained lower parts of the site have a cover of mosses and vascular plants. Lichen woodland *per se* is not present at Timmins 2.

Geologically, the site is similar to Timmins 4 in that it is underlain by units of the Knob Lake Group (for stratigraphy see Table I). The Timmins 2 deposit itself occurs within the faulted limb of a Sokoman Iron Formation syncline (IOCC, internal report). Its structure is similar to that illustrated for Timmins No. 1 Mine, by Séguin (1974b, Figure 4). In compiling the present prediction, it has been assumed that the physical and thermal properties of the rock types at Timmins 2 are identical with those recorded for Timmins 4 (Table V).

6.12 Permafrost distribution

The occurrence of frozen ground within the Timmins 2 site is poorly documented, due to a lack of ground temperature information. A subjective evaluation of the distribution of environmental parameters such as relief, vegetation and snow depth, however, allows tentative conclusions to be drawn, which can serve as a basis for further discussion.

Based on such an appraisal, it is concluded that, overall, permafrost is discontinuous at Timmins 2. It is essentially continuous beneath the upland ridge areas, but discontinuous or absent elsewhere. Talik zones are probably developed

beneath the upper portions of the two major channels. Comparison of relative snow cover thicknesses at the Timmins 2 and 4 sites would suggest that frozen ground thicknesses are not so great at Timmins 2.

6.2 GROUND TEMPERATURE CONDITIONS AT TIMMINS 2

The distribution of ground temperatures was modelled, in three dimensions, using the improved procedure described in sub-sections 5.21 and 5.23. Plans and sections, illustrating the projected geometry of permafrost and occurrence of frozen and unfrozen ground, are shown in Figures 20 through 22, and discussed in detail in sub-section 6.22.

6.21 Compilation of the prediction

The same procedure was used for the Timmins 2 prediction as was employed at Timmins 4 (sub-section 5.21 and 5.23). In this instance, however, a larger number of ground temperature profiles was employed (299 compared to 133). These are located at the intersections, 30m apart, of the approximately 700m by 450m grid, shown in Figure 18. A 30m grid was chosen in an attempt to avoid the problems encountered in interpolating between profiles on the 60m grid used at Timmins 4.

6.211 Data collection.

Snow depth, elevation and thermal conductivity variables were

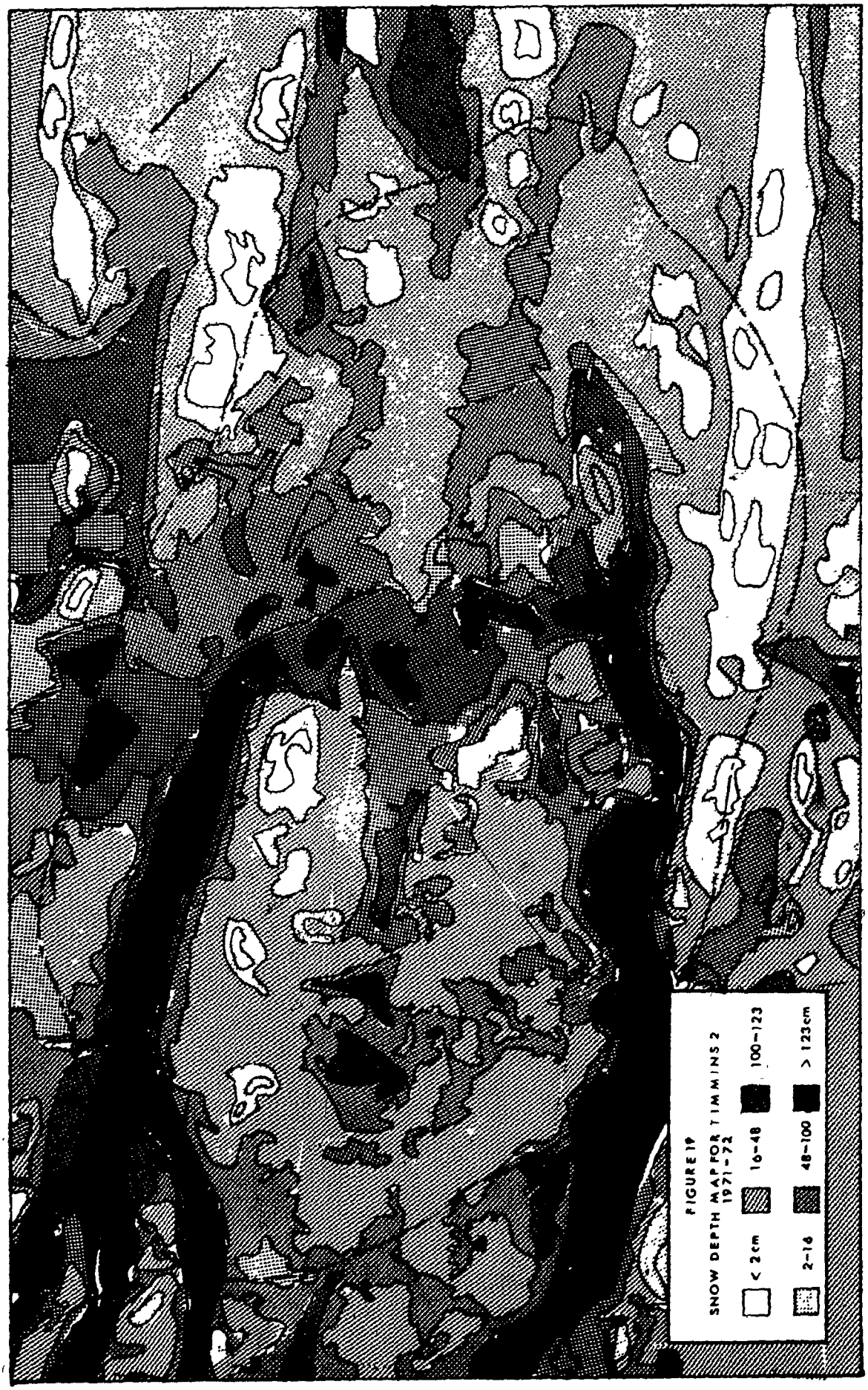
FIGURE 19
SNOW DEPTH MAP FOR TIMMINS 2
1971-72
< 2cm
2-16
16-48
48-100
100-123
> 123cm

evaluated for each grid point as described in the relevant sections of Chapter 3.

Elevations were obtained by interpolating between map contours. The resulting values all lie within the range of those employed in deriving the optimum predictive equations at Timmins 4, but with a somewhat smaller range.

Figure 19 is a map of peak snow accumulation for winter 1971-72 at Timmins 2. The map was produced from sequence melt air photography taken on the five flights documented in Table III (Plates 6 to 10). Details of the method employed, which is identical to that used at Timmins 4, are given in section 3.3. The same values (Table III) were adopted for the depth categories on both snow maps, snow melt rates being assumed uniform at both sites. Data were removed from the map by means of the procedure described in section 3.33, and illustrated in Figure 8.

Mining operations have now commenced at Timmins 2, so that detailed geological information is available. Thermal conductivity variables were compiled, for each prediction point using data on rock types and unit thicknesses obtained from IOCC sections and plans, and the conductivity data given in Table V.

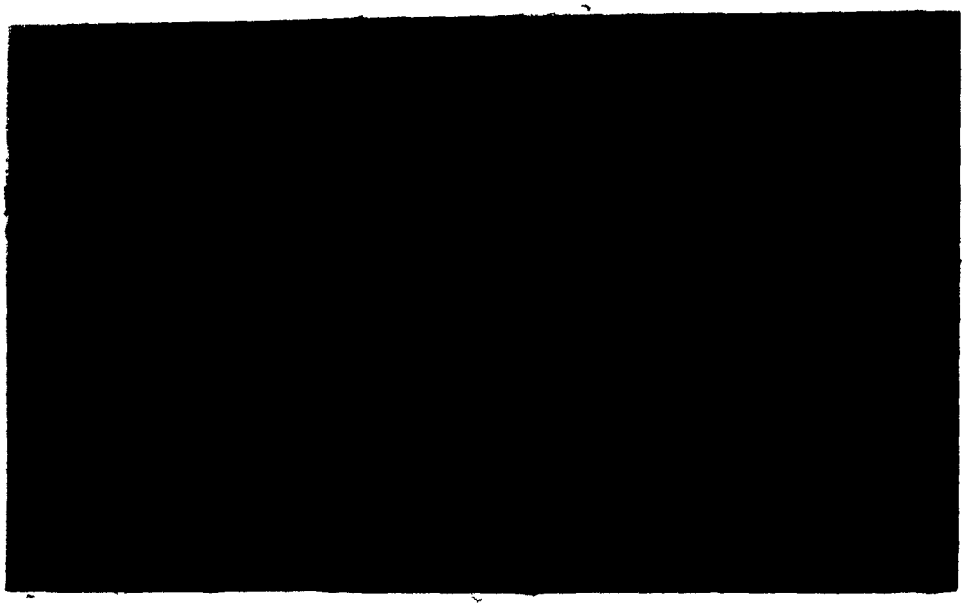

Plate 6: Snow distribution at Timmins 2, 27 April 1972

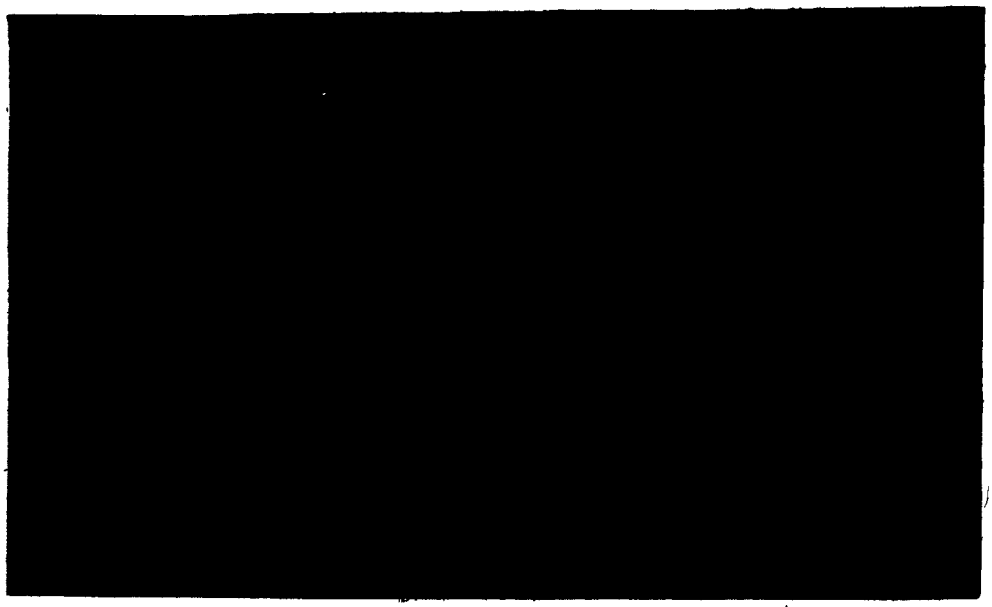

Plate 7: Snow distribution at Timmins 2, 16 May 1972

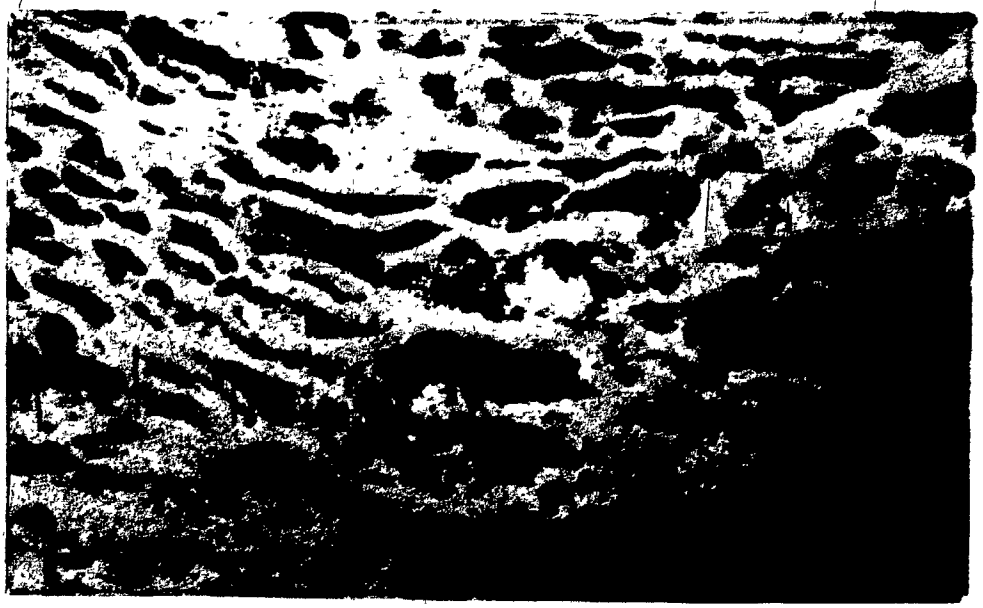

Plate 8: Snow distribution at Timmins 2, 30 May 1972

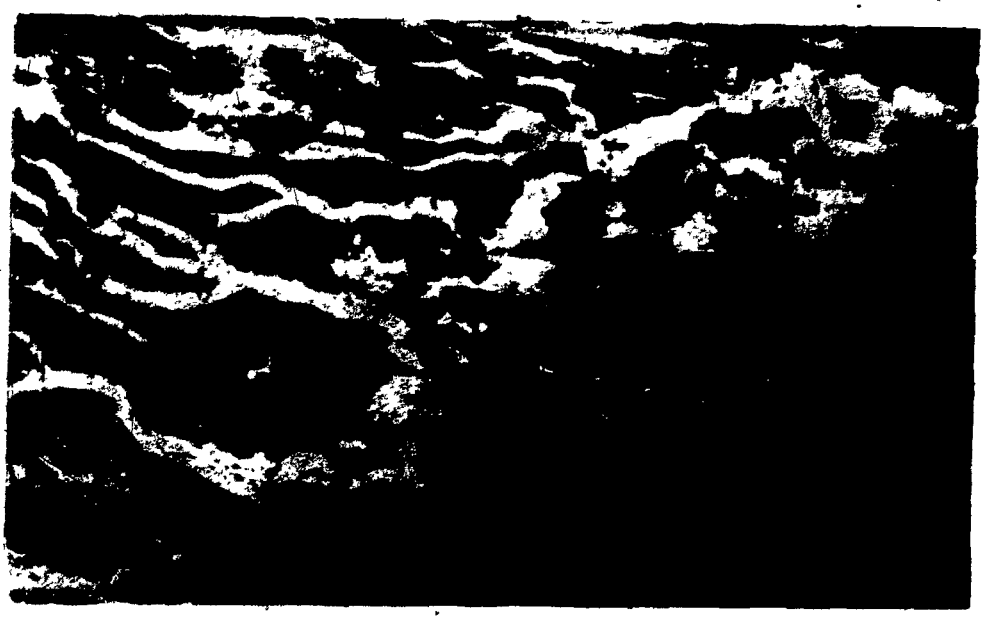

Plate 9: Snow distribution at Timmins 2, 6 June 1972

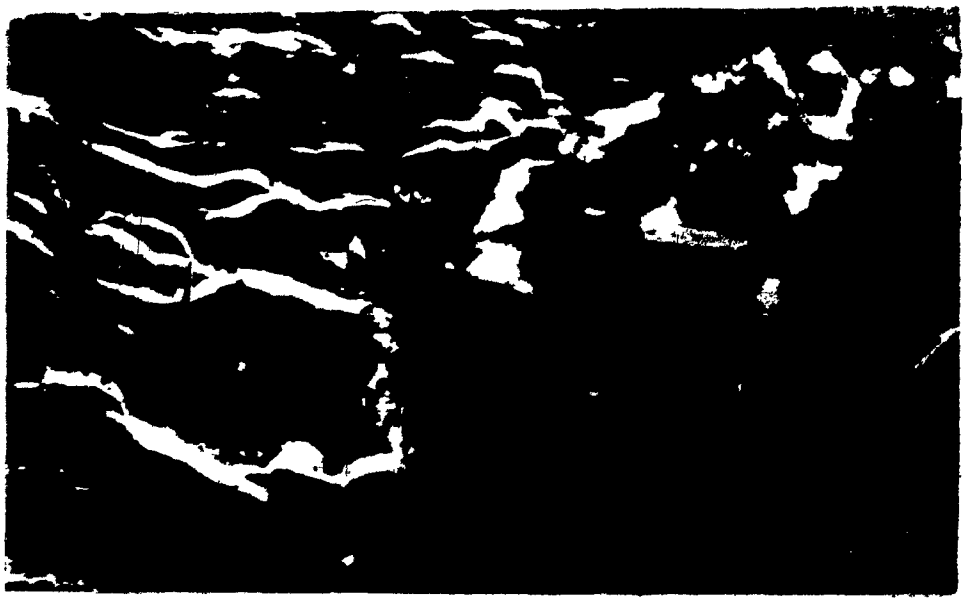

Plate 10: Snow distribution at Timmins 2, 18 May 1973

6.212 Construction of profiles, sections and plans

The three-dimensional prediction of ground temperature conditions was compiled by means of the procedure outlined in Chapter 5. Vertical sections were produced illustrating the ground thermal regime at 30m intervals across and along the site (Figure 20), as well as plans showing permafrost thicknesses (Figure 21) and the elevation of the base of permafrost (Figure 22).

6.22 Permafrost and unfrozen ground at Timmins 2

According to the model, approximately seventy percent of the site is underlain by perennially frozen ground. It occurs as steep-sided, frozen bodies surrounding a roughly horseshoe-shaped zone of unfrozen ground. Permafrost thicknesses are not as great as those proposed for Timmins 4, with a maximum predicted thickness of 106m.

6.221 Vertical sections

The distribution of ground temperatures along a longitudinal section and a series of cross-sections is shown in Figure 20. The location of each section is indicated on Figure 18. Together with Figures 21 and 22, the sections provide a three-dimensional impression of the occurrence of permafrost and unfrozen ground at this site.

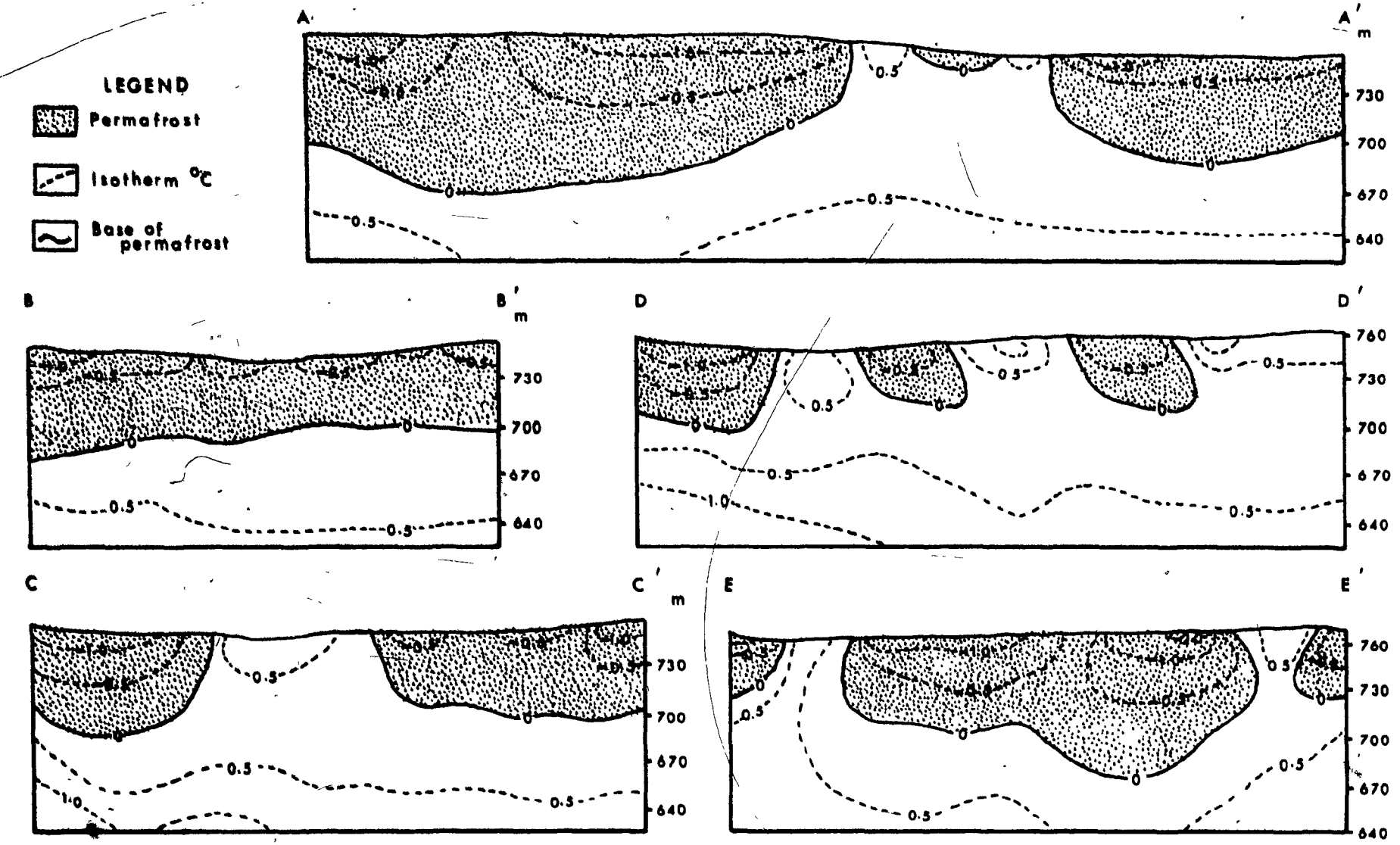

Figure 20: Longitudinal ground temperature profile and cross-sections, Timmins 2.

The pattern of isotherms indicates that, over most of the site, heat flow is essentially vertical at depths of greater than 30m. However, as at Timmins 4, non-vertical heat transfers are important near the surface and in the vicinity of channels, valleys and associated areas with ground water movement and deep snow accumulation. The existence of nearly vertical isotherms in such locations is reflected, on the sections, in the steep boundaries of the permafrost masses.

6.222 Permafrost thicknesses

Projected depths to the base of permafrost are shown in Figure 21. A maximum thickness of 106m is predicted beneath the ridge area in the north of the site. Elsewhere frozen ground is less extensively developed, rarely exceeding 40-50m in thicknesses. Small, shallow permafrost masses also occur within the unfrozen parts of the site. In general, thicknesses appear to increase from south to north along the axis of the site, a trend which is also visible in the sections (Figure 20).

6.223 Base of permafrost

The projected position and configuration of the lower boundary of frozen ground at Timmins 2 are shown in Figure 22. As at Timmins 4, the lower boundary appears to approximately mirror the surface relief, in that it occurs at the greatest depth beneath ridge areas. Permafrost is thin or absent beneath valley and

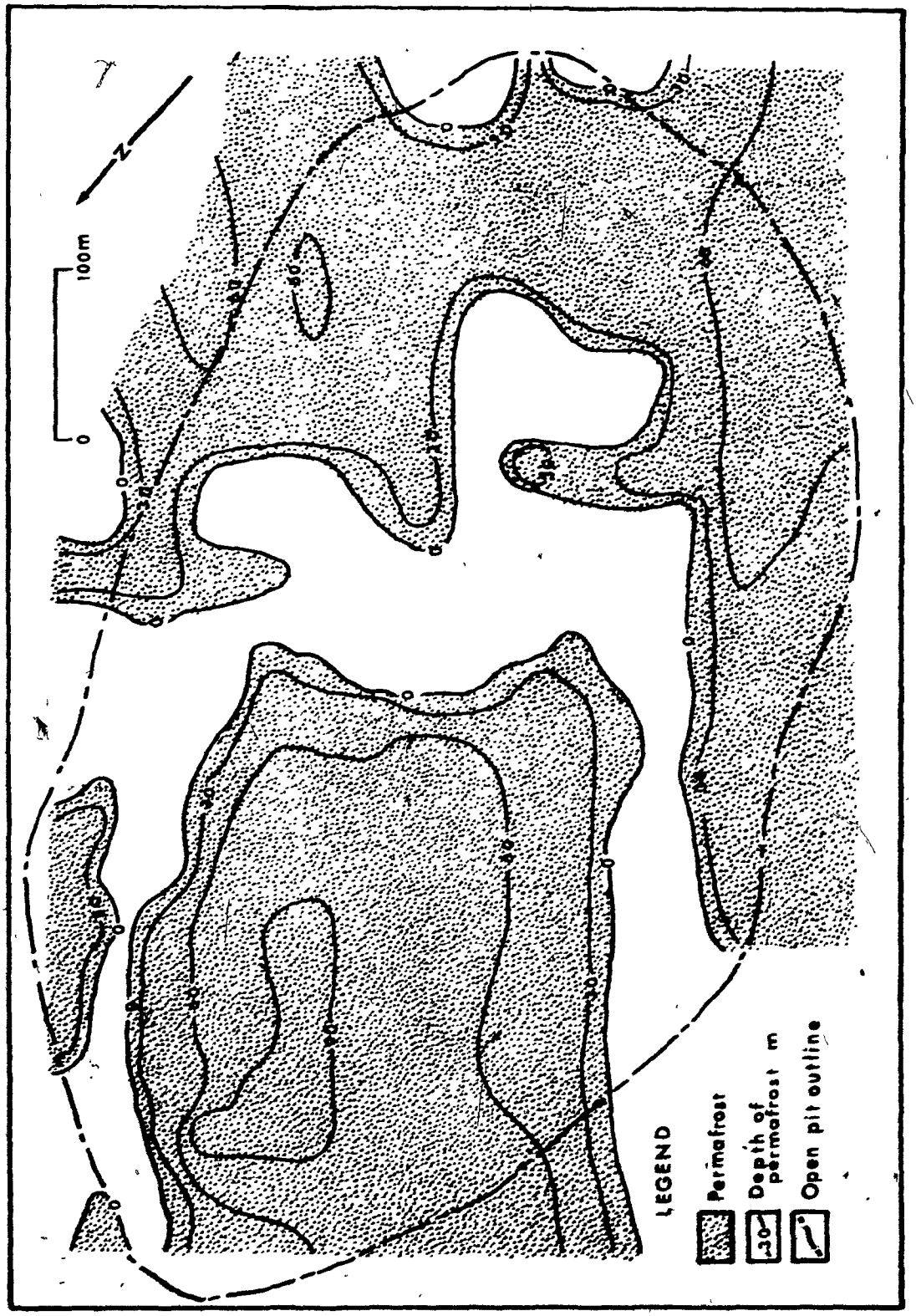

Figure 21: Permafrost depths, Timmins 2.

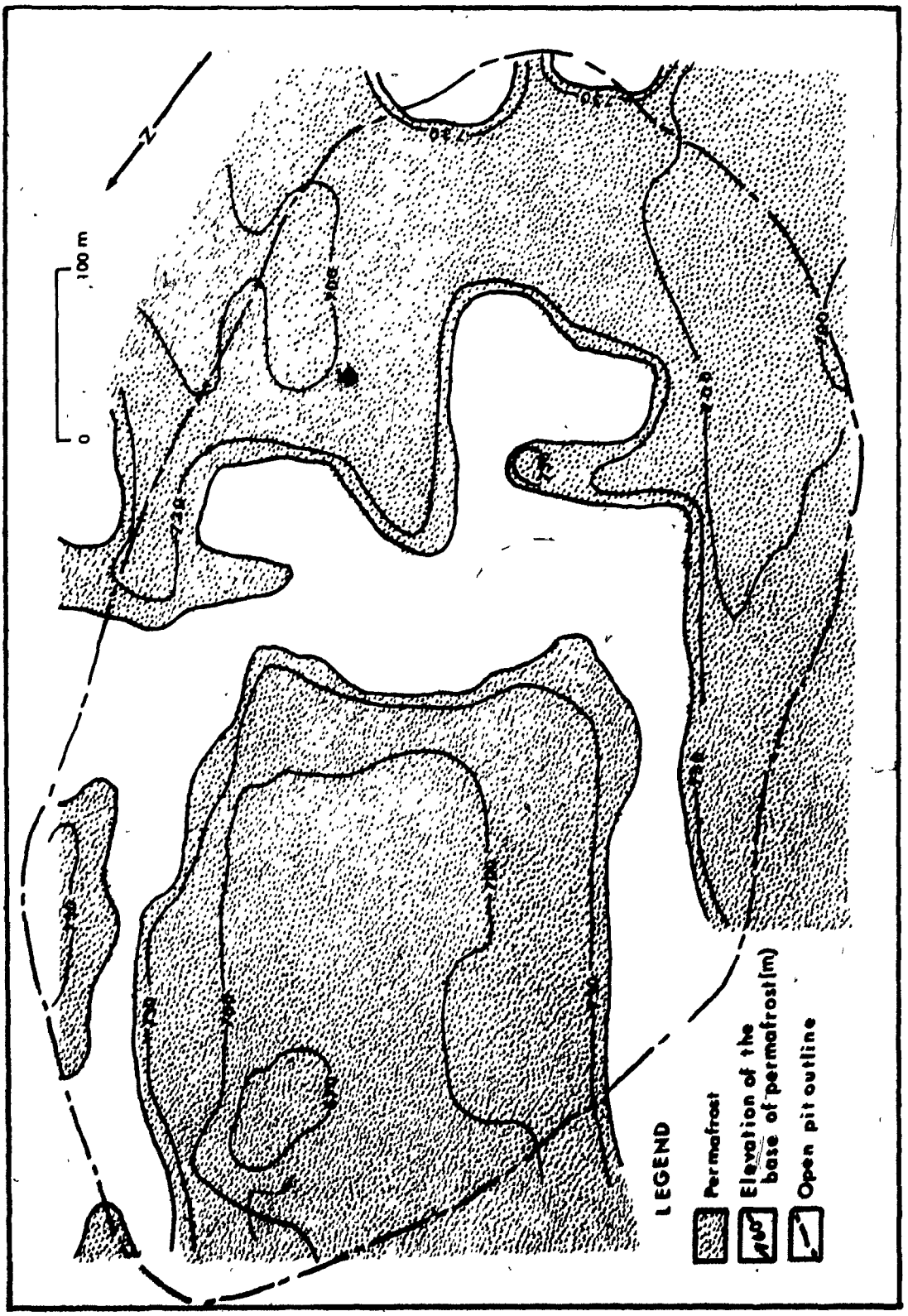

Figure 22: Elevation of the base of permafrost, Timmins 2.

channel locations. In the northern part of the site, the base of permafrost is situated at an elevation of 630-650m (IOCC datum). Elsewhere, it rarely occurs lower than 700m (IOCC datum).

6.224 Unfrozen areas

Approximately thirty percent of the site is predicted as unfrozen. These areas are indicated in Figure 20. Permafrost is not present beneath the channels, nor beneath deep snow areas in the central and southern parts of the site. There is little or no evidence, in the present prediction, of extensive talik development at Timmins No. 2.

6.23 Accuracy of the Timmins 2 prediction

As has already been suggested in sub-section 6.12, there are, unfortunately, neither thermocable data, nor measurements of permafrost thickness, to assist in an assessment of the validity of the present prediction. Observations by the author during the early stages in excavation of Timmins No. 2 Mine do, however, suggest a close spatial correlation between the actual distribution of permafrost and that projected here. It is difficult to draw firm conclusions regarding permafrost thicknesses, but the presence of an unfrozen, north-south zone, running through the centre of the mine (where a deep active layer or shallow talik zone amidst relatively uninterrupted permafrost is predicted) suggests that the projected distribution of frozen ground and

thicknesses, may be pessimistic. It is suggested that this situation may be attributable to an apparent underestimate in snow depths, as indicated on the Timmins 2 snow map (Figure 19).

The influence of dirt and dust in reducing the albedo of the snow-cover, and hence increasing melt rates, has been demonstrated at the nearby Fleming 7 site (for location, see Figure 1) by Nicholson (1974, Table 3). A similar situation can be postulated for Timmins 2, since this site lies adjacent to, and downwind from, Timmins No. 1 Mine, which was operating during the period preceding the 1972 aerial photography flights. When used in the model, the apparently shallower snow depths, produce a colder predicted ground temperature, and more extensive permafrost.

The magnitude of this effect is not readily estimated. At Fleming 7, snow depths were reduced by an average of 30 percent, as compared with Timmins 4 (Nicholson, op cit. Table 3). Using this figure as a gross approximation, it may be suggested that areas with an average snow depth on the Timmins 2 snow map of less than about 60cm are likely to be frozen, rather than the originally indicated 90 cm, and that 75m is a more realistic maximum permafrost thickness at this site.

In fact, 75m is closer to the permafrost thicknesses that are projected based on observed conditions. However, the

basis of such a correction is very tenuous and the main purpose of the example is to indicate that the discrepancy between actual and predicted conditions may quite reasonably be explained as a function of an underestimate in snow depths, rather than of the inadequacies of the predictive model *per se*. Once the three-dimensional distribution of permafrost at Timmins 2 is known with certainty, it will be possible to make a much more quantitative assessment of the accuracy of the proposed model.

CHAPTER 7

SUMMARY AND CONCLUSIONS

This study was concerned with assessing the influence of environmental parameters on ground temperature distribution, with deriving improved equations for shallow ground temperature prediction, and with development of a simple procedure for modelling the occurrence of permafrost and unfrozen ground. These objectives were pursued, with varying degrees of success, at the Timmins 4 Permafrost Experimental Site.

A review of the literature on the ground thermal regime in permafrost regions suggested that ground temperature at any shallow depth is a function of the influence of two sets of factors. Environmental parameters, such as snow depth, relief and vegetation, determine the upper (surface) boundary condition, while sub-surface factors modify heat flows in response to the boundary condition. Thus, variations in both surface and sub-surface factors control temperature distribution. Ground thermal properties and mass transfer effects associated with supra-permafrost groundwater movement are the main sub-surface factors. Variables representative of all these factors were compiled for twenty-one thermocable sites at Timmins 4, and related to ground temperature conditions in the ensuing analysis.

The relationship between ground temperature and the

environmental factors was examined by means of simple linear correlation analysis and step-wise multiple regression. The correlation coefficients indicated that, while snow depth is the single most important variable, almost all the other factors also appear to be significantly correlated with ground temperature. The regression results, however, suggested that few of the variables were truly independent, one from another. The fact that the snow depth variable, together with either thermal conductivity or elevation, was able to explain over 90 percent of the variance in ground temperature lent support to this contention. Thus, it was concluded that most of the correlations with the environmental parameters were, in fact, reflections of the relationship between ground temperature and snow depth, and were essentially false correlations.

Shallow temperature profiles were constructed for each Timmins 4 thermocable location, using equations derived from the regression results. Comparison with measured ground temperatures confirmed that the optimum equations, for predicting temperature as a function of snow depth and either thermal conductivity or elevation, were superior to equations which contain only the snow depth variable. The optimum equations were incorporated into a simple empirical model for ground temperature prediction. In developing this model, the ground was divided into two layers. Between the surface and 30 m depth, mean annual temperatures were

predicted using the optimum equations. Below this depth, the resulting profiles had to be extrapolated downwards assuming a simple heat flow model. The accuracy of this model varied spatially, so that while correspondence between predicted and observed conditions was good beneath ridge sites, it was not so good under the valleys. This situation was attributed to mass transfer effects due to groundwater movement, and to greater than average lateral heat flows.

When the model was then employed to construct a permafrost prediction for the entire Timmins 4 site, approximately 60 percent of the site was predicted frozen. A maximum permafrost thickness of about 150 m was projected. Although this figure could not be confirmed by direct temperature measurement, the predicted distribution of permafrost and unfrozen ground appeared to agree well with the results of previous studies.

An attempt to test the applicability of the model at Ferriman Ridge was less successful. Predicted temperatures were several degrees cooler than measured. It was hypothesised that this situation might be related to the elevation difference existing between the two sites, and that the procedure had become site-specific with inclusion of the elevation variable. As a further test, the model was then applied at the site of Timmins No. 2 Mine. Although topographically different from Timmins 4, this site lies within the same elevation range. Spatially, the predicted distribution of permafrost at Timmins 2 was in good

agreement with that observed during the early stages in excavation of the Mine. Projected permafrost thicknesses, however, appeared to be somewhat pessimistic. It was argued that this situation was related to an apparent increase in snow melt rates, due to wind-blown iron ore dust, rather than to any inadequacies in the model per se.

It is clear that there are a number of areas in which improvements to the model could be made. Indeed, as presently conceived the model has limited practical application, since the inclusion of elevation has made it site-specific. An obvious improvement would be to replace the elevation variable by one representative of, for example, the influence of groundwater, providing this variable could be simply and conveniently quantified on a large scale. The difficulties associated with assessing the accuracy of this and similar predictive procedures have been demonstrated. Any improvement which facilitates such assessments will be very useful. The importance of monitoring permafrost conditions during mining at the various sites considered here cannot be overemphasized.

In summary, the study confirmed that the winter snow cover is the most important single factor affecting the distribution of ground temperatures in the Schefferville area. Improved equations were derived for predicting shallow temperatures, and incorporated into a simple empirical model for prediction at greater depths. This model was tested at three sites in the area,

and found to be site-specific. At present, this limits application of the model to upland sites lying within the same elevation range as Timmins 4. However, the methods and procedures adopted in development of the model will probably be of lasting theoretical and practical value.

B I B L I O G R A P H Y

MSARP = McGill Sub-Arctic Research Papers
NRCC = National Research Council of Canada

ADDISON, A.P., 1972. Studies of evapotranspiration and energy budgets on the Truelove Lowland, Devon Island, N.W.T. p. 73-88, in L.C. Bliss (ed.), Devon Island I.B.P. Project -High Arctic Ecosystem, Project Report 1970 and 1971

AHRNSBRACK, W.F., 1968. Summertime radiation balance and energy budget of the Canadian tundra. Univ. Wisconsin, Dept. Meteorology, Tech. Rep. 37.

ANNERSTEN, L.J., 1962. Permafrost investigations. MSARP 12:102-111.

ANNERSTEN, L.J., 1964. Investigations of permafrost in the vicinity of Knob Lake, 1961-62. MSARP 16:51-143.

ANNERSTEN, L.J., 1966. Interaction between surface cover and permafrost. Biul. Peryglacj. 15:27-33.

BALOBAEV, V.T., 1973. Heat exchange between permafrost and the atmosphere in the presence of a vegetation cover. in Heat processes taking place in frozen soil. (NRCC Tech. Translation 1670).

BARANOV, I.Y., 1959. Geographical distribution of seasonally frozen ground and permafrost. in Principles of Geocryology, Pt. 1: General Geocryology. (NRCC Tech. Translation 1121).

BARNETT, D.M., 1963. Snow depth and distribution in relation to frozen ground in the Ferriman Mine and Denault Lake areas. MSARP 15:72-85.

BECKEL, D.K.B., 1957. Studies on seasonal changes in temperature gradient of the active layer of soil at Fort Churchill, Manitoba. Arctic 10:151-183.

BIRCH, F. 1948., The effects of Pleistocene climatic variations upon geothermal gradients. Am. J. Sci. 238:529-558.

BLISS, L.C. and R.W. WEIN, 1971. Changes in the active layer caused by surface disturbance. Proc. Conference on the permafrost active layer. NRCC Assoc. Comm. Geotech. Res., Tech. Memo. 103 Ottawa. p.37-46

BONNLANDER, B., 1958. Permafrost research. MSARP 4:56-58.

BONNLANDER, B. and G.M. MAJOR-MAROTHY, 1964. Permafrost and ground temperature observations, 1957. MSARP 16:33-50.

BROWN, R.J.E., 1965. Some observations on the influence of climatic and terrain features on permafrost at Norman Wells, N.W.T., Canada. Can. J. Earth Sci. 2:15-31.

BROWN, R.J.E., 1966a. Relation between mean annual air and ground temperatures in the permafrost region of Canada. p. 241-47, in Permafrost: Proceedings of an International Conference. National Academy of Sciences, Washington, D.C.

BROWN, R.J.E., 1966b. Influence of vegetation on permafrost. p.20-25, in Permafrost: Proceedings of an International Conference, National Academy of Sciences, Washington, D.C.

BROWN, R.J.E., 1967. Permafrost in Canada. Map NRC 9769. NRCC. Division of Building Research, and Geological Survey of Canada Map 1246A.

BROWN, R.J.E., 1969. Factors influencing discontinuous permafrost in Canada. p. 11-53, in T.L. Pewe (ed.) The Periglacial Environment, past and present. INQUA, 7th Congr., Alaska, 1965. McGill-Queens University Press, Montreal.

BROWN, R.J.E., 1970. Permafrost as an ecological factor in the Subarctic. p.129-140, in Ecology of Subarctic Regions. UNESCO. Paris.

BROWN, R.J.E., 1972a. Permafrost investigations on Devon Island, N.W.T. Canadian Tundra Biome Study Site. p. 30-45, in L.C. Bliss (ed.) Devon Island I.B.P. Project - High Arctic Ecosystem, Project Report 1970 and 1971.

BROWN, R.J.E., 1972b. Permafrost in the Canadian Arctic Archipelago. Z. Geomorphol. Suppl. 13:102-130.

BROWN, R.J.E., 1973. Influence of climatic and terrain factors on ground temperatures at three locations in the permafrost region of Canada. p. 27-35, in Permafrost: North American contributions to the Second International Conference on Permafrost. Yakutsk.

BROWN, R.J.E., and T.L. PEWE, 1973. Distribution of Permafrost in North America and its relationship to the environment: a review 1963-1973. p. 71-100, in Permafrost; North American contributions to the Second International Conference on Permafrost. Yakutsk.

BROWN, W.G., 1963. Graphical determination of temperature under heated or cooled areas on the ground surface. Trans. Eng. Inst. Can. 6 (B-14).

BROWN, W.G. 1964. Difficulties associated with predicting depth of freeze or thaw. Can. Geotech. J. 7:365-371.

BROWN, W.G., G.H. JOHNSTON, and R.J.E. BROWN, 1964. Comparison of observed and calculated ground temperatures with permafrost distribution under a northern lake. Can. Geotech. J. 1:147-154.

BUDYKO, M.I., 1958. Heat balance of the earth's surface. Translation by Office of Climatology, U.S. Dept. of Commerce.

CARSLAW, M.S. and J.C. JAEGER, 1947. Conduction of heat in solids. Clarendon Press, Oxford. 386 p.

COOK, F.A., 1956. Near surface temperature measurements at Resolute Bay, N.W.T., Canada. Arctic 18:237-49.

COURTIN, G.M., 1972. Meteorological studies in the Truelove Lowlands. p. 46-72, in L.C. Bliss (ed.), Devon Island I.B.P. Project-High Arctic Ecosystem Project Report 1970 and 1971.

CRREL. Bibliography on cold regions science and technology. CRREL Rept. 12. 1951 to date.

DAVIES, J.A., 1962. A survey of two years' weather records in the Ferriman Mine area. MSARP 12:79-96.

DINGMAN, S.L. and F.R. KOUTZ, 1974. Relations among vegetation, permafrost and potential insolation in Central Alaska. J. Arctic Alp. Res. 6(1):37-47.

EZEKIEL, M., and K.A. FOX, 1959. Methods of Correlation and Regression Analysis. Wiley, New York. 548 p.

FERRIANS, O.J. Jr., 1965. Permafrost map of Alaska. U.S. Geol. Surv., Misc. Geol. Investigations, Map 1-445.

FRENCH, H.M., 1970. Soil temperatures in the active layer, Beaufort Plain. Arctic 23:229-239.

GARG, O.P., 1973. In situ physiomechanical properties of permafrost using geophysical techniques. p. 508-517, in Permafrost: North American Contributions to the Second International Conference on Permafrost. Yakutsk.

GARG, O.P. and P.F. STACEY, 1973. Techniques used in the delineation of permafrost in the Schefferville, P.Q. area. Proc. Seminar on the thermal regime and measurement in

Permafrost. NRCC Assoc. Comm. Geotech. Res. Tech. Memo. 108 Ottawa. p.76-83.

GARNIER, B.J. and A. OHMURA, 1970. The evaluation of surface variations in solar radiation income. Solar Energy 13:21-34.

GILL, D., 1973. Permafrost table microtopography in the Mackenzie River Delta, N.W.T., Canada. p. 105-113, in Permafrost: North American contributions to the Second International Conference on Permafrost. Yakutsk.

GOLD, L.W., 1963. Influence of snow cover on average annual ground temperature at Ottawa, Canada. Proc. Int. Conf. Assoc. d'Hydrol. Sci. Berkeley. p.82-91.

GOLD, L.W. and A.H. LACHENBRUCH, 1973. Thermal conditions in Permafrost. p. 3-25, in Permafrost: North American contributions to the Second International Conference on Permafrost. Yakutsk.

GRANBERG, H.B., 1972. Snow depth variations in a forest-tundra environment, Schefferville, P.Q. Winter, 1968-69. Unpublished M. Sc. thesis McGill University, Montreal. 134 p.

GRANBERG, H.B., 1973. Indirect mapping of the snow cover for permafrost prediction at Schefferville, Quebec, Canada. p. 113-121, in Permafrost: North American contributions to the Second International Conference on Permafrost. Yakutsk.

GRAY, J.T., 1966. Permafrost studies at Knob Lake, Central Labrador-Ungava (1964-65). MSARP 21:129-35.

GROSS, G.A., 1968. Geology of Iron Deposits in Canada, Vol. III: Iron Ranges of the Labrador Geosyncline. Geol. Surv. Canada Econ. Geol. Rept. 22. 179 p.

HARE, F.K., 1959. Photo reconnaisance survey of Labrador-Ungava. Dept. of Mines and Tech. Surveys, Geogr. Branch, Memo. 6, Ottawa. 83 p.

HARLAN, R.A., 1971. Water transport in frozen and partially-frozen porous media. Proceedings of Hydrology Symposium No. 8, NRCC, Ottawa. p. 109-130.

HARRISON, J.M. J.E. HOWELLS, and W.F. FAHRIG, 1972. A geological cross-section of the Labrador Miogeosyncline near Schefferville, Quebec. Geol. Surv. Can. Paper 70-37. 34 p.

HEGINBOTTOM, J.A., 1973. The thermal regime of the permafrost active layer at Inuvik, N.W.T. Proc. Seminar on the thermal regime and measurement in permafrost. NRCC: Assoc. Comm. Geotech. Res. Tech. Memo. 108 Ottawa p.68-75.

HENDERSON, E.P., 1959. Glacial study of central Labrador-Ungava. Geol. Surv. Can. Bull. 50. 94 p.

HWANG, C.T., D.W. MURRAY, and E.W. BROOKER, 1972. A thermal analysis for structures on permafrost. Can. Geotech. J. 9:33-46.

IVES, J.D., 1961. A pilot project for permafrost investigation in central Labrador-Ungava. Dept. Mines and Tech. Surv. Geogr. Paper 28. 26 p.

JESSOP, A.M., 1971. The distribution of glacial perturbation of heat flow in Canada. Can. J. Earth Sci. 8:162-166.

JOHNSTON, G.H. and R.J.E. BROWN, 1964. Some observations on permafrost distribution at a lake in the Mackenzie Delta, N.W.T., Canada. Arctic 17:162-175.

JOHNSTON, G.H., R.J.E. BROWN, and D.N. PICKERSGILL, 1963. Permafrost investigations at Thompson, Manitoba: Terrain studies. NRCC, Div. Build. Res., Tech. Paper 158. 55 p.

JUDGE, A.S., 1973a. Deep permafrost observations in the Canadian North. p. 35-41, in Permafrost: North American contributions to the Second International Conference on Permafrost. Yakutsk.

JUDGE, A.S., 1973b. The thermal regime of the Mackenzie Valley: Observations of the natural state. Environmental-Social Committee, Northern Pipelines. Report 73-38. Information Canada, Ottawa. 177p.

JUDGE, A.S., 1973c. The prediction of permafrost thickness. Can. Geotech. J. 10:1-11.

KELLEY, J.J. and D.F. WEAVER, 1969. Physical processes at the surface of the Arctic tundra. Arctic 22:425-437.

KRINSLEY, D.B., 1963. Influence of snow cover on frost penetration. U.S. Geol. Surv. Prof. Paper 475-B, B144-B147.

KUDRYAVTSEV, V.A., 1965. Temperature, thickness and discontinuity of permafrost. in Principles of Geocryology, pt. 1: General Geocryology (NRCC Tech. Translation 1187).

LACHENBRUCH, A.H., 1957a. Thermal effects of the ocean on permafrost. Geol. Soc. Am. Bull. 68:1515-1530.

LACHENBRUCH, A.H., 1957b. Three-dimensional heat conduction in permafrost beneath heated buildings. U.S. Geol. Surv. Bull. 1052-B, p. 51-69.

LACHENBRUCH, A.H., 1959. Periodic heat flow in a stratified medium with application to permafrost problems. U.S. Geol. Surv. Bull. 1083-A. 36 p.

LACHENBRUCH, A.H., 1968a. Permafrost. p.833-839, in R.W. Fairbridge (ed). The Encyclopedia of Geomorphology. Reinhold, New York.

LACHENBRUCH, A.H., 1968b. Rapid estimation of the topographic disturbance to superficial thermal gradients. Rev. Geophys. 6:365-400.

LACHENBRUCH, A.H., G.W. GREENE and B.V. MARSHALL, 1966. Permafrost and the geothermal regimes. p. 149-163, in Environment of the Cape Thompson Region, Alaska. USAEC Div. Tech. Information.

LINELL, K.A., 1973. Long-term effects of vegetative cover on permafrost stability in an area of discontinuous permafrost. p. 688-693, in Permafrost: North American contributions to the Second International Conference on Permafrost. Yakutsk.

MACKAY, J.R., 1967. Permafrost depths, Lower Mackenzie Valley, Northwest Territories. Arctic 20:21-26.

MACKAY, J.R. and D.K. MACKAY, 1974. Snow cover and ground temperatures, Garry Island, N.W.T. Arctic 27:287-296.

MISENER, A.D., 1955. Heat flow and depth of permafrost at Resolute Bay, Cornwallis Island, N.W.T. Canada. Trans. Am. Geophys. Union 36:1055-60.

MULLER, S.W., 1947. Permafrost or permanently frozen ground and related engineering problems. J.W. Edwards Inc., Ann Arbor, Michigan. 231 p.

NICHOLSON, F.H., 1974. Prediction of permafrost distribution for sub-arctic mining operations - Report on the first 10 months of work. Unpublished Report, NRCC Special Project. 63 p.

NICHOLSON, F.H. and H.B. GRANBERG, 1973. Permafrost and snow cover relationships near Schefferville, Quebec. p. 151-158, in Permafrost: North American contributions to the Second International Conference on Permafrost. Yakutsk.

NICHOLSON, F.H. and B.G. THOM, 1973. Studies at the Timmins 4 Permafrost Experimental Site, Schefferville, Quebec. p. 159-166, in Permafrost: North American contributions to the Second International Conference on Permafrost. Yakutsk.

NICHOLSON, H.M., 1973. Pedological studies in a sub-arctic environment, Schefferville, Quebec. Unpublished M. Sc. thesis, McGill University, Montreal. 248 p.

NIE, N., D.H. BENT and C.H. HULL, 1970. Statistical Package for the Social Sciences. McGraw-Hill, New York.

PRICE, L.W., 1971. Vegetation, microtopography and depth of active layer on different exposures in subarctic alpine tundra. Ecology 52(4): 638-647.

ROUSE, W.R. and K.A. KERSHAW, 1971. The effects of burning on the heat and water regimes of lichen-dominated subarctic surfaces. J. Arctic Alp. Res. 3(4):291-304.

SEGUIN, M.K., 1974a. The use of Geophysical Methods in Permafrost Investigation: Iron Ore Deposits of the Central Part of the Labrador Trough, Northeastern Canada. Geoforum 18:55-67.

SEGUIN, M.K., 1974b. Etat des recherches sur le pergélisol dans la partie centrale de la fosse du Labrador, Québec subarctique. Rev. Géogr. Montr. 28:343-356.

SEGUIN, M.K. and O.P. GARG, 1974. Delineation of frozen rocks from the Labrador-Ungava Peninsula using bore-hole geophysical logging. Proc. 9th Canadian Symposium on Rock Mechanics (1972). p.53-75.

SELLERS, W.D., 1970. Physical climatology. Univ. Chicago Press, Chicago. 272 p.

SHVETSOV, P.F., 1964. General mechanisms of the formation and development of permafrost in Principles of Geocryology Pt. 1:General Geocryology (NRCC Tech. Translation 1117).

SHIRTLIFFE, C.J., 1971. Optimum polynomials for representing temperature-EMF data for thermocouples over limited ranges. NRCC, Div. Build. Res., Tech. Paper 355 (NRCC 12231).

SHUL'GIN, A.M. 1957. Temperature regime of soils. (Trans) U.S. Dept. of Agriculture, and Israel Program for Scientific Translation.

SMITH, M.W., 1972. Observed and predicted ground temperatures, Mackenzie Delta, N.W.T. p. 95-106, in D.E. Kerfoot (ed) Mackenzie Delta area Monograph. 22nd Int. Georg. Congress

SMITH, M.W. and C.T. HWANG, 1973. Thermal disturbance due to channel shifting, Mackenzie Delta, N.W.T. p.51-60, in Permafrost: North American contributions to the Second International Conference on Permafrost. Yakutsk.

STUBBINS, J.B., R.A. BLAIS, and I.F. ZAJAC, 1960. Origin of the soft iron ores of the Knob Lake Range. Trans. Can. Inst. Mining Met. 64:37-52.

THOM, B.G., 1969. New permafrost investigations near Schefferville P.Q., Rev. Géogr. Montr. 23(3):317-327.

THOM, B.G., 1970. Comprehensive report on the Timmins 4 Permafrost Experimental Site. T.S. Report 6907-4, IOCC. 40 p.

TOUT, D.G., 1964. The climate of Knob Lake. MSARP 17:36 p.

TYRTIKOV, A.P., 1959. Perennially frozen ground and vegetation. in Principles of Geocryology, Pt. 1: General Geocryology (NRCC Tech. Translation 1163).

WILLIAMS, J.R., 1965. Groundwater in Permafrost regions - An annotated bibliography. U.S. Geol. Surv. Water Supply Paper 1792. 294 p.

WILLIAMS, P.J., 1964: Unfrozen water content of frozen soils and soil moisture suction. Geotechnique 14(3): 213-246.

WILLIAMS, G.P., 1971. Surface heat exchange and permafrost. Proc. Conference on the permafrost active layer. NRCC Assoc. Comm. Geotech. Res. Tech. Memo 103 Ottawa. p.8-11.

WILSON, C.V., 1971. The climate of Quebec. Part I Climatic Atlas. Can. Met. Serv.

WOODSIDE, W. and J.H. MESSMER, 1961. Thermal conductivity of porous media. II. Consolidated rocks. J. Appl. Phys. 32:1699-1706.

YAP, S.-M., 1972. Engineering properties of frozen ores from Labrador. Unpublished M. Eng. thesis, McGill University, Montreal.

ZAJAC, I.F., 1974. The stratigraphy and mineralogy of the Sokoman Formation in the Knob Lake area, Quebec and Newfoundland. Geol. Surv. Can. Bull. 220. 159 p.

APPENDIX I

PEAK AND MELT PERIOD SNOW SURVEYS AT TIMMINS 4

The Timmins 4 snow course was read at the time of peak snow in 1972 (15 April) and 1973 (30 March), as well as after each of the aerial photography flights made in connection with this study. Data from these surveys are presented here.

The snow course comprises 147 measurement stakes arranged on a rectangular grid with 21 rows and 7 columns. The survey readings given in this Appendix are arranged on such a grid, assuming that the northwest end of the snow course lies towards the top of the page. All readings are given in centimetres, water equivalent.

Date: 15 April, 1972 (Peak snow survey, 1972)

	A	B	C	D	E	F	G
21	95	47	96	82	120	108	101
20	103	48	100	101	95	127	50
19	194	1	61	63	109	75	94
18	11	1	95	66	163	93	99
17	0	27	111	106	36	*	161
16	123	76	154	132	87	123	75
15	72	122	135	59	8	68	18
14	7	50	82	61	*	113	50
13	179	119	47	55	133	58	65
12	174	3	14	121	117	65	5
11	*	7	144	167	102	17	*
10	1	0	41	131	98	17	95
9	7	115	80	22	79	36	62
8	0	116	81	24	55	44	60
7	21	89	1	160	2	62	*
6	15	46	55	142	13	37	*
5	58	1	79	150	30	10	*
4	0	50	155	54	37	6	*
3	34	88	165	31	15	22	67
2	47	105	*	36	10	66	92
1	42	5	196	*	59	*	28

* = missing data

Date: 2 May, 1972 (Survey following Flight No. 1)

	A	B	C	D	E	F	G
21	90	45	100	80	113	103	107
20	100	50	95	92	90	123	46
19	85	0	55	57	109	67	97
18	5	0	90	61	132	96	94
17	0	25	110	112	32	143	116
16	65	72	50	126	89	116	54
15	67	120	140	55	4	66	10
14	10	45	85	57	146	106	62
13	165	115	35	39	26	55	58
12	160	0	10	114	114	61	*
11	150	15	140	146	94	14	5
10	0	0	140	135	89	12	85
9	0	140	76	20	72	50	56
8	0	110	85	30	60	43	59
7	18	90	0	150	0	56	*
6	15	45	65	145	11	20	*
5	55	0	75	140	*	16	*
4	0	60	*	45	38	7	14
3	30	90	105	30	*	16	61
2	57	100	*	35	19	62	89
1	45	0	90	145	50	*	28

* = missing data

Date: 17 May, 1972 (Survey following Flight No. 2)

	A	B	C	D	E	F	G
21	73	15	70	50	82	80	70
20	70	12	76	66	73	106	22
19	30	0	31	34	89	44	72
18	0	*	67	33	135	64	124
17	0	9	83	76	2	130	88
16	72	34	24	105	60	91	28
15	35	96	113	22	0	42	0
14	0	21	59	28	124	85	30
13	133	84	*	0	1	34	36
12	134	2	*	75	90	38	0
11	*	2	108	125	67	0	0
10	0	0	7	95	58	0	*
9	0	*	55	2	49	17	52
8	0	*	57	9	28	10	33
7	4	62	0	145	0	24	32
6	0	18	32	111	0	8	*
5	28	2	47	114	*	0	*
4	0	31	*	38	5	0	*
3	15	64	76	11	*	5	43
2	16	82	*	6	0	42	63
1	17	0	58	112	25	*	0

* = missing data

Date: 31 May, 1972 (Survey following Flight No. 3)

	A	B	C	D	E	F	G
21	39	0	44	31	62	52	47
20	26	0	52	48	43	74	0
19	16	0	0	0	68	0	41
18	0	0	32	0	95	39	44
17	0	0	57	48	0	106	71
16	0	0	0	72	36	56	0
15	0	72	67	0	0	17	0
14	0	0	24	0	86	52	0
13	109	62	0	0	0	0	5
12	116	0	0	53	64	0	0
11	48	0	81	89	31	0	0
10	0	0	0	61	0	0	10
9	0	0	34	0	0	0	26
8	0	46	33	0	0	0	5
7	0	28	0	100	0	0	0
6	0	0	0	73	0	0	0
5	0	0	30	83	0	0	*
4	0	0	87	0	0	0	12
3	0	44	39	0	0	0	8
2	0	68	*	0	0	0	36
1	0	0	22	89	0	0	0

* = missing data

Date: 6 June, 1972 (Survey following Flight No. 4)

	A	B	C	D	E	F	G
21	0	0	0	0	0	0	0
20	0	0	0	0	0	0	0
19	31	0	0	0	0	0	0
18	0	0	0	0	0	0	0
17	0	0	0	0	0	24	0
16	0	0	0	0	0	0	0
15	0	26	14	0	0	0	0
14	0	0	0	0	41	12	0
13	74	14	8	0	0	0	0
12	91	0	0	0	0	0	0
11	109	0	34	48	0	0	0
10	0	0	0	27	0	0	0
9	0	0	0	0	0	0	0
8	0	0	0	0	0	0	0
7	0	0	0	58	0	0	0
6	0	0	0	32	0	0	0
5	0	0	20	39	0	0	0
4	0	0	58	0	0	0	0
3	0	0	45	0	0	0	0
2	0	0	*	0	0	0	0
1	0	0	44	42	0	0	0

* = missing data

Date: 30 March, 1973 (1973 Peak Snow Survey)

	A	B	C	D	E	F	G
21	82	28	62	53	88	104	74
20	93	12	105	74	82	126	41
19	172	0.5	61	38	115	56	78
18	3	1	93	55	144	70	44
17	1	21	92	104	44	96	98
16	155	52	81	102	94	101	10
15	38	97	151	45	7	14	0
14	10	43	42	23	132	61	43
13	160	83	27	29	32	74	28
12	150	1	32	73	122	76	0
11	152	3	107	104	43	25	0
10	3	0.5	27	97	28	8	19
9	1	83	94	4	23	32	20
8	1	46	29	0	31	28	9
7	39	11	0	78	0	54	51
6	26	63	80	74	14	0	30
5	65	14	88	38	8	0	86
4	1	68	137	2	7	13	51
3	36	110	107	11	33	32	35
2	*	137	131	4	0	51	26
1	14	15	92	79	32	51	17

* = missing data